

**A STUDY ON THE ANTIOXIDANT EFFECTS OF
ALPINIA GALANGA AND *CURCUMA AROMATICA* RHIZOME
EXTRACTS ON THE INHIBITION OF
UV-INDUCED CELLULAR MELANOGENESIS**

KANNIKA JAEMSAK

**A THESIS SUBMITTED IN PARTIAL FULFILLMENT
OF THE REQUIREMENTS FOR
THE DEGREE OF MASTER OF SCIENCE (PHARMACOLOGY)
FACULTY OF GRADUATE STUDIES
MAHIDOL UNIVERSITY**

2007

COPYRIGHT OF MAHIDOL UNIVERSITY

Thesis
Entitled

**A STUDY ON THE ANTIOXIDANT EFFECTS OF *ALPINIA GALANGA*
AND *CURCUMA AROMATICA* RHIZOME EXTRACTS ON THE
INHIBITION OF UV-INDUCED CELLULAR MELANOGENESIS**

.....
Miss Kannika Jaemsak
Candidate

.....
Uraivan ketsawatsakul
M.D., Ph.D. (Pharmacology)
Major-Advisor

.....
Assist.Prof.Adisak Wongkajornsilp,
M.D.,Ph.D. (Pharmacology)
Co-Advisor

.....
Assoc.Prof.Pravit Akarasereenont,
M.D.,Ph.D. (Pharmacology)
Co-Advisor

.....
Prof.M.R.Jisnuson Svasti, Ph.D.
Dean
Faculty of Graduate Studies

.....
Assist.Prof.Adisak Wongkajornsilp,
M.D.,Ph.D. (Pharmacology)
Chair
Master of Science Programme in
Pharmacology
Faculty of Medicine Siriraj Hospital

Thesis
Entitled

**A STUDY ON THE ANTIOXIDANT EFFECTS OF *ALPINIA GALANGA*
AND *CURCUMA AROMATICA* RHIZOME EXTRACTS ON THE
INHIBITION OF UV-INDUCED CELLULAR MELANOGENESIS**

was submitted to the Faculty of Graduate Studies, Mahidol University
For the degree of Master of Science (Pharmacology)

on
May 29, 2007

.....
Miss Kannika Jaemsak
Candidate

.....
Assoc.Prof.Parkpoom Tengamnuay,
B.Pharm, Ph.D. (Pharmaceutics)
Chair

.....
Uraivan ketsawatsakul,
M.D., Ph.D. (Pharmacology)
Member

.....
Assoc.Prof.Pravit Akarasereenont,
M.D.,Ph.D. (Pharmacology)
Member

.....
Assist.Prof.Adisak Wongkajornsilp,
M.D.,Ph.D. (Pharmacology)
Member

.....
Prof.M.R.Jisnuson Svasti, Ph.D.
Dean
Faculty of Graduate Studies
Mahidol University

.....
Clin.Prof.Piyasakol Sakolsatayadorn,
M.D.,F.R.C.S.T
Dean
Faculty of Medicine Siriraj Hospital
Mahidol University

ACKNOWLEDGEMENTS

This study could not be successful without the valuable advice of my major advisor Dr. Uraiwan Ketsawatsakul. I would like to express my heartfelt gratitude for her kind attention, the guidance, supervision and continual encouragement. I am very grateful to my advisor. She always made time for me when I need her assistance in completing my research. I am very grateful to my co-advisors Asst. Prof. Dr. Adisak Wongkajornsilp and Assoc. Prof. Dr. Pravit Akarasereenont for their kindness, encouragement and constructive comments.

I would like to thank the staff of Department of Pharmacology, Faculty of Medicine Siriraj Hospital, Mahidol University for their co-operation and generous assistance. I am also indebted to Assoc. Prof. Dr. Supornchai Kongpatanakul, Head of the Department of Pharmacology, Faculty of Medicine, Siriraj hospital, to Assoc. Prof. Parkpoom Tengamnuay, Faculty of pharmaceutical sciences, Chulalongkorn University for great support, advice, and who was the external examiner of the thesis defense.

I would like to thank Mrs. Sirikul Chotewutakorn and Mrs. Valla Wamanuttajinda for her helpful and advice. In particular, I would like to extend my appreciation to Mr. Athiwat Thaworn for great assistance, valuable suggestions and his kindness would always be remember. I would like to thank Miss Wanlapha Ananta and Miss Chiraporn Ninchawee for all help and always a best friend, I feel very appreciate to her. I would like to give my special thank to Mr. Sukit Huabprasert, Miss Kanda Kasetsilpsombat, for great assistance and wonderful friendships. I would like to thank Mrs. Pimolvann Tappayuthipijarn, Mr. Tharis Hincheranundana, Mr. Chaiporn Manochanon, Mrs. Piyapat Pongnarin and Miss Phornnapa chareonkij for great support during my study. I would like to thank Mrs. Srisamorn Sudthim for great assistance and for UVA instrument technique.

I would like to acknowledge my classmate in the Department of Pharmacology, Faculty of Medicine, Siriraj hospital especially Mr. Theera Somchitprasert, a good brother who always help me in everything and take care for me, Miss Yuvadee Saecheung, a lovely sister who a lot of kindness, Miss sookrutai boonmasawai, kindness sister for helping me and take care everybody. I would like to thank Kaew, Pla, Top, Nis and Da, a lovely young sister and brother who make me feel good all time and for the wonderful time we shared together.

A special acknowledgement is extend to the Prasart Neurological Instituted Hospital and faculty of graduate studies, mahidol university who supported research grant for in part of this thesis.

Finally, I wouldn't have been able to success my study without my family for their endless love, understanding and greatest support. The usefulness of this thesis, I dedicate to my mother, father, sisters and all the teachers who have taught me since my childhood.

Kannika Jaemsak

A STUDY ON THE ANTIOXIDANT EFFECTS OF *ALPINIA GALANGA* AND *CURCUMA AROMATICA* RHIZOME EXTRACTS ON THE INHIBITION OF UV-INDUCED CELLULAR MELANOGENESIS**KANNIKA JAEMSAK 4736161 SIPM/M
M.Sc. (PHARMACOLOGY)****THESIS ADVISORS: URAIWAN KETSAWATSAKUL, M.D., Ph.D.,
ADISAK WONGKAJORN SILP, M.D., Ph.D.,
PRAVIT AKARASEREENONT, M.D., Ph.D.****ABSTRACT**

The skin is a very susceptible target organ to ultraviolet radiation (UVR). UVR is believed to contribute to skin problems including melasma, possibly, by generating reactive oxygen species (ROS) and depleting endogenous antioxidant defenses, thereby leading to oxidative stress. UVR-induced oxidative stress in skin is postulated to play a crucial role in melanogenesis by aggravating tyrosinase activities and melanin contents. Therefore, the roles of exogenous antioxidants found in medicinal plants in the inhibition of UV-dependent oxidative stress involved in melanogenesis are intensively studied in order to develop effective depigmentating agents. *Alpinia galanga* (*A. galanga*) and *Curcuma aromatica* (*C. aromatica*) possessing antioxidant activities have traditionally been used in skin problems. Hence, this study investigated the antioxidant properties and phenolic contents of *A. galanga* and *C. aromatica* extracts using TLC-DPPH (Thin layer chromatography-1,1-diphenyl-2-picrylhydrazyl) and folin assay. In addition, melanoma cell culture model was performed to study their roles in inhibiting cellular melanogenesis induced by UVR to assess cell cytotoxicity by 3-(4,5-dimethylthiazol-2-yl)-2,5-diphenyltetrazolium bromide (MTT) reduction assay, intracellular oxidative stress or ROS formation by dichlorofluorescein diacetate (DCF-DA) assay, activities of antioxidant enzymes including catalase (CAT) and glutathione peroxidase (GPx), contents of cellular glutathione (GSH).

A. galanga and *C. aromatica* extracts were shown to inhibit UVR-dependent induction of tyrosinase activity and melanin content in G361 cells. In addition, both extracts were able to decrease UVR-induced cytotoxicity and oxidative stress of G361 cells. In studying the effects of plant extracts on antioxidant defenses, *C. aromatica* extract was able to protect against depletion of antioxidant enzyme (both CAT and GPx) activities and GSH contents caused by UVR. However, *A. galanga* extract did not significantly prevent a decrease in CAT activities, although its ability to inhibit UVR-induced reduction of GPx activities was higher than that of *C. aromatica* extract. This study concludes that improving antioxidant defense systems could be a mechanism by which both extracts-derived antioxidant phenolics provide inhibitory effects on UVA-dependent cellular melanogenesis.

**KEY WORDS: ULTRAVIOLET RADIATION/ OXIDATIVE STRESS/
REACTIVE OXYGEN SPECIES / MELANOGENESIS/
Alpinia galanga/ *Curcuma aromatica*/ ANTIOXIDANT DEFENSE**

165pp.

การศึกษากฤทธิ์ต้านอนุมูลอิสระของสารสกัดจากเหง้าข่า ว่านนางคำ ต่อการยับยั้งผลของรังสีอัลตราไวโอเลตในการกระตุ้นการเพิ่มขึ้นของสีผิว (A STUDY ON THE ANTIOXIDANT EFFECTS OF *ALPINIA GALANGA* AND *CURCUMA AROMATICA* RHIZOME EXTRACTS ON THE INHIBITION OF UV-INDUCED CELLULAR MELANOGENESIS)

นางสาวกรรณิการ์ แจ่มศักดิ์ 4736161 SIPM/M

วท.ม. (เภสัชวิทยา)

คณะกรรมการควบคุมวิทยานิพนธ์: อุไรวรรณ เกศสวัสดิ์สกุล, M.D., Ph.D., อติศักดิ์ วงศ์จรศิลป์, M.D., Ph.D., ประวิทย์ อัครเสรินนท์, M.D., Ph.D.

บทคัดย่อ

ผิวหนังเป็นอวัยวะเป้าหมายที่สำคัญสำหรับรังสีอัลตราไวโอเลต รังสีอัลตราไวโอเลตเป็นสาเหตุที่สำคัญในการทำให้เกิดความผิดปกติของผิวหนัง รวมทั้งเป็นสาเหตุในการทำให้เกิดฝ้า โดยทำให้มีการเพิ่มขึ้นของ reactive oxygen species ส่งผลให้เกิดการลดลงของสารต้านอนุมูลอิสระภายในร่างกาย จนทำให้เกิดภาวะ oxidative stress เกิดขึ้น โดยบทบาทของรังสีอัลตราไวโอเลตในการเหนี่ยวนำให้เกิด oxidative stress ในผิวหนังถือเป็นปัจจัยหนึ่งที่สำคัญในการทำให้มีการเพิ่มขึ้นของสีผิวโดยส่งผลให้มีการเพิ่มขึ้นของ activities ของเอนไซม์ tyrosinase รวมทั้งการเพิ่มขึ้นของเม็ดสีเมลานิน ในการทดลองนี้ได้ทำการศึกษาบทบาทของสารต้านอนุมูลอิสระในพืชสมุนไพรต่อ การยับยั้งรังสีอัลตราไวโอเลตที่เหนี่ยวนำให้เกิดภาวะ oxidative stress และส่งผลต่อการเพิ่มขึ้นของสีผิวเพื่อเป็นแนวทางในการพัฒนาสารลดความเข้มข้นของสีผิว ข่าและว่านนางคำมีฤทธิ์ต้านอนุมูลอิสระ รวมทั้งมีประวัติการใช้ในการรักษาปัญหาเกี่ยวกับโรคผิวหนัง ดังนั้นในงานวิจัยนี้จึงได้ทำการศึกษาฤทธิ์ต้านอนุมูลอิสระและปริมาณของสารประกอบ phenolic ในสารสกัดจากข่าและว่านนางคำ โดยใช้วิธี TLC-DPPH (Thin layer chromatography-1,1-diphenyl-2-picrylhydrazyl) และ folin นอกจากนี้ได้มีการศึกษาบทบาทของการยับยั้งการเพิ่มขึ้นของสีผิวที่เหนี่ยวนำโดยรังสีอัลตราไวโอเลตโดยใช้เซลล์ melanoma และทำการประเมินพิษของสารสกัดต่อเซลล์โดยใช้ 3-(4,5-dimethylthiazol-2-yl)-2,5-diphenyltetrazolium bromide (MTT) การศึกษาภาวะ oxidative stress ในเซลล์โดยวิธี Dichlorofluorescein Diacetate (DCF-DA) การศึกษา activities ของเอนไซม์ที่มีฤทธิ์ต้านอนุมูลอิสระ คือ catalase (CAT) และ glutathione peroxidase (GPx) รวมทั้งการศึกษาระดับของ glutathione (GSH) ภายในเซลล์

สารสกัดจากข่า (*Alpinia galanga*) และว่านนางคำ (*Curcuma aromatica*) สามารถยับยั้งผลของรังสีอัลตราไวโอเลตต่อการเพิ่มขึ้นของสีผิวในเซลล์ได้ โดยการลด activities ของเอนไซม์ tyrosinase และปริมาณของเม็ดสีเมลานิน รวมทั้งยังสามารถลดพิษและภาวะ oxidative stress ในเซลล์ G361 ที่เหนี่ยวนำด้วยรังสีอัลตราไวโอเลตได้ ผลของสารสกัดต่อการปกป้องสารต้านอนุมูลอิสระในภาวะที่เหนี่ยวนำโดยรังสีอัลตราไวโอเลตพบว่าสารสกัดจากว่านนางคำสามารถป้องกันการลดลงของ activities ของเอนไซม์ที่มีฤทธิ์ต้านอนุมูลอิสระ คือ เอนไซม์ CAT และ GPx รวมทั้งปริมาณของ GSH แต่อย่างไรก็ตามสารสกัดจากข่าไม่สามารถป้องกันการลดลงของ activities ของเอนไซม์ CAT ได้ แต่สามารถป้องกันการลดลงของ activities ของเอนไซม์ GPx ได้มากกว่าสารสกัดจากว่านนางคำ สารสกัดสมุนไพรทั้งสองชนิดมีความสามารถในการพัฒนาระบบของสารต้านอนุมูลอิสระ โดยสารสกัด มีสารประกอบ phenolic ที่มีฤทธิ์ต้านอนุมูลอิสระน่าจะเป็นกลไกในการยับยั้งผลของรังสีอัลตราไวโอเลตต่อการเพิ่มขึ้นของสีผิว

CONTENTS

	Page
ACKNOWLEDGEMENT	iii
ABSTRACT	iv
LIST OF TABLES	x
LIST OF FIGURES	xiii
LIST OF ABBREVIATIONS	xviii
CHAPTER	
I INTRODUCTION	1
II OBJECTIVES	3
III LITERATURE REVIEWS	4
3.1 Pathology and pathogenesis of melasma	4
3.1.1 Structure and pigmentation of skin	4
3.1.2 Melanogenesis pathway and tyrosinase enzyme	11
3.1.3 Treatment of melasma	15
3.2 Effect of ultraviolet irradiation on skin	17
3.2.1 UVR generates reactive oxygen species	21
3.2.1.1 Free radicals and reactive oxygen species	21
3.2.1.2 UVR and reactive oxygen species	25
3.2.2 UVR and oxidative stress-induced melanogenesis	31
3.2.3 The effect of UVR on cellular antioxidants	34
3.2.3.1 Non-enzymatic antioxidant	37
3.2.3.1.1 Glutathione (GSH)	37
3.2.3.1.2 Vitamin C	39
3.2.3.1.3 Vitamin E	40
3.2.3.2 Enzymatic antioxidants	41
3.2.3.2.1 Glutathione peroxidase (GPx)	41

CONTENTS (continued)

	Page
3.2.3.2.2 Superoxide dismutase (SOD)	42
3.2.3.2.3 Catalase (CAT)	43
3.3 Antioxidants as inhibitor of UV- induced melanogenesis: the effects of Thai medicinal plants	44
IV MATERIALS AND METHODS	55
4.1 Chemicals, Materials and Instruments	55
4.1.1 Chemicals	56
4.1.2 Materials	58
4.1.3 Instruments	58
4.2 Methods	59
4.2.1. Quanlitative study of plant extracts	59
4.2.1.1 Preparation of the plant extracts	59
4.2.1.2 Thin layer chromatography (TLC) analysis	59
4.2.2 Determination of total phenolics	60
4.2.3 Free radical scavenging activity assay	61
4.2.4 Antityrosinase activity	62
4.2.5 Cell culture	62
4.2.5.1 Cell culture	62
4.2.5.2 MTT assay	63
4.2.5.3 Tyrosinase activity	64
4.2.5.4 Melanin contents	65
4.2.5.5 Cellular antioxidants	65

CONTENTS (continued)

	Page
4.2.5.5.1 Antioxidant enzyme activities	65
4.2.5.5.1.1 Glutathione peroxidase (GPx)	66
4.2.5.5.1.2 Catalase (CAT)	67
4.2.5.5.2 Cellular glutathione contents in melanoma exposed to UV	70
4.2.5.6 Dichlorofluorescein Diacetate Assay	72
4.2.5.7 Procedure of protein assay	73
V RESULTS	74
5.1 Identification of antioxidant activity, the presence of phenolic and antityrosinase activities of the plant extracts	74
5.1.1 Thin layer chromatography	74
5.1.2 Determination of total phenolics	95
5.1.3 Free radical scavenging activity assay	98
5.1.3 Antityrosinase activities	101
5.2 Cellular study of the effects <i>A. galanga</i> and <i>C. aromatica</i> extracts in inhibiting UVR-induced melanogenesis.	104
5.2.1 Assessment of cell viability by MTT reduction assay	104
5.2.1.1 Cytotoxic effect on CC2511 and G361	104
5.2.1.2 Effects of <i>A. galanga</i> and <i>C. aromatica</i> extracts on G361 and CC2511 cells exposed to UVR	104
5.2.2 Effect on tyrosinase activities	111
5.2.3 Effect on melanin contents	115
5.2.4 Assessment of cellular antioxidants	120
5.2.4.1 Antioxidant enzyme activities	120
5.2.4.1.1 Glutathione peroxidase (GPx) activities	120
5.2.4.1.2 Catalase (CAT) activities	125
5.2.4.2 Cellular glutathione contents	130
5.2.5 Effect on intracellular oxidative stress	135

CONTENTS (continued)

	Page
VI DISCUSSION	137
VII CONCLUSION	144
REFERENCES	147
APPENDIX	161
PUBLICATIONS	163
BIOGRAPHY	165

LIST OF TABLES

TABLE	Page
3.1 Classification of melasma	5
3.2 Steps of mammalian melanogenesis	10
3.3 Nomenclature of reactive species	22
3.4 Evidence of phenolic compounds as protective agents against skin damage induced by UVR	46
4.1 Preparation of antityrosinase activity assay	62
4.2 Preparation of formaldehyde standards	68
4.3 Amount of substances to each well for CAT assay	69
5.1 Solvent system of mobile phase detected phenolic	75
5.2 R_f and rRF value of <i>C. aromatica</i> and curcuminoids in solvent system1.(Lot.1)	78
5.3 R_f and rRF value of <i>C. aromatica</i> and curcuminoids in solvent system1.(Lot.2)	79
5.4 R_f and rRF value of <i>C. aromatica</i> and curcuminoids in solvent system1.(Lot.3)	80
5.5 R_f and rRF value of <i>C. aromatica</i> 3 lots detected by FBS staining in solvent system 1.	81
5.6 R_f and rRF value of <i>C. aromatica</i> and curcuminoids in solvent system2.(Lot.1)	82
5.7 R_f and rRF value of <i>C. aromatica</i> and curcuminoids in solvent system2.(Lot.2)	83
5.8 R_f and rRF value of <i>C. aromatica</i> and curcuminoids in solvent system2.(Lot.3)	84
5.9 R_f and rRF value of <i>C. aromatica</i> 3 lots detected by FBS staining in solvent system 2.	85

LIST OF TABLES (continued)

TABLE	Page
5.10 R _f and rRF value of <i>A. galanga</i> and curcuminoids in solvent system1.(Lot.1)	86
5.11 R _f and rRF value of <i>A. galanga</i> and curcuminoids in solvent system1.(Lot.2)	87
5.12 R _f and rRF value of <i>A. galanga</i> and curcuminoids in solvent system1.(Lot.3)	88
5.13 R _f and rRF value of <i>A. galanga</i> 3 lots detected by FBS staining in solvent system 1.	89
5.14 R _f and rRF value of <i>A. galanga</i> and curcuminoids in solvent system2.(Lot.1)	90
5.15 R _f and rRF value of <i>A. galanga</i> and curcuminoids in solvent system2.(Lot.2)	91
5.16 R _f and rRF value of <i>A. galanga</i> and curcuminoids in solvent system2.(Lot.3)	92
5.17 R _f and rRF value of <i>A. galanga</i> 3 lots detected by FBS staining in solvent system 2.	93
5.18 The effects of UVA on tyrosinase activity and melanin content in G361 cells.	118
5.19 EC ₅₀ values of herbal extracts on GPx activity in G361 cells exposed with UVA	122
5.20 The effects of UVA on CAT and GPx activities in G361 cells	128
5.21 The effects of UVA on GSH contents in G361 cells	133

LIST OF TABLES (continued)

TABLE	Page
6.1 Comparative effects of <i>C. aromatica</i> and <i>A. galanga</i> on cytotoxicity by MTT reduction and GSH content in G361 cells	139
6.2 Comparative effects of <i>C. aromatica</i> and <i>A. galanga</i> on the inhibition of UVR-induced reduction of CAT and GPx activity and GSH contents in G361 cells	143
7.1 Summary table of the inhibitory effects of <i>A. galanga</i> and <i>C. aromatica</i> extracts on UVA-induced cellular melanogenesis in association with antioxidant defense system.	145

LIST OF FIGURES

FIGURE	Page
3.1 The layers of the skin	6
3.2 Epidermal melanin unit	7
3.3 The formation of the melanosome	7
3.4 Histology of melanocyte in normal skin	8
3.5 Structure of melanin	9
3.6 Biosynthetic pathway of melanin synthesis	12
3.7 Gene and protein structures of tyrosinase, TRYP1 and TRYP2	13
3.8 Tyrosinase compartmentalization in the melanosome	14
3.9 Summary of the effects of UVR on skin	18
3.10 Formation of ROS and organic free radicals by photosensitization reactions type I and type II	19
3.11 Action of UV radiation on cellular biomolecules	20
3.12 An imbalance between production of ROS and antioxidant defence is proposed to lead to oxidative stress	23
3.13 Major sources of free radicals in the body and the consequences of free radical damage	24
3.14 UVA-photosensitizers with possible involvement in skin photodamage	26
3.15 Excited states of non - DNA chromophores and UVA - induced DNA damage	27
3.16 Structure of the major UV- induced DNA base photodimer	29
3.17 Structure of the major UV – induced oxidative DNA damage	29
3.18 Effect of UVA induced ROS on skin photodamage	30
3.19 The possible role of UV-produced free radicals in melanogenesis	33
3.20 Subcellular location of endogenous antioxidants	34

LIST OF FIGURES(continued)

FIGURE	Page
3.21 The various pathways of antioxidants in the management of oxidative stress.	36
3.22 Structures of reduced (GSH) and oxidised (GSSG) glutathione	37
3.23 Effect of GSH on tyrosinase activity	38
3.24 UV-tyrosinase interaction	39
3.25 Various forms of vitamin C and its reaction with radicals(R [*])	40
3.26 Structure of α -tocopherol	40
3.27 Interacting network of nonenzymic antioxidant	41
3.28 Diagrammatic representation of relationship between cellular antioxidants	44
3.29 Structural groups and antioxidant capacity	45
3.30 Pictures of <i>A. galanga</i> and <i>C. aromatica</i>	48
3.31 Chemical structures of phenylpropanoids from <i>A. galanga</i>	49
3.32 Chemical structures of curcuminoids	51
3.33 Strategy planed for a study on the antioxidant effects of <i>Alpinia galanga</i> and <i>Curcuma aromatica</i> rhizome extracts on the inhibition of UV-induced cellular melanogenesis.	54
4.1 DPPH Scavenging	61
4.2 Cellular metabolism resulting in the conversion of MTT to formazan	63
4.3 Standard curve of tyrosinase activity	64
4.4 Standard curve of melanin content	65
4.5 Standard curve of formaldehyde	70
4.6 The reaction of GSH with OPA	70
4.7 Standard curve of GSH	71
4.8 The interaction of fluorescent probe with cell and oxidants	72
4.9 Standard curve of protein assay	73

LIST OF FIGURES (continued)

FIGURE	Page
5.1 Phenolic screening (solvent system 1): Bands were detected by UV 254 nm, UV 366 nm and FBS spray.	77
5.2 Phenolic screening (solvent system 2): Bands were detected by UV 254 nm, UV 366 nm and FBS spray.	77
5.3 Densitometer analysis of <i>C. aromatica</i> and curcuminoids in solvent system1.(Lot.1)	78
5.4 Densitometer analysis of <i>C. aromatica</i> and curcuminoids in solvent system1.(Lot.2)	79
5.5 Densitometer analysis of <i>C. aromatica</i> and curcuminoids in solvent system1.(Lot.3)	80
5.6 Densitometer analysis of <i>C. aromatica</i> and curcuminoids in solvent system2.(Lot.1)	82
5.7 Densitometer analysis of <i>C. aromatica</i> and curcuminoids in solvent system2.(Lot.2)	83
5.8 Densitometer analysis of <i>C. aromatica</i> and curcuminoids in solvent system2.(Lot.3)	84
5.9 Densitometer analysis of <i>A. galanga</i> and curcuminoids in solvent system1.(Lot.1)	86
5.10 Densitometer analysis of <i>A. galanga</i> and curcuminoids in solvent system1.(Lot.2)	87
5.11 Densitometer analysis of <i>A. galanga</i> and curcuminoids in solvent system1.(Lot.3)	88
5.12 Densitometer analysis of <i>A. galanga</i> and curcuminoids in solvent system2.(Lot.1)	90
5.13 Densitometer analysis of <i>A. galanga</i> and curcuminoids in solvent system2.(Lot.2)	91

LIST OF FIGURES (continued)

FIGURE	Page
5.14 Densitometer analysis of <i>A. galanga</i> and curcuminoids in solvent system ² .(Lot.3)	92
5.15 Determination of total phenolics contents in extracts of <i>A. galanga</i> and <i>C. aromatica</i> by Folin-Ciocalteu method.	96
5.16 The effect of <i>A. galanga</i> and <i>C. aromatica</i> extracts on free radical scavenging activity	99
5.17 Inhibitory effect of <i>A. galanga</i> and <i>C. aromatica</i> extracts on tyrosinase activities	102
5.18 Cytotoxicity of <i>A. galanga</i> and <i>C. aromatica</i> extracts on CC2511 cells	105
5.19 Cytotoxicity of <i>A. galanga</i> and <i>C. aromatica</i> extracts on G361 cells	105
5.20 Effect of dose of UVA on viability of G361 cells.	107
5.21 The effect of <i>A. galanga</i> and <i>C. aromatica</i> extracts on CC2511 cells exposed with UVA	109
5.22 The effect of <i>A. galanga</i> and <i>C. aromatica</i> extracts on G361 cells exposed with UVA	109
5.23 The effect of <i>A. galanga</i> and <i>C. aromatica</i> extracts on tyrosinase activity in G361 cells	112
5.24 The effect of <i>A. galanga</i> and <i>C. aromatica</i> extracts on melanin contents in G361 cells exposed with UVA	113
5.25 The effect of <i>A. galanga</i> and <i>C. aromatica</i> extracts on melanin contents in G361 cells	116
5.26 The effect of <i>A. galanga</i> and <i>C. aromatica</i> extracts on melanin contents in G361 cells exposed with UVA	117
5.27 The effects of UVA on tyrosinase activity and melanin content in G361 cells	118
5.28 The effect of <i>A. galanga</i> and <i>C. aromatica</i> extracts on GPx activity in G361 cells	121

LIST OF FIGURES (continued)

FIGURE	Page
5.29 The effect of <i>A. galanga</i> and <i>C. aromatica</i> extracts on GPx activity in G361 cells exposed with UVA	123
5.30 The effect of <i>A. galanga</i> and <i>C. aromatica</i> extracts on CAT activity in G361 cells	126
5.31 The effect of <i>A. galanga</i> and <i>C. aromatica</i> extracts on CAT activity in G361 cells exposed with UVA	127
5.32 The effects of UVA on CAT and GPx activities in G361 cells	128
5.33 The effect of <i>A. galanga</i> and <i>C. aromatica</i> extracts on intracellular GSH contents in G361 cells	131
5.34 The effect of <i>A. galanga</i> and <i>C. aromatica</i> extracts on intracellular GSH contents in G361 cells exposed with UVA	132
5.35 The effects of UVA on GSH content in G361 cells	133
5.36 The effects of <i>A. galanga</i> and <i>C. aromatica</i> extracts on the inhibition of ROS in G361 cells	136
5.37 The effects of <i>A. galanga</i> and <i>C. aromatica</i> extracts on the inhibition of ROS in G361 cells exposed with UVA	136
7.1 The photoprotective effect of <i>A. galanga</i> and <i>C. aromatica</i> extracts against UVA-radiation-induced the oxidative stress.	146

LIST OF ABBREVIATIONS

%	percentage
AOX	Antioxidant
BSA	Bovine serum albumin
CAT	Catalase
DCF	2', 7'-dichlorofluorescein
DCFH	Dichlorofluorescein
DCF-DA	2', 7'-Dichlorofluorescein diacetate
DMEM	Dulbecco's modified Eagle's media
DMSO	Dimethyl sulfoxide
EDTA	Ethylenediaminetetra-acetic acid
EPR	Electron paramagnetic resonance
GSH	Glutathione reduced
GPx	Glutathione peroxidase
GR	Glutathione reductase
GSSG	Oxidized glutathione
H ₂ O ₂	Hydrogen peroxide
H ₃ PMo ₁₂ O ₄₀	Phosphomolybdic acid
H ₃ PW ₁₂ O ₄₀	Phosphotungstic acid
KH ₂ PO ₄	Potassium dihydrogen orthophosphate
K ₂ HPO ₄	Dipotassium hydrogen orthophosphate
KOH	Potassium hydroxide
OD	optical density
OPA	<i>o</i> -phthalaldehyde
ROS	Reactive oxygen species
SEM	Standard error of the mean
SOD	Superoxide dismutase
vol	volume

LIST OF ABBREVIATIONS (continued)

°C	degrees Celsius
M	molar
MeOH	Methanol
mM	millimolar
EC-SOD	extracellular superoxide dismutase
MnSOD	Manganese superoxide dismutase
MTT	3-(4,5-dimethylthiazol-2-yl)-2,5-diphenyltetrazolium bromide
n	number of experiments
NaCl	Sodium chloride
NAD ⁺	Nicotinamide adenine dinucleotide, oxidised
NADPH	Nicotinamide adenine dinucleotide phosphate, reduced
NaOH	Sodium hydroxide
NBT	Nitroblue tetrazolium
nm	Nanometer
nM	Nanomolar
O ₂ ^{•-}	Superoxide radical
OH [•]	Hydroxyl radical
OH ⁻	Hydroxyl anion
PBS	Phosphate buffered saline
μM	micromolar
g	gram
mg	milligram
μg	microgram
ml	milliliter
μl	microlitre
U	unit
h	hour
min	minute
RFU	relative fluorescence unit

LIST OF ABBREVIATIONS (continued)

sec	Second
TCA	Trichloroacetic acid
TLC	Thin layer chromatography
UVA	Ultraviolet A radiation
UVB	Ultraviolet B radiation
UVC	Ultraviolet C radiation

CHAPTER I

INTRODUCTION

Skin is the largest organ of the body and forms the critical barrier protecting the body against the exterior environment. Ultraviolet radiation (UVR) is likely the most frequently encountered stress causing oxidative stress, an imbalance between reactive oxygen species and antioxidant defenses. Oxidative stress causing harmful effect on skin is postulated to play a crucial role in several skin pathogenesis including melasma (1-9).

Melasma, one of the most common skin problems, is an acquired skin hyperpigmentation or melanogenesis caused by an increased amount of melanin and tyrosinase is a key enzyme in modulating melanin production (10-13). Melanocytes thus are central to pathology of this skin disorder. Although melasma can affect all people, Asian and Hispanic females are most commonly affected (14). While the exact cause of melasma is unknown, both genetic and environmental factors are play a role in its development. Of the many etiology factors associated with melasma, environmental factors especially UVR is believed to be a major factor contributed to melanogenesis(14-16).

Many studies showed that UVR from the sun could provide potentially harmful effects on the skin. UVR reaching us on earth comprises mostly Ultraviolet A (UVA) 90-99 % and Ultraviolet B (UVB) 1-10 % (17). UVA penetrates deep into the dermis and epidermis of the skin. UVR can reach the depth of melanocytes higher in the UVA region than in UVB (18). UVR is a potent inducer of oxidants including superoxide radical($O_2^{\bullet-}$), hydrogen peroxide (H_2O_2) and hydroxyl radical(OH^{\bullet}) (5,19-20). To protect cells from oxidative damage, the skin is thus equipped with a network of complex antioxidant defense system (19-21).

The skin antioxidant defense system consists of a network of enzymatic and non-enzymatic antioxidants. Among enzymatic antioxidants, glutathione peroxidase, catalase and superoxide dismutase play a pivotal role (20-22). When there is an imbalance between antioxidant defense system and oxidants produced from UVR, oxidative stress could occur, as shown by a decrease in the level of antioxidants and inactivation of antioxidant enzyme (23-28). Since UVR-mediated oxidative stress is suggested to be involved in melanogenesis and endogenous antioxidants may not be sufficient to protect skin cells, there is a need to develop potentially exogenous antioxidants to promote antioxidant defense against oxidative stress capable of damaging skin cells.

In recent years the roles of herbal compounds such as phenolics, flavonoids, and high molecular weight polyphenols have been widely studied as beneficial protective agents of skin damage induced by UV irradiation (29-45). Several studies showed that phenolic compounds, major components of several herbs, possessed antioxidant properties responsible for their pharmacological activity. Traditionally, plants in Zingiberaceae family including *Alpinia galanga* (*A. galanga*) and *Curcuma aromatica* (*C. aromatica*) have been used in skin problem. The plants of Zingiberaceae family were previously shown to yield powerful antioxidant activity in several *in vitro* studies (46-47). While there is no gold standard, adverse side effects from depigmentating agents and recurrences are common (15,48-50). Hence developing therapeutic agents to effectively treat melasma is a challenge. Therefore, the role of antioxidant in the inhibition of UVR-dependent oxidative stress involved in melanogenesis are intensively explored. In addition, the potential herbs, as an important source of antioxidant phenolics need to be developed as effective depigmentating agents in the treatment of melasma.

The aim of this study is therefore to examine the roles of herbal extracts containing phenolic antioxidants in inhibiting melanogenesis induced by ultraviolet radiation using melanoma cell culture model.

CHAPTER II

OBJECTIVES

1. To study the antioxidant activities and the presence of phenolic compounds in the ethanol extracts of *Alpinia galanga* Sw. and *Curcuma aromatica* Salisb.
2. To elucidate the roles of the above plant extracts in the inhibition of cellular melanogenesis induced by UVR using different test systems in melanoma cell culture studying;
 - Cytoprotective effects
 - The activities of antioxidant enzymes and contents of GSH
 - Tyrosinase enzyme activities
 - Melanin contents

CHAPTER III

LITERATURE REVIEW

3.1 Pathology and pathogenesis of melasma

Melasma is an acquired skin hyperpigmentation. Lesions are irregular hypermelanosis characterized by light to dark brown macules and patches. Although melasma can affect all people, Asian and Hispanic female are most commonly affected (14). Melasma is classified both clinically and histologically. There are three clinical patterns of melasma: central facial pattern (most common), malar pattern and mandibular pattern (14-16). Histologically, melasma can be divided into 4 types based on Wood's light examination (Table 3.1): epidermal type with increased melanin in the epidermis, dermal type with melanin in the dermis, a mixed epidermal-dermal, and an indeterminate type found in type V and VI skin.

In comparison to normal skin, melasma lesional skin was found to contain an increased amount of melanin pigmentation in the epidermis (epidermal type), dermis (dermal type), or both (mixed type). in contrast to melanocytes of normal skin (14-16).

3.1.1 Structure and pigmentation of skin

The skin is the largest and the first line of defense organs from exterior environment. Skin is constantly exposed to pro-oxidant environmental stresses from a wide array of sources, including exposure to solar UVR. Acute or chronic exposure of the skin to UVR results in the development of inflammation, oxidative stress, and DNA damage leading to several skin disorders, including hyperpigmentation, photoaging or premature aging of the skin, and melanoma and nonmelanoma skin cancers (1-9).

Table 3.1 Classification of melasma (16).

Type	Normal light	Wood's light	Histology
Epidermal	Light brown	Enhancement of color contrast	Melanin deposition is found in the basal and suprabasal layers of epidermis.
Dermal	Ashen/Bluish gray	No enhancement of color contrast	Melanin deposition is found in the superficial and middermis
Mixed	Deep brown	Enhancement of color contrast in some areas, while not in others	Melanin deposition is found in the epidermis and dermis
Wood's light not apparent	Ashen gray or unrecognized	Not evident under Wood's light	Melanin deposition is found in the dermis

Skin can be divided into three layers: the outer epidermis, the middle dermis, and the inner subcutaneous. The dermis contains a complex extracellular matrix comprising many types of collagen, fibroblasts, and a range of supporting structures. The hypodermis (subcutaneous fat) spreads all over the body as a fibrofatty layer, with the exception of the eyelids and of the male genital region. The cells manufacture and store lipids in large quantities and bundles of collagen fibers weave between aggregates of fat cells providing flexible linkages between the underlying structures and the superficial skin layers. The epidermis consists of layers made of stratified epithelium which composed predominantly of keratinocytes. Keratinocytes within the basal layer proliferate and differentiate as they move through the stratum spinosum and granulosum to form the dead but chemically non inert stratum corneum (Figure 3.1). The outer layers are dead and cornified. The process of living cells moving upward and changing to dead cells is known as keratinization. The total turnover time,

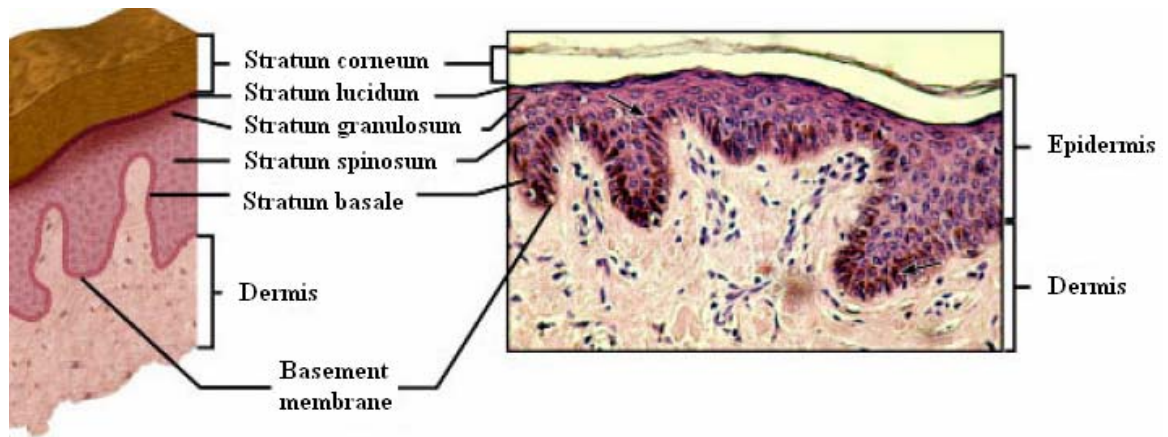


Figure 3.1 The layers of the skin.

from the basal layer to shedding, averages 28 days in healthy skin. In addition to the keratinocytes, an estimated 10% of the cellular component of the epidermis is composed of neural crest–derived melanocytes and Langerhans cells.

Melanocytes, derived from neuroectoderm, are oval and have a smooth cytoplasmic membrane and a round nucleus. In human, melanocytic development begins with the migration of melanoblast neural crest during embryogenesis to reach the basal layer of the epidermis. Melanocytes are dendritic cells with dendrites extending outward from the cell body. The dendritic processes of differentiated melanocytes are interspersed between neighbouring keratinocytes. The melanogenic pathway in melanocytes occurs within a discrete cytoplasmic compartment, melanosome. Melanocytes synthesize melanin in melanosome before passing the melanosomes to surrounding keratinocytes (Figure 3.2).

The formation of the melanosome has been divided into 4 stages (Figure 3.3). Stage I melanosomes contain a few filaments with a characteristic periodic banding and the enzyme tyrosinase in an inactive form; stage II melanosomes are oval with numerous filaments organized into a lamellar structure in which melanin is not present; Stage III melanosomes are partially filled with melanin; and Stage IV melanosomes are completely filled with melanin (51). Contact between dendrites of melanocytes and keratinocytes is important for transfer of melanin-containing melanosomes. Melanocyte will contact with keratinocytes, call “epidermal melanin unit”. The human epidermal melanin unit is composed of melanocytes and keratinocytes in a 1:40 ratio. Histology of melanocyte in normal skin as shown in (Figure 3.4).

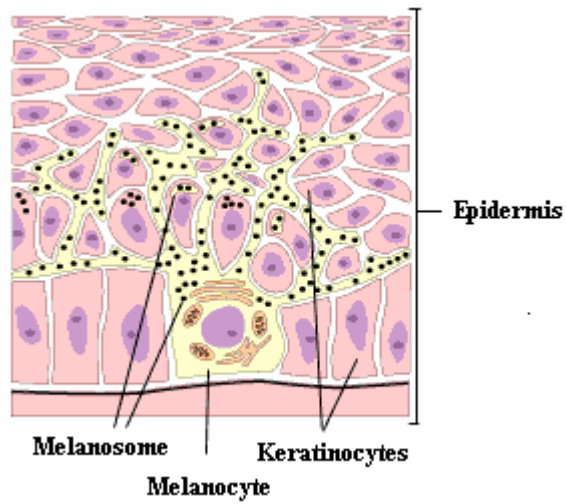


Figure 3.2 Epidermal melanin unit

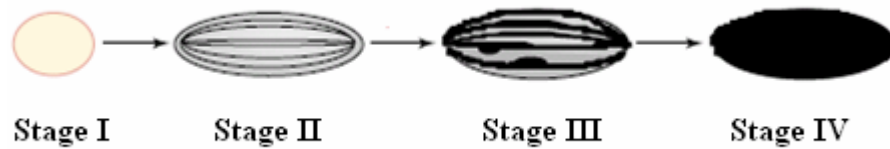


Figure 3.3 The formation of the melanosome (51).

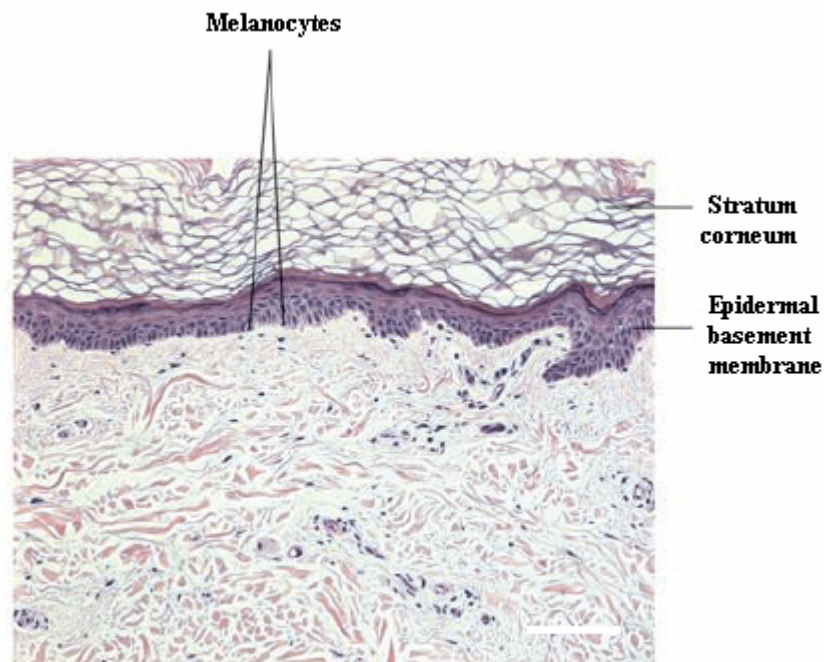
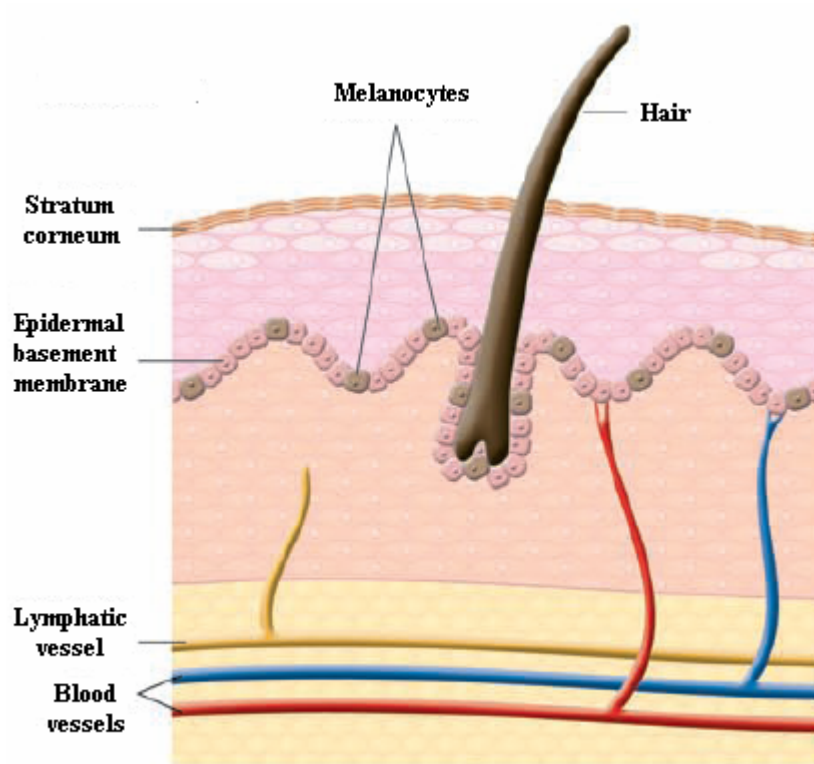


Figure 3.4 Histology of melanocyte in normal skin (52).

The basic structural unit of melanins is usually represented by covalently linked indoles. Structure of melanin shown as a region of 4²-7 linked substituted indoles indicating the high degree of conjugation of such domains (Figure 3.5). Carboxylic acid groups are attached to the C2 and the 5,6 functionalities are shown (top to bottom) as carbonyls in the orthoquinone form, deprotonated hydroxyls in the catecholic form, and an equilibrium form of linked semiquinones. The three major functions are indicated as electronic reactions, which render the polymer a potential free radical generator or scavenger, photon absorption and cation binding through the carboxyl groups. Some cationic binding also may involve the deprotonated hydroxyl groups or semiquinones.

The critical step in melanin biogenesis is the oxidation of tyrosine by the enzyme tyrosinase. In vertebrates this enzyme is active only in specialized organanelles in retinal pigment epithellum and melanocytes. In mammals melanin is formed as intracellular granules. Melanin granules are transferred from melanocytes to epithellal cells and form the predominant pigment of hair and epidermis (53). Steps of mammalian melanogenesis are shown in Table 3.2.

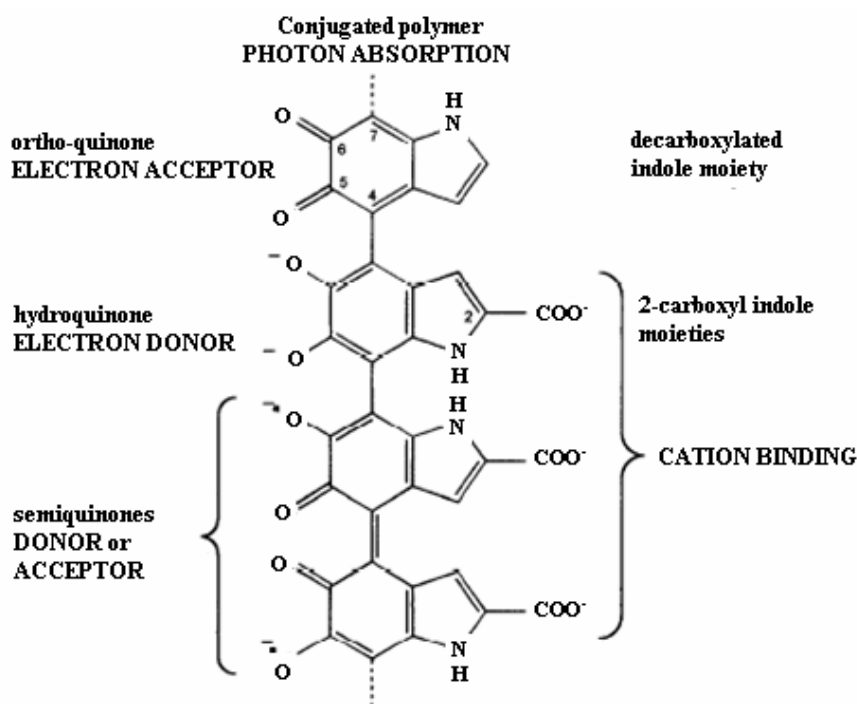


Figure 3.5 Structure of melanin (53).

Melanin is a nitrogenous polymer produced and concentrated in melanosome within melanocytes located in the basal layer of the skin. Depending on skin type, melanocytes produce varying ratios of eumelanin or pheomelanin synthesis by tyrosinase. In the skin, tyrosinase can be regarded as an important system for elimination reactive oxygen species. It has been established that this enzyme is able to utilize superoxide radical to produce melanin and an increase in melanin production associated with an enhancement in tyrosinase activities was found in melanocytes during exposure to UV (54). As human have approximately the same numbers of melanocytes in the skin, differences in color are due primarily to the ratio of eumelanin to pheomelanin, their distribution in keratinocytes, degree of melanocyte activity, and environmental factors such as solar irradiation that stimulates melanin production (55).

Table 3.2 Steps of mammalian melanogenesis (56).

Step I	Melanoblast migrate from the neural crest
Step II	Melanoblast differentiates to melanocyte. Clonal population of skin by melanocytes
Step III	Melanosome matrix formation
Step IV	Melanogenic genes such as tyrosinase, tyrosinase related proteins and melanosomal matrix components are induced tyrosinase and related melanogenic proteins are synthesized
Step V	Posttranslational processing and glycosylation of tyrosinase.
Step VI	Fusion of vesicles to form melanosomes and initiation of melanogenesis
Step VII	Control of tyrosinase activities
Step VIII	Control of the activities of tyrosinase related protein
Step IX	Post tyrosinase modification of biosynthesis
Step X	Modification of melanin
Step XI	Melanosome transfer to keratinocytes
Step XII	Melanosome degradation
Step XIII	Melanin removal with loss of cornified cell

Melanin is an irregular tight-absorbing polymer derived from the oxidation of tyrosine. Melanin is one of the most widely distributed pigments and is found in bacteria, fungi, plants and animals. It is the major pigment present in the surface structures of vertebrates (53). It is a heterogeneous polyphenol-like biopolymer with a complex structure and color varying from yellow to black. The color of mammalian skin and hair is determined by a number of factors, the most important of which is the degree and distribution of melanin pigmentation. Various dermatological disorders result in the accumulation of an excessive level of epidermal pigmentation. These hyperpigmented include melasma, age spots and sites of actinic damage.

Melanin synthesis results in the generation of hydrogen peroxide that, if inappropriately processed, can lead to the generation of hydroxyl radicals and other reactive oxygen species. The synthesis of melanin intermediates through tyrosinase involves the production of cytotoxic free radicals (12,18,20). The photoprotective properties of pigment melanin and its precursors in cultured melanocytes and melanoma cells have been the subject of many studied. This situation is complex because the composition as well as the quantity of melanin in the skin is of importance for photoprotection or photosensitization. Two types of melanin are considered to make up the mixed melanosomal melanin polymer.

3.1.2 Melanogenesis pathway and tyrosinase enzyme

The intracellular pathway for melanogenesis has been well characterized. First, L-tyrosine is hydroxylated to form dihydroxyphenylalanine (L-DOPA). Subsequently, L-DOPA is oxidized to L-dopaquinone which is either processed into eumelanin or pheomelanin. When thiols are absent, eumelanin is produced. Cysteine reacts with quinone intermediates, diverting melanin pigment synthesis from eumelanin (brown/black) to pheomelanin (red/yellow). In the absence of thiol compounds dopaquinone is immediately converted to dopachrome.

Otherwise, dopachrome tautomerase also known as tyrosinase-related protein-2 (Trp2/DCT) can convert dopachrome into a more stable intermediate called 5, 6- dihydroxyindole-2-carboxylic acid (DHICA). Spontaneous decarboxylation of dopachrome can also occur, leading to 5,6-dihydroxy indole(DHI). Tyrosinase-related protein-1(Trp1) and tyrosinase catalyse the conversion of DHICA to indolequinone 5,6-quinone-2-carboxylic acid a carboxylated indolequinone (Figure 3.6).

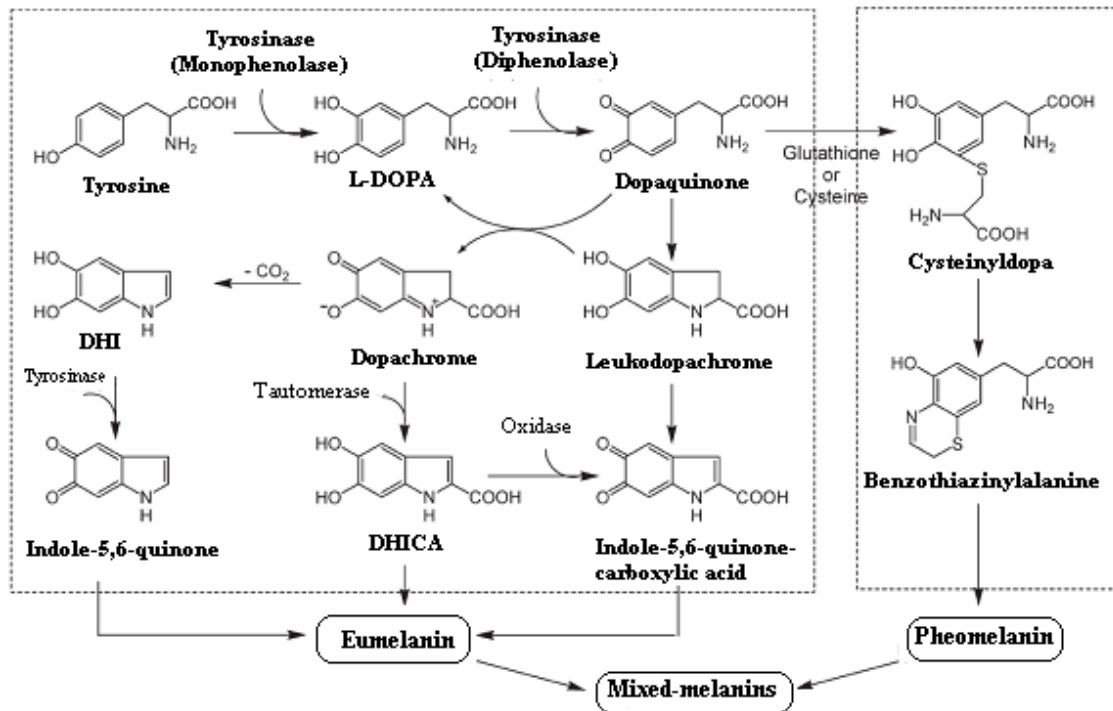


Figure 3.6 Biosynthetic pathway of melanin synthesis (57).

To regulate melanin synthesis, cells are equipped with melanogenic enzymes such as tyrosinase (TYR), tyrosinase-related protein 1 (TRP-1) and tyrosinase-related protein 2 (TRP-2). Gene and protein structures of tyrosinase, TRYP1 and TRYP2 are shown in figure 3.7. TYR, TYRP-1 and TYRP-2 contain an N-terminal signal sequence, an epidermal growth factor (EGF) repeat and other conserved cysteine residues that may be involved in protein-protein interactions, two metal binding domain that serve as the catalytic site, and a C-terminal transmembrane domain with a short cytoplasmic tail. These proteins share a common tertiary structure, have the potential to associate in a higher order melanosomal protein complex and contribute to the stability of complex formation. TYR to be encoded by five exons, TYRP-1 protein by eight exons and TYRP-2 by eight exons (11). Among those enzymes, tyrosinase is known to play a pivotal role in modulating melanin production.

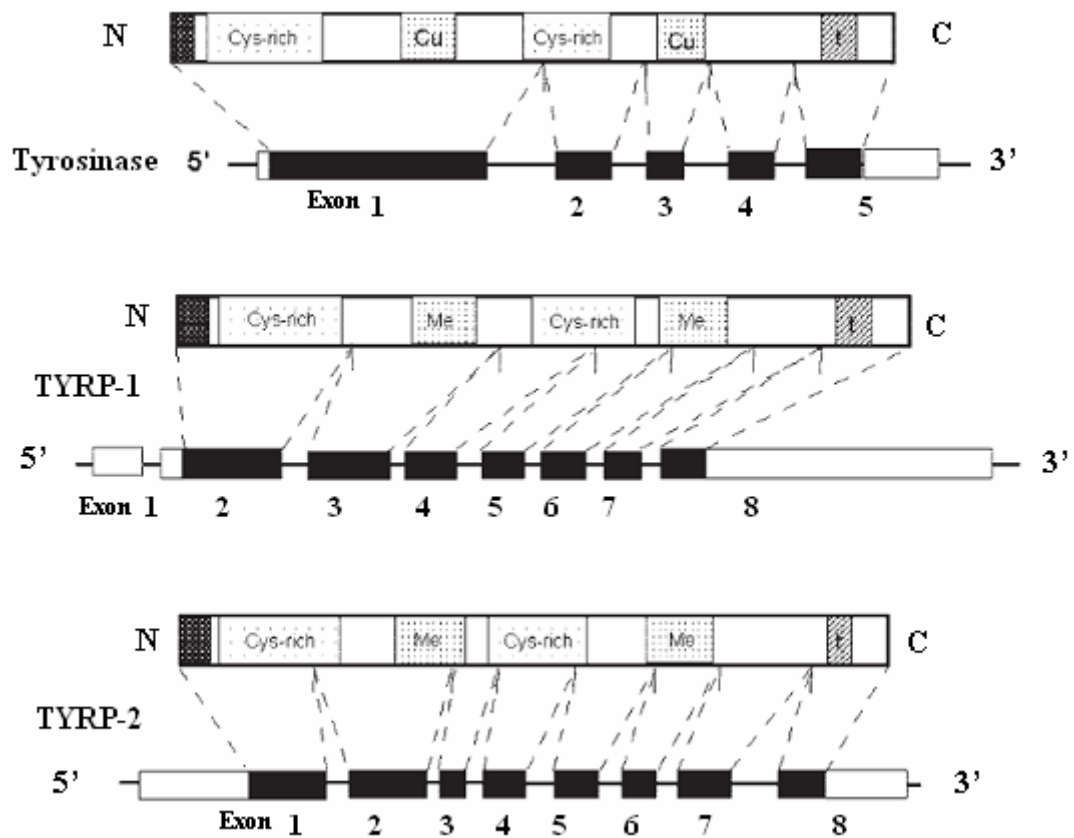


Figure 3.7 Gene and protein structures of tyrosinase, TRYP1 and TRYP2 (58).

N and C are the amino and carboxy protein terminus, respectively; Cy-rich, cysteinerich segments; Cu, Cu binding domains; t, transmebrane segment.

In the gene structure, numbers represent exons.

Human tyrosinase is a bifunctional, copper-dependent glycoprotein composed of 548 amino acids with a molecular mass of 62.6 kilodalton (kDa). Tyrosinase catalyses conversion steps in the biosynthetic pathway for melanin pigment synthesis. Tyrosinase (EC 1.14.18.1) is a copper-containing enzyme that catalyzes two distinct reactions of melanin synthesis: the hydroxylation of tyrosine by monophenolase action and the oxidation of 3,4-dihydroxyphenylalanine (L-DOPA) to *o*-dopaquinone by diphenolase action. The first catalytic function of tyrosinase, the hydroxylation of tyrosine to dihydroxyphenylalanine (DOPA), is the rate-limiting step for melanogenesis. Accordingly, melanin production has been suggested to be primarily controlled by the expression and activation of tyrosinase (10-13,53).

Synthesis of tyrosinase occurs on the ribosomes of the rough endoplasmic reticulum (RER). Nascent tyrosinase is transported to the golgi complex, where asparagines-linked glycosylation of tyrosinase is completed before exported into the melanosomes. At the golgi complex, glycosylation is essential for the normal structure and function of tyrosinase (56).

Tyrosinase has been divided into three domains: an inner domain that resides inside the melanosomes, a transmembrane domain and a cytoplasmic domain that extends into the cytoplasm of melanocytes (Figure 3.8). Over 90% of the tyrosinase copper binding site is localized to the inner domain. The inner domain has been shown to contain virtually all of the catalytic activity resulting in melanin formation exclusively in the melanosome. The transmembrane and cytoplasmic domains of tyrosinase consist of short amino acid sequences residing in the melanocyte cytoplasm. The cytoplasmic domain is critical for its melanogenic function and the cellular trafficking of tyrosinase. The cytoplasmic domain facilitates transport from the RER through the golgi complex to the melanosome (56).

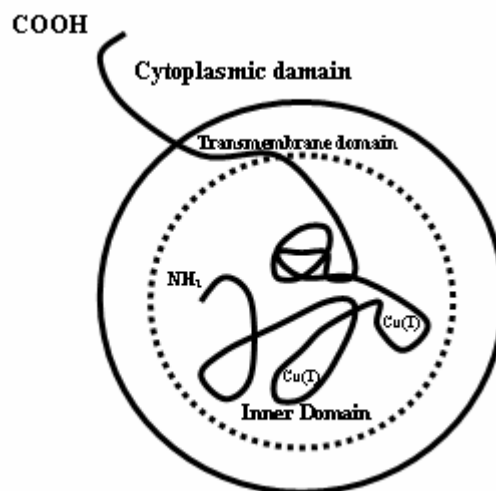


Figure 3.8 Tyrosinase compartmentalization in the melanosome (56).

Key: **NH₂**: Amino terminal of tyrosinase, **COOH**: Carboxyl terminal of tyrosinase, **Cu(I)**:Copper atoms found at the active site.

3.1.3 Treatment of melasma

Several therapeutic agents to treat melasma have been widely studied and developed. Although management of melasma is a challenge as there is no gold standard treatment and recurrences are common (15, 48-50). Various types of topical treatments are presently available as the following;

Sunscreens

Sunscreens are agents that physically or chemically block the penetration of UV light into the skin. Products providing against both UVB and UVA are called full or broad spectrum sunscreens. When used as directed, a sunscreen rated SPF 15 is usually adequate for most skin types. They may also increase the possibility of irritation and contact allergy because they contain multiple sunscreen agents in higher concentrations.

Hydroquinone

Hydroquinone inhibits melanogenesis. It is likely that hydroquinone interrupts one or more steps in the tyrosine-tyrosinase pathway of melanin synthesis. Hydroquinone is available as a 2% cream and a 4% cream. Hydroquinone produces variable depigmentation results. Prolonged use of hydroquinone, especially of high concentration, may cause a paradoxical hyperpigmentation.

Topical tretinoin

Topical 0.1% tretinoin was found to be effective in the treatment of facial melasma but may take up to 24 weeks for clinical improvement (applied once at night). The mechanism of action of tretinoin lightening melasma is poorly understood, although the reduction in epidermal melanin, correlates with clinical improvement. Topical tretinoin may cause transient stinging. It produces some erythema and peeling. Photosensitivity may occur. Tretinoin is applied as a cream, gel or alcoholic solution, usually containing 0.01% to 0.1%.

Topical steroids

The more potent the topical steroids used, the more pronounced the depigmentation. For example, 0.025% fluocinolone acetonide and 0.1% betamethasone valerate gives more pronounced effect than 0.1% triamcinolone acetonide or 0.1% dexamethasone. Their mechanism of action in depigmentation has not been adequately explained. The general effect of steroids on many cell systems is

antimetabolic. Steroids are cytotoxic or at least cytostatic to the epidermis; they decrease epidermal turnover and eventually produce atrophy. Caution is necessary when using potent fluorinated corticosteroids for prolonged periods on the face, as telangiectasia, atrophy, or acne rosacea can develop. The use of topical steroids as a single agent to treat melasma is therefore not encouraged.

Hydroquinone in combination

It was noticed that hydroquinone itself was not sufficiently efficacious to accomplish lightening in some hyperpigmentary disorders. Topical hydrophilic ointment containing 5% hydroquinone, 0.1% dexamethasone and 0.1% tretinoin was more effective and depigments melasma more rapidly than does topical hydroquinone alone.

Glycolic acid

Glycolic acid (an alpha hydroxyacid or AHA) is used as a chemical peel (chemabrasion). Treatment involves a series of peels in progressive concentrations. For better results, it has been recommended that AHA chemabrasion be accompanied by the use of hydroquinone and sunscreens. AHAs cause transient, mild stinging. In higher concentrations for peeling, erythema which lasts for a few days may develop. Scarring, hyperpigmentation and hypopigmentation are possible reactions. Experience of the therapeutic potential of AHAs in melasma treatment is still evolving.

Azelaic acid

Azelaic acid has been shown to be effective in melasma. A possible explanation for the efficacy of azelaic acid in melasma is related to its selective effects on hyperactive melanocytes. Azelaic acid inhibits the activities of tyrosinase and other oxidoreductases as well as mitochondrial respiratory enzymes and restores the hypermelanotic response to normal. The most commonly reported adverse symptoms with azelaic acid were transient stinging and itching.

Many of the most popular depigmentating agents in use today exhibit toxicity to melanocytes and are known to produce adverse side effects. The ideal treatment for melasma should allow depigmentation without bleaching of normal skin as well as should not be sensitizing or irritating and be cosmetically acceptable. Whichever modality is selected, proper skin protection from the sun is absolutely necessary for good results.

3.2 Effect of ultraviolet irradiation on skin

Epidermal melanocytes and even other epidermal and dermal cells may be targets of Ultraviolet irradiation (UVR), but melanocytes as the cells capable of synthesizing melanin themselves seem to be the first candidates for being the major target (59). The activation and differentiation of melanocytes can be induced directly by UVR or indirectly through their interaction with surrounding UV-irradiated keratinocytes (46). UV can generate acute and long-term effects on the skin. Example of UV-induced acute cytotoxicity include DNA damage and apoptosis, exemplified by the generation of sunburn keratinocytes, erythema, immune suppression and increased pigmentation. The long-term effects of UV on the skin are for example, photoaging and skin cancers, including melanoma (1-2, 5-6, 9, 60-64).

UV light region occurs between 100–400 nm. According to the International Commission on Illumination, UVR is divided into three categories depending on wavelength – UVC (200-280 nm), UVB (280-320 nm) and UVA (320 – 400 nm). UVR reaching us on earth comprises mostly UVA (90-99%) and UVB (1-10%). UVC has the highest energy and is the most biologically damaging region of UVR. The ozone layer efficiently absorbs UV radiation up to about 310 nm and it thus consumes all UVC and most of UVB (95 %). However, UVA is not absorbed at all (17).

When human skin is exposed to UVR, approximately, 5% of the UVR is reflected from the surface of the stratum corneum and 10% is scattered in the epidermis. The remaining UVR is absorbed by other molecules such as DNA, protein. These UVR-absorbing molecules are called chromophores. DNA absorbed UVR maximally at wavelengths from 245-290 nm. DNA is not capable of absorbing UVR at wavelengths longer than 320 nm, but the longer wavelengths can cause damage to genetic material by reacting with other chromophores, which transfer the energy further towards the DNA, a process call photosensitization (1). UVB absorbed within the epidermis and upper dermis causes erythema and sunburn. It is generally agreed that non-melanoma skin cancer is primarily elicited by UVB. UVA is a major component of sunlight that penetrates deep into the epidermis and dermis of the skin. Epidermiological studies indicate a relationship between high dose of UVA exposure and increased risk of melanoma in humans (65-68).

UVR can be both beneficial and harmful to normal human skin (Figure 3.9). The beneficial effects comprise killing pathogens on the skin, inducing vitamin D synthesis and treating certain skin diseases such as psoriasis vulgaris. The harmful effects include immune suppression and DNA damage (9). Excessive exposure of skin to UVR can result in acute and chronic damage. Exposure of UVR induces various dermal changes, including tanning, skin aging, and skin cancer. Up to 50% of UVA can reach the depth of melanocytes and the dermal compartments, whereas only 14% of UVB reaches the lower epidermis. Additionally, it has been estimated that the total photon energy delivered into the lower epidermis and upper dermis is 100 fold higher in the UVA than in UVB (20). UVA penetrates deeper than UVB through the epidermal layers of human skin to the basal layer and the underlying dermis, it can readily reach the melanocytes residing on the epidermal-dermal junction, and possibly lead to oxidative DNA damage and mutagenesis (18). In addition, UVA component of solar radiation may induce lipid peroxidation, which can subsequently stimulate the migration of important immune-mediating skin resident cells from the epidermis, thereby leading to skin immune suppression. Furthermore, only 40% of cytotoxic effects from sunlight (290-434 nm) was due to the UVB component (69).

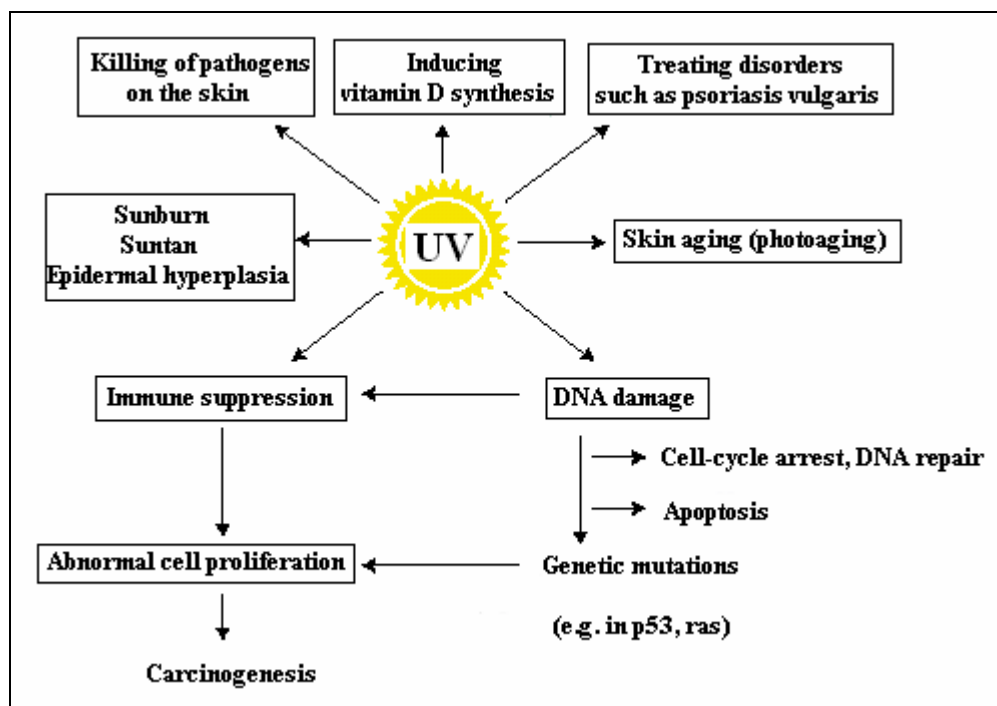


Figure 3.9 Summary of the effects of UVR on skin (9).

UVR induces damage of skin cells via two different mechanisms. Firstly, UV photons directly absorbed by cellular chromophores can lead to photo-induced reactions. This kind of injury is typical for DNA bases. Secondly, sensitizers can indirectly through photosensitization processes absorb UV light. Although ROS are widely known as mediators of UV photodamage, the exact mechanism of their generation in UV-irradiated skin is poorly understood. However, photosensitization by endogenous non-DNA chromophores of skin appears to be a key mechanism of UVR derived ROS production in human skin.

Photosensitization occurs as a consequence of photon absorption by endogenous non-DNA chromophores responsible for solar light-driven ROS production. The photoexcited state, most often the triplet state of the sensitizer, is the key photoreactive intermediate and exerts skin photodamage by direct reaction with substrate molecules including DNA bases (type I photosensitization) or molecular oxygen (type II photosensitization) leading to ROS formation as shown in simplified form in figure 3.10. Photon absorption by sensitizer chromophores in the electronic ground state (S) induces formation of photo excited states (S*). These can directly interact with substrate molecules (R), such as DNA bases (type I reaction) or activate molecular oxygen by electron or energy transfer reactions (type II reactions). Superoxide radical anions formed by type I or II mechanisms can then give rise to H₂O₂ formation by spontaneous dismutation. Hence, oxidative stress may play an important role in melanogenesis as it is involved in DNA damage (20). The effect UVR on cellular biomolecules are shown in figure 3.11.

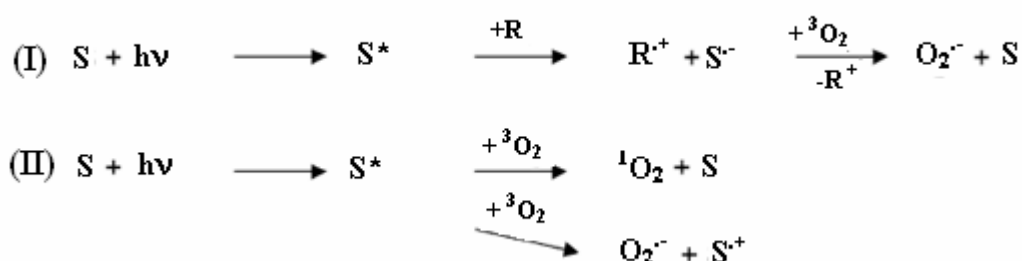


Figure 3.10 Formation of ROS and organic free radicals by photosensitization reactions type I and type II (17,20).

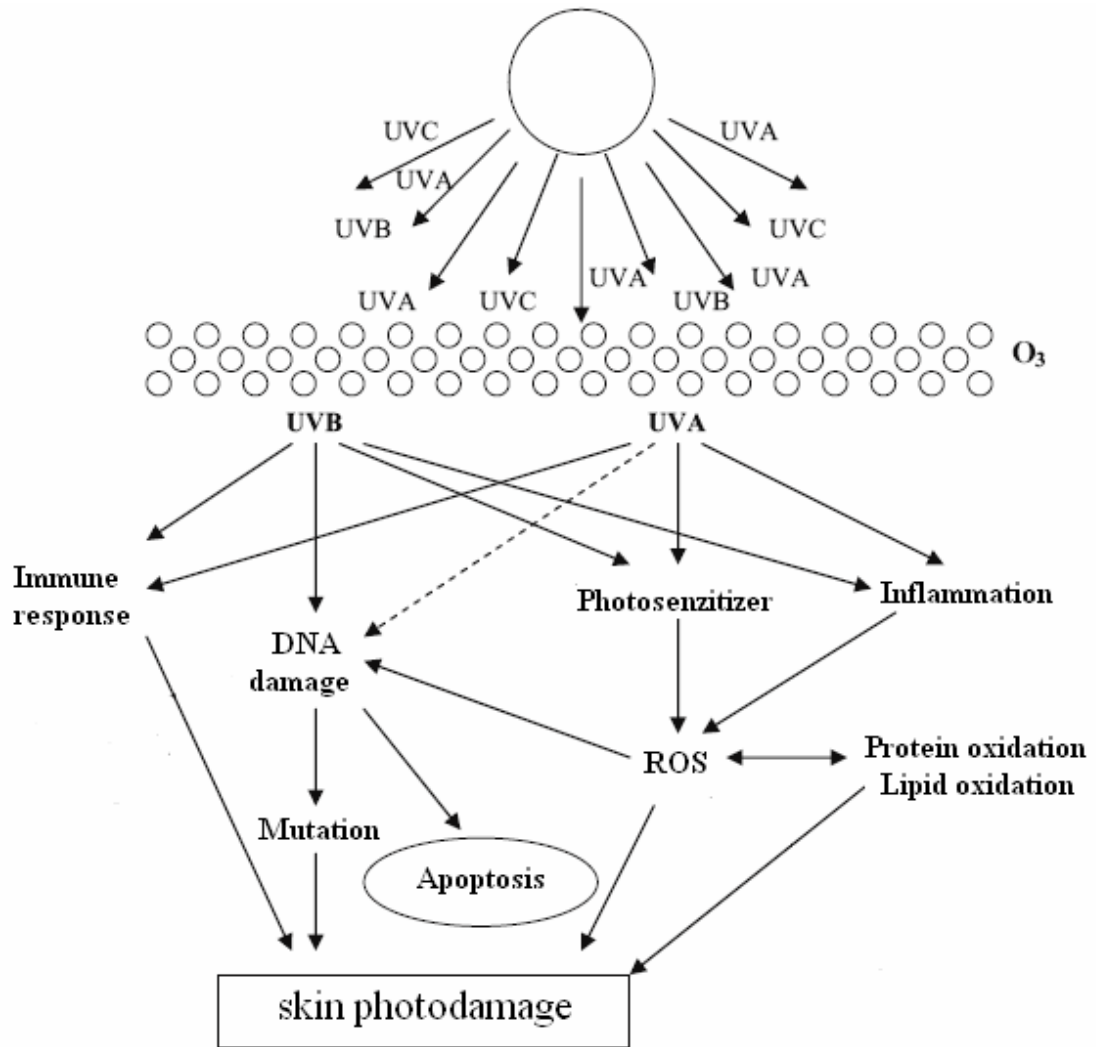


Figure 3.11 Action of UV radiation on cellular biomolecules (modified from 17).

3.2.1 UVR generates reactive oxygen species (ROS)

3.2.1.1 Free radicals and reactive oxygen species

A free radical is an any chemical species that has an odd number of electrons, because it contains one more unpaired electrons, that is an electron that occupies an atomic or molecular orbital by itself. An unpaired electron can be formed by the loss of a single electron from a non-radical, or by the gain of a single electron by the non-radical. They are often highly reactive and have short half-life. They can easily be formed when a covalent bond is broken if one electron from each of the pair shared remains with each atom. Nomenclature of reactive species as shown in table 3.3.

Oxygen free radicals are products of normal cellular metabolism. ROS is playing a dual role as both harmful and beneficial species to living systems. Beneficial effects of ROS occur at low/moderate concentrations and involve physiological roles in cellular responses to noxia, as for example in defence against infectious agents and in the function of a number of cellular signalling systems. One further beneficial example of ROS at low/moderate concentrations is the induction of a mitogenic response. The harmful effect of free radicals causing potential biological damage is termed oxidative stress and nitrosative stress. This occurs in biological systems when there is an overproduction of ROS or deficiency of enzymatic and non-enzymatic antioxidants. The excess ROS can damage cellular lipids, proteins, or DNA inhibiting their normal function. Oxidative stress has been implicated in a number of human diseases. The balance between beneficial and harmful effects of free radicals is a very important aspect of living organisms and is achieved by mechanisms called “redox regulation”. The process of “redox regulation” protects living organisms from various oxidative stresses and maintains “redox homeostasis” by controlling the redox status *in vivo* (21, 70-71). ROS can thus play a very important physiological role as secondary messengers (22).

Oxidative stress results from imbalance between the levels of antioxidants (AOX) and reactive oxygen species (ROS). Cells are normally able to balance the production of oxidants and antioxidants to maintain redox equilibrium. Oxidative stress occurs when this equilibrium is upset by excess levels of ROS, or depletion of antioxidant defenses (Figure 3.12).

Table 3.3 Nomenclature of reactive species (72).

Type	Reactive species
Reactive oxygen species (ROS)	Superoxide, $O_2^{\bullet-}$ Hydroxyl, OH^{\bullet} Hydroperoxyl, HO_2^{\bullet} Peroxyl, RO_2^{\bullet} Alkoxy, RO^{\bullet} Carbonate, $CO_3^{\bullet-}$ Carbon dioxide, $CO_2^{\bullet-}$ Ozone O_3 Hydrogen peroxide, H_2O_2 Singlet oxygen ($O^1_2\Delta g$) Hypobromous acid, $HOBr$ Peroxynitrous acid, $ONOOH$ Hypochlorous acid, $HOCl$ Peroxynitrite, $ONOO^-$ Organic peroxides, $ROOH$
Reactive chlorine species (RCS)	Chloramines Chlorine gas (Cl_2) Atomic chlorine, Cl^{\bullet} Hypochlorous acid, $HOCl$ Nitryl (nitronium) chloride, NO_2Cl
Reactive nitrogen species (RNS)	Nitric oxide, NO^{\bullet} Nitrogen dioxide, NO_2^{\bullet} Nitrosyl cation, NO^+ Nitroxyl anion, NO^- Nitrous acid, HNO_2 Dinitrogen trioxide, N_2O_3 Dinitrogen tetroxide, N_2O_4 Peroxynitrite, $ONOO^-$ Alkyl peroxynitrites, $ROONO$ Peroxynitrous acid, $ONOOH$ Nitryl (nitronium) chloride, NO_2Cl Nitronium (nitryl) cation, NO_2^+

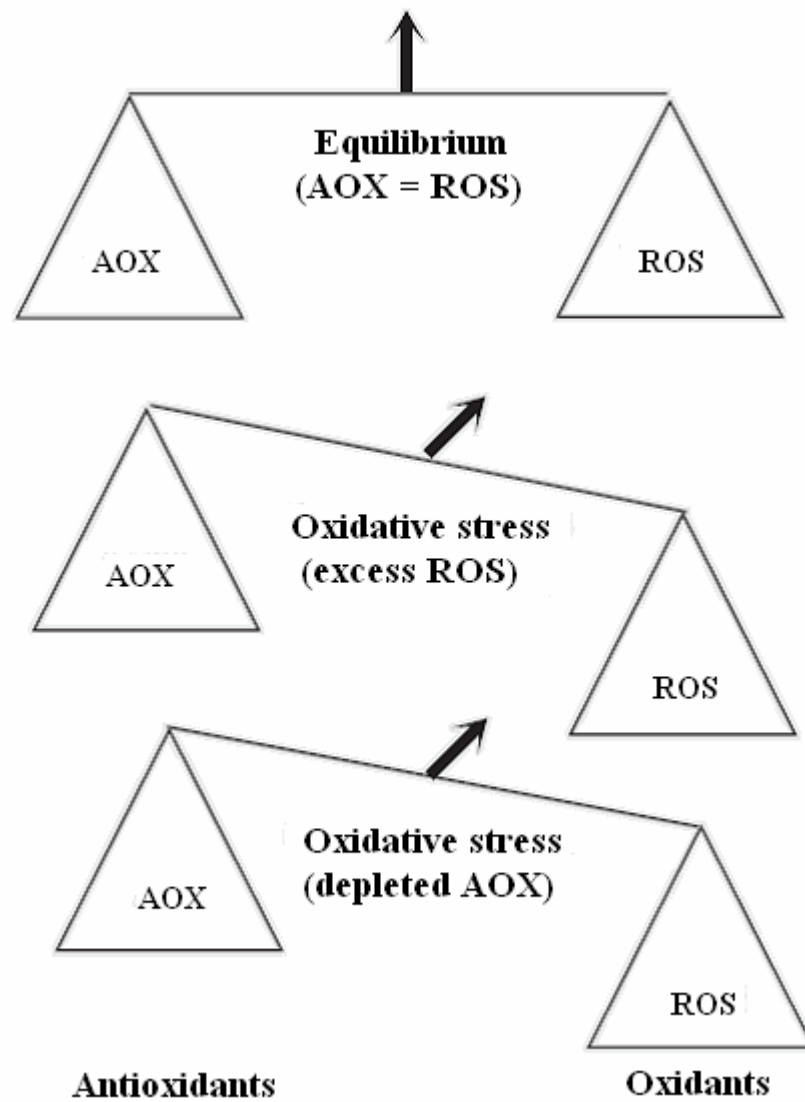


Figure 3.12 An imbalance between production of ROS and antioxidant defence is proposed to lead to oxidative stress (73).

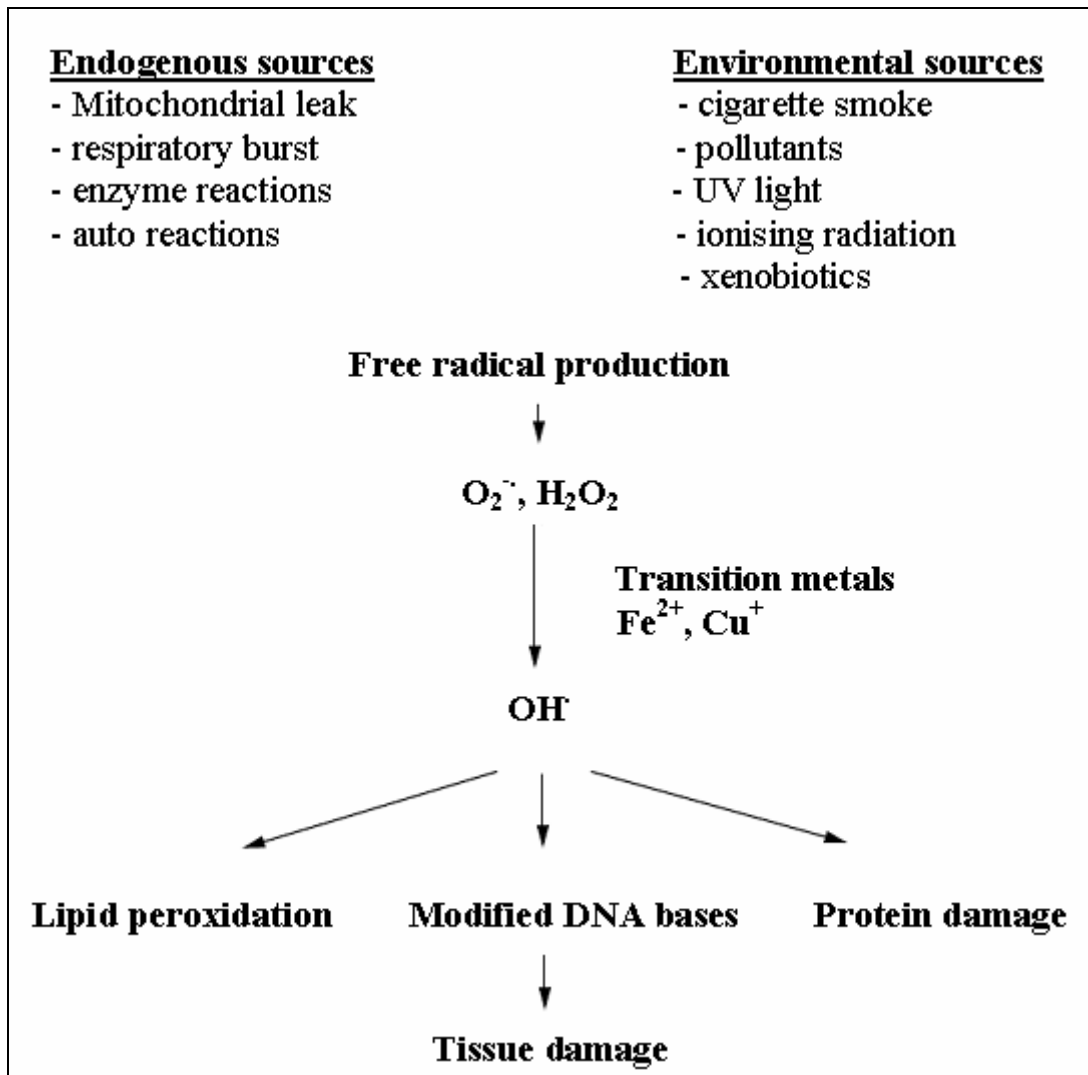


Figure 3.13 Major sources of free radicals in the body and the consequences of free radical damage (74).

ROS can be produced from both endogenous and exogenous substances as shown in figure 3.13. Singlet oxygen¹O₂, superoxide radical (O₂^{•-}) and hydroxyl radical (OH[•]) are predominant cellular free radical. Hydrogen peroxide (H₂O₂), although not itself radical containing molecules is referred as reactive oxygen species (ROS). Potential endogenous sources include mitochondria, cytochrome P450 metabolism, peroxisomes, and inflammatory cell activation (22).

ROS are formed through a variety of events and pathways. It has been estimated that one human cell is exposed to approximately 1.x10⁵ oxidative hits a day from

hydroxyl radicals and other such reactive species (22). The electron transport system in the mitochondrial is a major source that generate ROS.

A fraction of the oxygen is incompletely reduced by one-electron transfer (mostly via ubiquinone) to generate ROS and free radicals, which are usually disposed of by the coordinated function of antioxidant enzymes. If defected, they may cause oxidative damage and mutation of mtDNA molecules that are attached. mtDNA damage can lead to increase in ROS generation. Moreover, UV irradiation was reported to induce large-scale deletions of mtDNA in human skin and in cultured human skin fibroblast. ROS and free radicals generated by UVR may induce the occurrence and accumulation of mtDNA mutations in cells (75).

3.2.1.2 UVR and reactive oxygen species (ROS)

UV-driven ROS production has been demonstrated in cultured human skin cells, skin homogenates and intact murine and human skin (20, 76-77). Exposure of skin to UV light presents a potent oxidative stress, a condition when there is an imbalance of ROS and antioxidant defenses. Exterior oxidative stress as well as imbalanced production of oxidants such as $O_2^{\bullet-}$, OH^{\bullet} , H_2O_2 and 1O_2 can eventually lead to skin pathogenesis (5,19-20,78).

Cellular damage via an excited photosensitizer may occur by two major pathways often called Type I and Type II. The mechanisms are dependent on the chemical properties of photosensitizers. Human skin is an abundant source of numerous chromophores with strong particularly in the UVA (Figure 3.14) (20). Type I mechanisms involve one electron transfer through a direct interaction between an excited photosensitizer and other biomolecules, resulting in free radical formation. This mechanism does not require oxygen for the induction of molecule damage. The Type II mechanism involves energy transfer from an excited sensitizer to molecular oxygen that leads to production of reactive oxygen species (ROS). Mostly singlet oxygen, an excited state of oxygen, which is a very powerful oxidant with relatively long lifetime, is generated (Figure 3.15) (17).

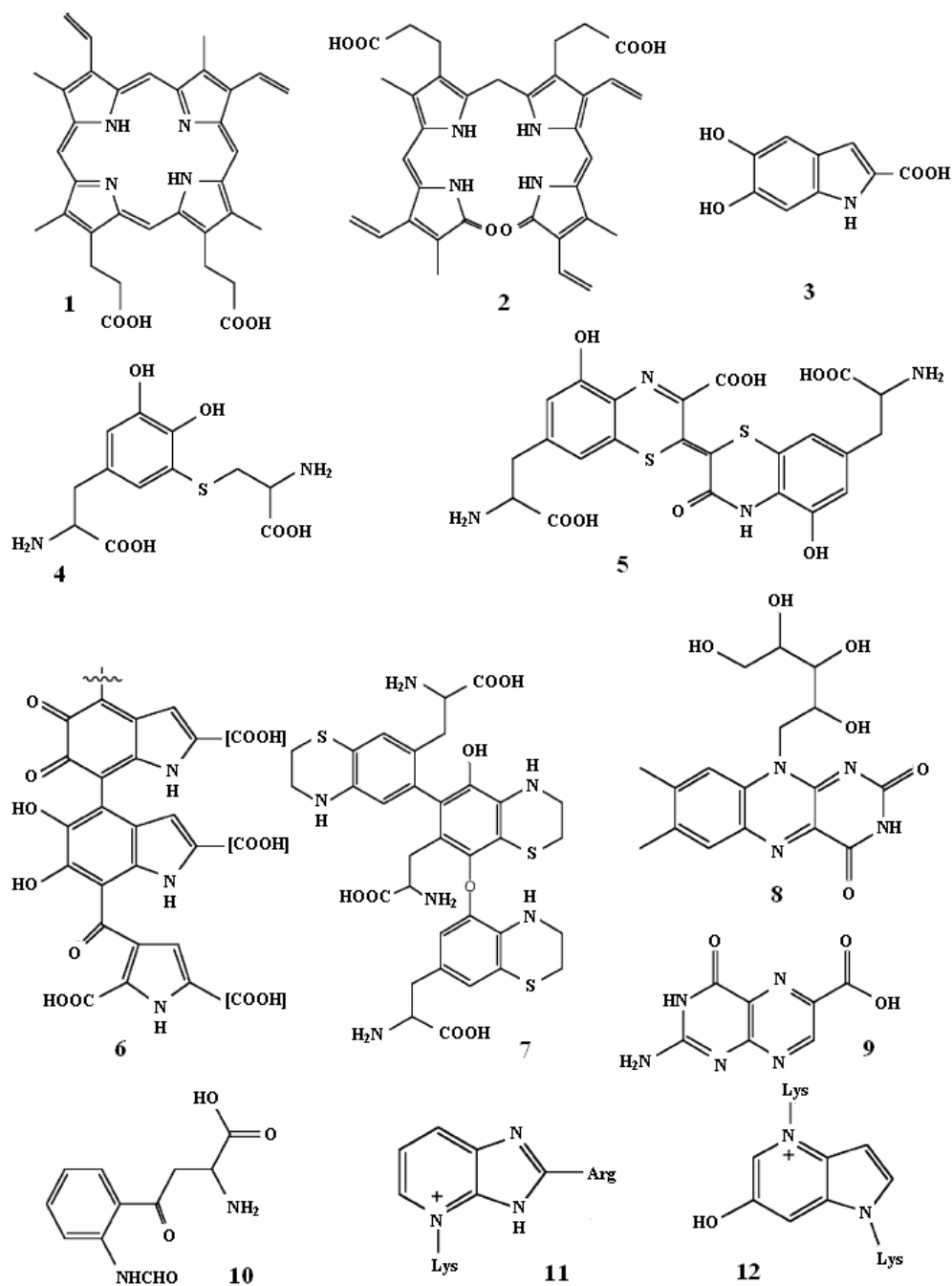


Figure 3.14 UVA-photosensitizers with possible involvement in skin photodamage (20).

- Selected examples: **1.** protoporphyrin IX, **2.** (Z,Z)-bilirubin, **3.** 5,6-dihydroxyindole-2-carboxylate, **4.** 5-S-cysteinyl dihydroxyphenylalanine, **5.** trichochrome C, **6.** eumelanin, **7.** pheomelanin, **8.** riboflavin, **9.** 6-carboxypterin, **10.** *N*⁷-formylkynurenine, **11.** pentosidine, **12.** vesperlysine A

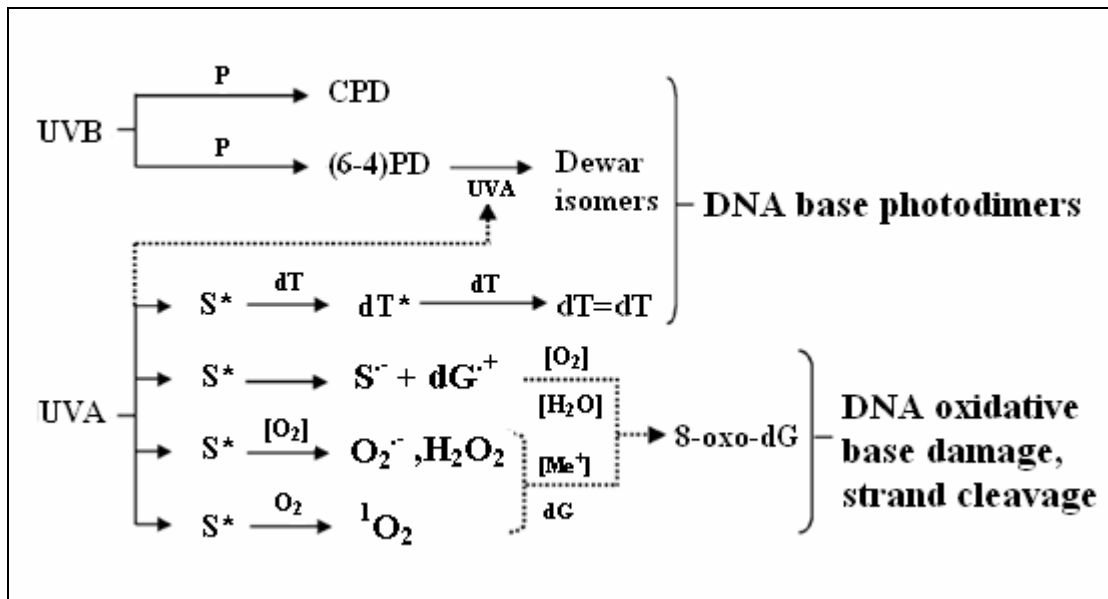


Figure 3.15 Excited states of non - DNA chromophores and UVA - induced DNA damage. Direct UVB absorption by DNA bases induces Cyclobutane pyrimidine dimers (CPD) from pyrimidine residues (P) and formation of pyrimidine (6–4) pyrimidone dimers [(6–4)PD]. UVA directly induces photoisomerization of (6–4)PDs to Dewar isomers. Photoexcited states of sensitizers (S*) are involved in UVA induced DNA base photodimerization. (dT = dT), particularly at deoxythymidine residues(dT) after triplet energy transfer from sensitizer to dT sites.Oxidative base damage can occur as a consequence of single electron transfer with formation of base radical cations (dG•+) and sensitizer radical anions(S•-). Most frequently, UVA-induced oxidative DNA damage occurs by sensitizer-induced formation of ¹O₂ and other ROS, that directly or after metal ion catalyzed decay oxidize DNA bases, especially guanine residues (dG) with formation of 8-oxo-7,8-dihydro-2-deoxyguanosine (8-oxo-dG) (20).

Both UVA and UVB induce photo-oxidative stress in skin. Structure of DNA damage including DNA base photodimers and DNA oxidative base damage as shown in figure 3.16 and 3.17. However, in contrast to the formation of mutagenic pyrimidine base photoproducts as a consequence of direct absorption of UVB by skin cell DNA, UVA results in little photoexcitation of DNA directly and generation of reactive oxygen species (ROS) seems to be the key mechanism of UVA. UVA causes DNA damage primarily by the generation of ROS that result in single-strand breaks in DNA and in DNA-protein crosslink (20).

UVA induced formation of ROS such as singlet oxygen and superoxide ion promotes biological damage in exposed tissues (79-81). Many mechanism likely contribute to ROS formation during UVR of skin, such as UV-enhanced electron leakage from the mitochondria respiratory chain and UV-induced remodeling of plasma membrane lipid rafts. However, photosensitization by endogenous non-DNA chromophores of skin appears to be a key mechanism of light-driven ROS production in human skin. Photoexcited states of endogenous skin sensitizer chromophores are rapidly emerging as key intermediates of skin photooxidative damage operating upstream of ROS formation. Exposure of human skin to solar UVA radiation induces the formation of photoexcited states (S^*) of endogenous skin chromophores (S). Some photoexcited chromophores act as toxic photosensitizers by direct chemical interaction with cellular target molecules or by interaction with oxygen leading to the formation of ROS. Energy transfer from S^* to molecular oxygen induces the formation of photoexcited oxygen (1O_2), being both a ROS and a photoexcited state species. Molecular damage inflicted by ROS and S^* on cellular targets in skin, leading to mutagenesis and altered signal transduction, contribute ultimately to photodamage of skin (Figure 3.18).

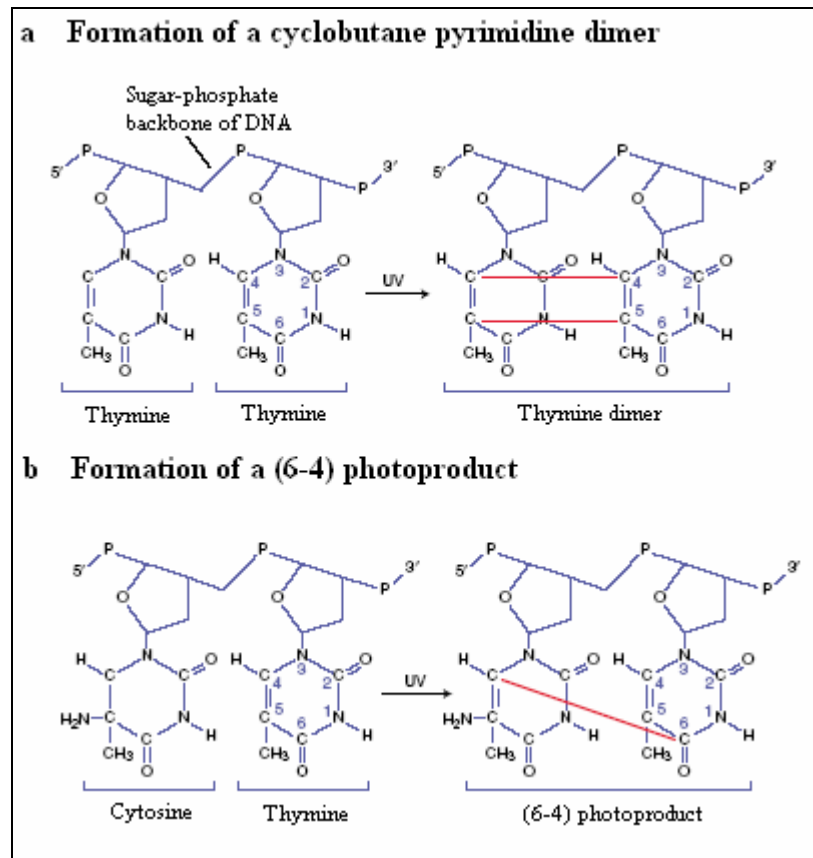


Figure 3.16 Structure of the major UV- induced DNA base photodimer (12).

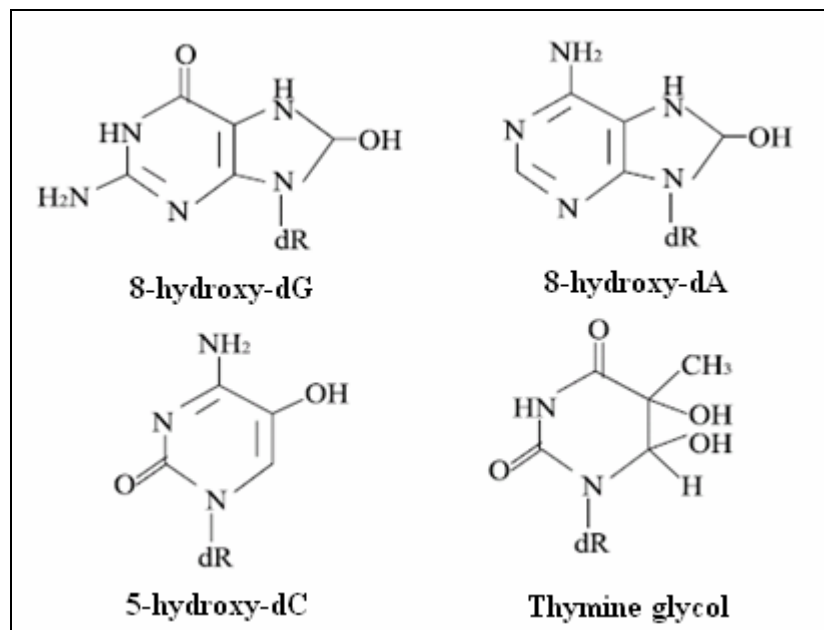


Figure 3.17 Structure of the major UV – induced oxidative DNA damage (8).

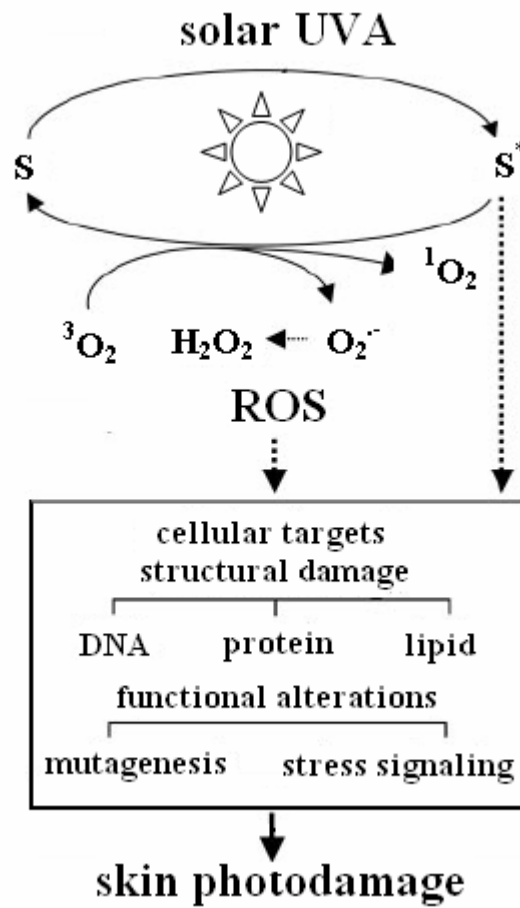


Figure 3.18 Effect of UVA induced ROS on skin photodamage (modified from ref 82).

The primary intermediates of Type II reactions, mediated by singlet oxygen, are endoperoxides generated by cycloaddition reaction of the imidazole ring with singlet oxygen. The major decomposition product of these endoperoxides is 8-oxo-dG. Modified bases, particularly 8-oxo-dG, are produced more frequently than single-strand breaks or DNA-protein crosslinks by UVA. 8-oxo-dG is a characteristic mutagenic lesion, which generates GC → TA transversion by pairing with an adenine instead of a cytosine during replication. The guanine bases are the most susceptible to oxidation via both Type I and Type II mechanisms. Adenine is the second, followed by approximately equal reactions for thymine and cytosine (17).

DNA in mitochondria may also be altered by UV-induced oxidative stress. As DNA repair is less efficient in mitochondria compared to nuclei, mutations accumulate at a relative rapid rate. Identified mutations are deletions, which can be mediated by UVA-induced $^1\text{O}_2$. These mutations may alter the cells capacity to carry out oxidative phosphorylation (17). While significant knowledge of the DNA repair mechanisms in nuclear DNA exists, much less is known about the repair systems in the mitochondria. However, compared with nuclear DNA repair mechanisms, DNA repair capacity in the mitochondrion appears to be rather low. The impaired repair capacity may lead to mitochondrial dysfunction and the onset of skin pathogenesis (22).

3.2.2 UVR and oxidative stress-induced melanogenesis

Exposure to UVR is associated with significant long-term deleterious effects such as skin cancer. A well recognized short-term consequence of UVR is increased skin pigmentation. In human, a major stimulus for facultative pigmentation is UVR. A putative melanocytic mutagen, UVR is the most potent stimulant for growth and differentiation of melanocytes. UVR induced skin pigmentation involves an increase in the melanocyte number as well as a stimulation of melanin neosynthesis and melanocyte dendricity (83). The activation and differentiation of melanocytes can be induced directly by UVR or indirectly through their interaction with surrounding UV-irradiated keratinocytes. UVR can act directly on melanocytes to induce melanogenesis. UV has been found to increase tyrosinase activities and expression. Clinical and histological changes occurring during tanning responses in humans have been extensively studied, but the mechanisms by which solar radiation stimulates melanogenesis are poorly understood.

However, if the ROS load reaches a critical concentration, subsequently overwhelming the antioxidative defense, oxidative or, if mediated by UV irradiation, photooxidative damage to all cellular components including DNA, proteins, and membranes, eventually occurs (84). There is some evidence that melanization is increased in relation to oxidative stress(85), and hyper-pigmentation seems to be associated with inflammatory responses. Localized hyper-pigmentation is a sign of abnormal pigment cell function (e.g. malignant melanoma). The fact that most melanomas exhibit a high degree of pigmentation has encouraged to the study of melanogenic pathway (86-89).

Addition, a new concept suggest that DNA damage and DNA repair play relevant roles in the UV-induced melanogenic response of melanocytes. It has also been reported that DNA damage enhance melanogenesis (90-93). Oxygen radicals also cause lipid peroxidation that can result in membrane and protein damage. Compared to UVB, UVA is about 1000 times more effective in the production of an immediate tanning effect which is caused by darkening of the melanin in the epidermis (17). However, it has been suggested that intracellular glutathione plays an important role in the inhibition of melanogenesis in cultured melanoma cells by dampening the action of tyrosinase (94).

Melanin production is the main known function of normal melanocytes of the epidermis. Identification of the genes involved in melanin formation and how they may be influenced by exposure of melanocytic cells to UVR should provide a molecular understanding of the processes of skin photoprotection. There is also the possibility that there may be protective effects or the production of mutagenic photoproducts, depending on the type of melanin produced. It has been established that melanins and their precursors have a photosensitizing action on DNA and generate radicals after exposure to UV light

While the exact cause of melasma is unknown, both genetic and environmental factors play a role in the development of this condition. Multiple factors have been postulated to involve in the etiology and pathogenesis of melasma include pregnancy, oral contraceptives, genetics, sun exposure, cosmetics and race. Of the many etiology factors associated with melasma, sunlight exposure appears to be the most significant and excessive reactive oxygen species is believed to be involved in melasma.

UVR causes the generation of ROS and therefore cell membrane lipid peroxidation and disintegrativity of the cellular functions of the skin as well as the depletion or direct damage of the antioxidant system in the skin tissue. Exterior oxidative stress and interior imbalanced production of oxidants can eventually lead to skin pathogenesis. The redox state of the skin is regulated by the balance between a variety of antioxidant enzymes, low molecular-weight antioxidants, and oxidants (19-22). It has also been reported that irradiation with UVA produces a decrease in the level of antioxidants, inactivation of antioxidant enzymes, and an increase in the marker of lipid peroxidation in skin homogenates (95). In addition to solar stimulated irradiation modulates gene expression and activities of antioxidant enzymes in cultured human dermal fibroblasts (23). The possible role of UV-produced free radicals in melanogenesis are shown in figure 3.19.

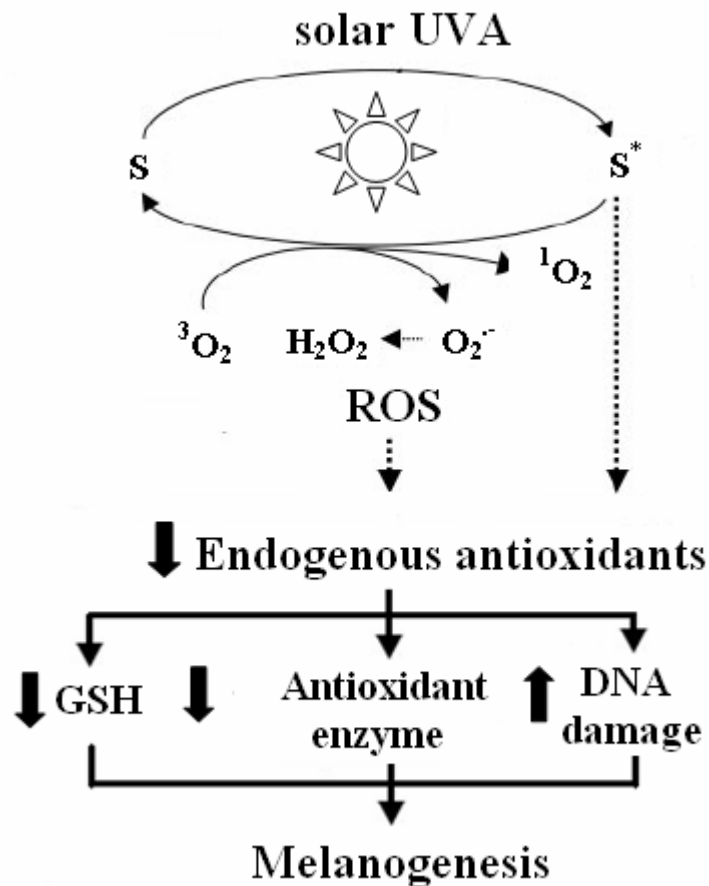


Figure 3.19 The possible role of UV-produced free radicals in melanogenesis.

3.2.3 The effect of UVR on cellular antioxidants

ROS are found in virtually all intracellular organelles or compartments as a consequence of normal metabolic activity. Each organelle or compartment has potential targets for oxidative damage, as well as mechanisms for the elimination of excess ROS accumulation. To minimize the damaging effects of ROS, aerobic organisms evolved both non-enzymatic and enzymatic antioxidant defenses are shown in figure 3.20.

Exposure to free radicals from a variety of sources has led organisms to develop a series of defence mechanisms. Defence mechanisms against free radical-induced oxidative stress involve: (i) preventative mechanisms, (ii) repair mechanisms, (iii) physical defences, and (iv) antioxidant defences. Enzymatic antioxidant defences include SOD, GPx, CAT. Non-enzymatic antioxidants are represented by ascorbic acid (Vitamin C), α -tocopherol (Vitamin E), glutathione (GSH), carotenoids, flavonoids, and other antioxidants. Under normal conditions, there is a balance between both the activities and the intracellular levels of these antioxidants. This balance is essential for the survival of organisms and their health.

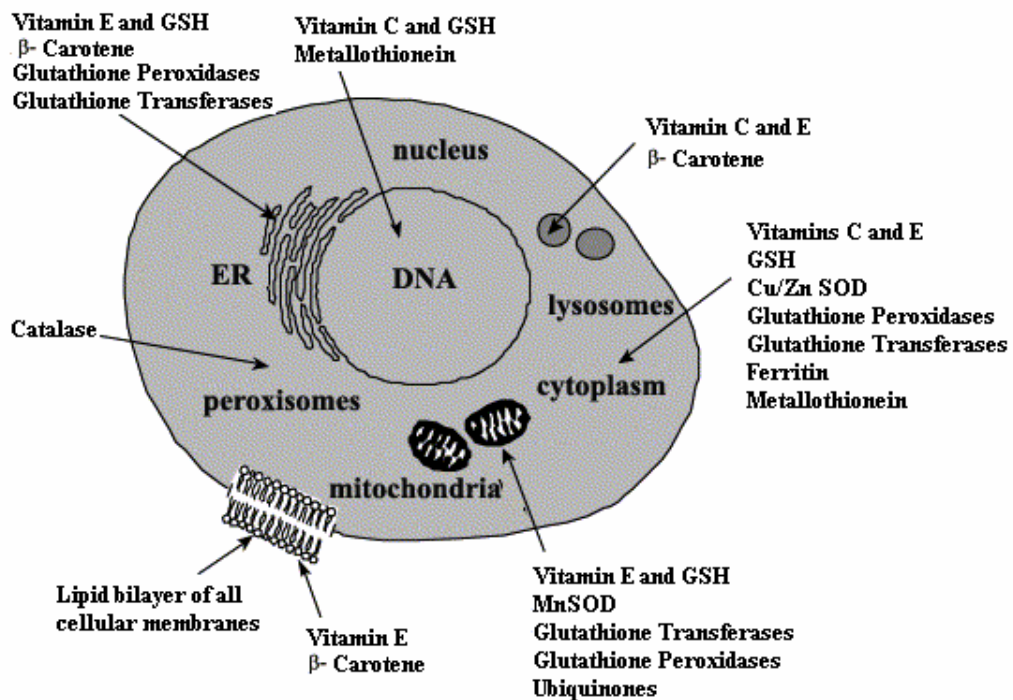


Figure 3.20 Subcellular location of endogenous antioxidants.

Various pathways for the management of oxidative stress by antioxidants are shown in figure 3.21 Reaction 1: superoxide is dismutated by the superoxide dismutase (SOD) to hydrogen peroxide. Reaction 2: hydrogen peroxide is most efficiently scavenged by the enzyme glutathione peroxidase (GPx) which requires GSH as the electron donor. Reaction 3: the oxidised glutathione (GSSG) is reduced back to GSH by the enzyme glutathione reductase (Gred) which uses NADPH as the electron donor. Reaction 4: some transition metals (e.g. Fe^{2+} , Cu^+ and others) can breakdown hydrogen peroxide to the reactive hydroxyl radical (Fenton reaction). Reaction 5: the hydroxyl radical can abstract an electron from polyunsaturated fatty acid (LH) to give rise to a carbon-centred lipid radical (L^{\bullet}). Reaction 6: the lipid radical (L^{\bullet}) can further interact with molecular oxygen to give a lipid peroxy radical (LOO^{\bullet}). Reaction 7: the lipid peroxy radical (LOO^{\bullet}) is reduced within the membrane by the reduced form of vitamin E (T-OH) resulting in the formation of a lipid hydroperoxide and a radical of Vitamin E (T-O^{\bullet}). Reaction 8: the regeneration of Vitamin E by Vitamin C: the Vitamin E radical (T-O^{\bullet}) is reduced back to Vitamin E (T-OH) by ascorbic acid (the physiological form of ascorbate is ascorbate monoanion, AscH^-) leaving behind the ascorbyl radical ($\text{Asc}^{\bullet-}$). Reaction 9: the regeneration of Vitamin E by GSH: the oxidised Vitamin E radical (T-O^{\bullet}) is reduced by GSH. Reaction 10: The oxidized glutathione (GSSG) and the ascorbyl radical ($\text{Asc}^{\bullet-}$) are reduced back to GSH and ascorbate monoanion, AscH^- , respectively, by the dihydrolipoic acid (DHLA) which is itself converted to α -lipoic acid (ALA). Reaction 11: the regeneration of DHLA from ALA using NADPH. Reaction 12: lipid hydroperoxides can break down into aldehydes, such as the strong oxidant 4-hydroxynonenal. Reaction 13: 4-hydroxynonenal is rendered into an innocuous glutathionyl adduct (GST: glutathione *S*-transferase). Reaction 14: lipid hydroperoxides are reduced to alcohols and dioxygen by GPx using GSH as the electron donor (21, 22).

The skin is constantly exposed to environmental sources of ROS such as UVR, ozone and air pollution. To protect from oxidative damage, the skin is equipped with a network of complex antioxidant defense system. The skin antioxidant system consists of a network of enzymatic and non-enzymatic antioxidants.

3.2.3.1 Non-enzymatic antioxidant

3.2.3.1.1 Glutathione (GSH)

GSH is well known as a biological antioxidant and acts as a quencher of oxidative stress in human cells. L-glutathione, synthesized by the actions of γ -glutamylcysteine synthetase and glutathione synthetase, is a biological active sulfur amino acid tripeptide of L-cysteine, L-glutamate and glycine (Figure 3.22). GSH acts as a major cellular antioxidant maintaining the intracellular redox balance. Its scavenging properties toward oxidants are due to its sulphhydryl groups.

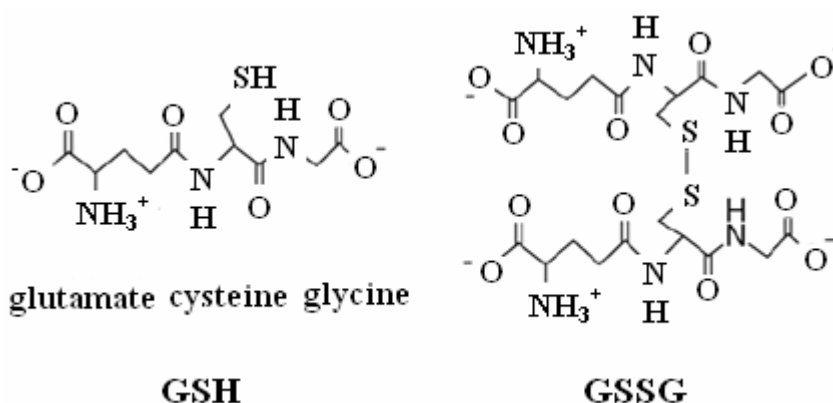


Figure 3.22 Structures of reduced (GSH) and oxidised (GSSG) glutathione (22).

Glutathione is highly abundant in the cytosol (1–11 mM), nucleus (3–15 mM), and mitochondria (5–11 mM) and is the major soluble antioxidant in these cell compartments. The reduced form of glutathione is GSH, glutathione, and the oxidised form is GSSG, glutathione disulphide. Too high a concentration of GSSG may damage many enzymes oxidatively (21, 22).

The main protective roles of glutathione against oxidative stress are: that (i) glutathione is a cofactor of several detoxifying enzymes against oxidative stress, e.g. glutathione peroxidase (GPx), glutathionetransferase and others; (ii) GSH participates in amino acid transport through the plasma membrane; (iii) GSH scavenges hydroxyl radical and singlet oxygen directly, detoxifying hydrogen peroxide and lipid peroxides by the catalytic action of glutathione peroxidase; (iv) glutathione is able to regenerate the most important antioxidants, vitamins C and E back to their active forms;

glutathione can reduce the tocopherol radical of vitamin E directly, or indirectly, via reduction of semidehydroascorbate to ascorbate as shown in figure 3.21 (22).

Glutathione depletion-induced chromosomal DNA fragmentation associated with apoptosis and necrosis. Mitochondria plays an important role in apoptosis and necrosis under GSH depletion (96-97).

GSH is also involved in regulation of melanin synthesis are shown in figure 3.23&3.24 (46). UVR reduced the levels of GSH. That leads to lessens the inhibition of tyrosinase activities and increase the synthesis of melanin. Several studies indicate that glutathione depletion may have effect to melanogenesis (86-89, 98-99).

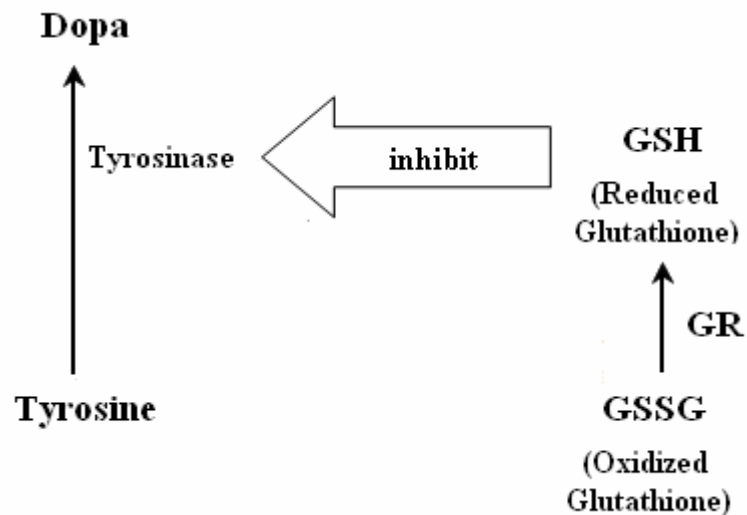


Figure 3.23 Effect of GSH on tyrosinase activities

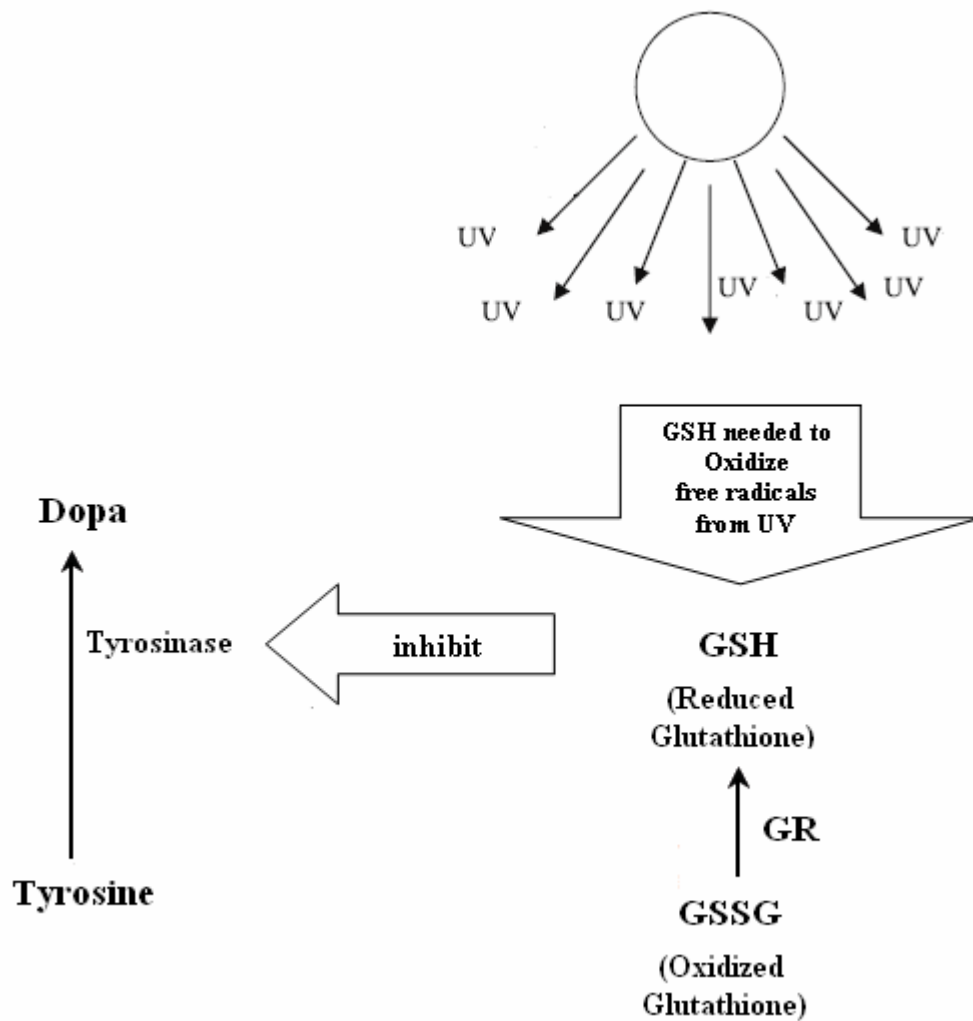


Figure 3.24 UV-tyrosinase interaction

3.2.3.1.2 Vitamin C

Vitamin C (ascorbic acid) found in cytosolic, mitochondrial and nuclear aqueous compartments is a very important free radical scavenger. It can exert a synergistic effect with other antioxidants (e.g. GSH, α -tocopherol). Vitamin C cooperates with vitamin E to regenerate α -tocopherol from α -tocopherol radicals in membranes and lipoproteins. Its concentration typically is \approx 1-10 mM intracellular fluids and \approx 20-150 μ M in human plasma.

Ascorbic acid has two ionisable hydroxyl groups and therefore is a di-acid (AscH_2). At physiological pH, 99.9% of Vitamin C is present as AscH^- , and only very small proportions as AscH_2 (0.05%) and Asc_2^- (0.004%). The antioxidant chemistry of

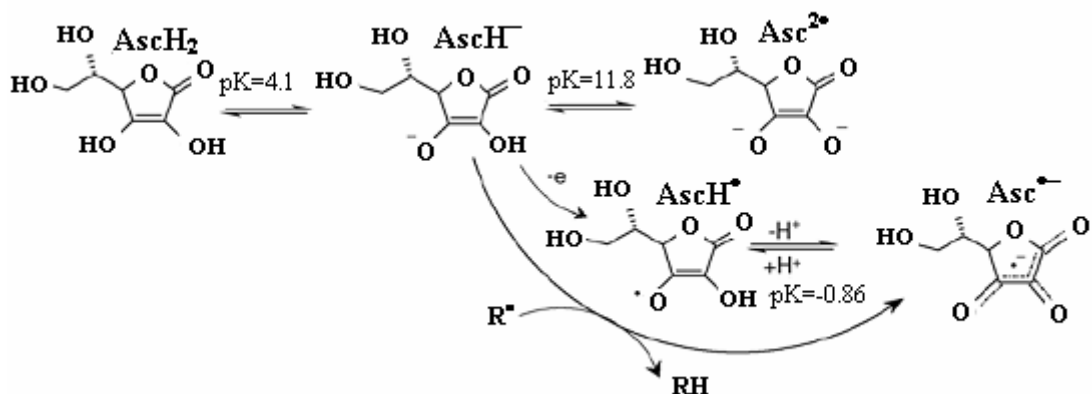


Figure 3.25 Various forms of vitamin C and its reaction with radicals(R^\bullet) (22).

vitamin C is thus the chemistry of $AscH^-$. $AscH^-$ has a unique 2,3-enediol moiety in the five member rings, which has a strong electron donating ability and reacts with radicals to produce the resonance stabilised tricarbonyl ascorbate free radical ($AscH^\bullet$) (Figure 3.25).

3.2.3.1.3 Vitamin E

Vitamin E (α -Tocopherol) is a fat-soluble vitamin that tends to concentrate in the cell membrane. α -Tocopherol, is a highly effective antioxidant found in the lipoproteins and cell membranes. Structure of α -tocopherol is shown in figure 3.26. The α -tocopherol and ascorbic acid function together in a cyclic-type of process. During the antioxidant reaction, α -tocopherol is converted to an α -tocopherol radical by the donation of a labile hydrogen to a lipid peroxy (ROO^\bullet) and alkoxy radical (RO^\bullet). α -Tocopherol scavenges lipid LOO^\bullet through a transfer of hydrogen atom to give the tocoperoxy radical (αTO^\bullet). The α -tocopherol radical can thus be reduced to the original α -tocopherol form by ascorbic acid (Figure 3.27).

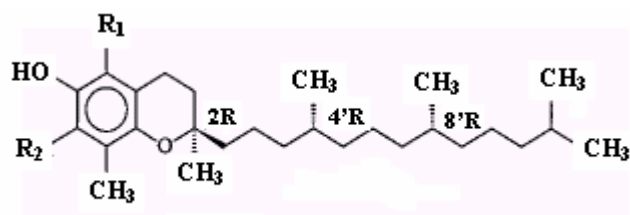


Figure 3.26 Structure of α -tocopherol. ($R_1, R_2 = CH_3$)

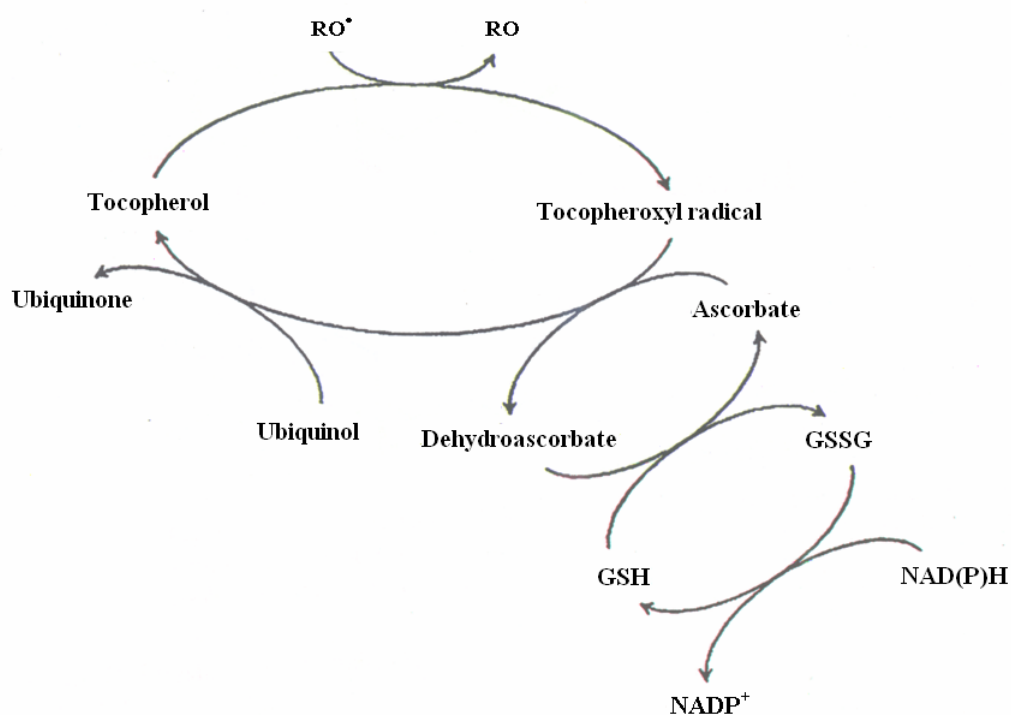


Fig 3.27 Interacting network of nonenzymic antioxidant (100).

When a ROS attacks membrane structure, it can be reduced by α -tocopherol that, in turn, can be regenerated by ubiquinol or ascorbic acid. Reduced ascorbic acid can be regenerate by GSH that, in turn, can be reduced by nicotinamide adenine dinucleotide phosphate reduced (NAD[P]H) pool. RO, reduced reactive oxygen free radical; RO^\bullet reactive oxygen free radical (100).

3.2.3.2 Enzymatic antioxidants

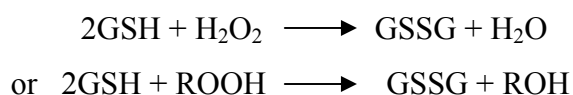
Among enzymatic antioxidants, glutathione peroxidase(GPx), catalase(CAT) and superoxide dismutase(SOD) play a pivotal role. It has been reported solar stimulated irradiation initially decrease glutathione peroxidase, superoxide dismutase and catalase (33).

3.2.3.2.1 Glutathione peroxidase (GPx) (EC 1.11.1.19)

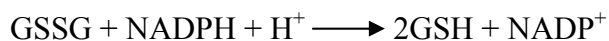
Glutathione peroxidase is a tetramer of four identical subunits, with a molecular weight of 84,000. GPx was first described as an enzyme that protects hemoglobin from oxidative degradation in red blood cells. GPx is intracellularly located in the cytosol and mitochondrial matrix. GPx is a selenoenzyme containing selenocystein amino acid residue in the active site of each monomer that participates in the actual mechanism of the enzyme. Lack of selenium leads to a deficiency in GPx activities

and consequently decreased ability to oxidize glutathione and adequately catabolize H_2O_2 (101).

GPx is capable of reducing hydrogen peroxides as well as lipid peroxide (LOOH). The glutathione cycle metabolizes H_2O_2 by using reduced glutathione as a substrate for H_2O_2 in a reaction catalyzed by GPx producing oxidized glutathione and H_2O .

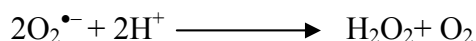


The regeneration of GSH from oxidized form, GSSG is achieved by an enzyme called glutathione reductase (GR), using NADPH as a reducing agent. Significantly, GPx competes with CAT for H_2O_2 as a substrate and is the major source of protection against low levels of oxidative stress (22).



3.2.3.2.2 Superoxide dismutase (SOD) (EC1.15.1.1)

SOD is a metalloenzyme which catalyzes the dismutation of $O_2^{\bullet-}$ to H_2O_2 and O_2 in the following reaction:



Superoxide dismutase exists in several isoforms, differing in the nature of the active metal centre and amino acid constituency, as well as their number of subunits, cofactors and other features. In humans, there are three forms of SOD identified: cytosolic Cu/Zn-SOD (16kDa), mitochondrial MnSOD (96 kDa), and extracellular-SOD (EC-SOD).

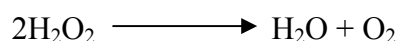
Cu, Zn-SOD is composed of two identical subunits (homodimer). Cu, Zn-SOD specifically catalyzes the dismutation of the superoxide anion to oxygen and water. Each subunit contains as the active site, a dinuclear metal cluster constituted by copper and zinc ions. Enzyme activities is relatively independent of pH in the range of 5–9.5.

Mn-SOD is a homotetramer (96 kDa) containing one manganese atom per subunit. Mn-SOD is one of the most effective antioxidant enzymes that has anti-tumour activity. A set of studies on different cell lines has confirmed that overexpression of Mn-SOD leads to tumour growth retardation.

EC-SOD is a secretory, tetrameric, copper and zinc containing glycoprotein, with a high affinity for certain glycosaminoglycans such as heparin and heparin sulphate. Its regulation in mammalian tissues occurs primarily in a manner coordinated by cytokines, rather than as a response of individual cells to oxidants (22).

3.2.3.2.3 Catalase (CAT) (EC 1.11.1.6)

CAT is a tetrameric haem-enzyme consisting of four identical tetrahedrally arranged subunits of 60 kDa and containing four ferriprotoporphyrin groups per molecule with 240 kDa molecular mass. It contains one molecule of nicotinamide adeninedinucleotide phosphate (NADPH) to help stabilize the enzyme. It catalyzes H_2O_2 to form H_2O and O_2 in the following reaction:



Catalase is located in a cell organelle called the peroxisomes, to a limited extent in mitochondria and other intracellular organelles. Catalase has one of the highest turnover rates for all enzymes: one molecule of catalase can convert ~6 million molecules of hydrogen peroxide (22). It is well documented that the catalase activities is lower after an acute dose of UVA. This has been demonstrated in mouse skin, as well as in human skin fibroblasts and keratinocytes. Chronic UVA exposure suppressed the catalase activities in hairless mouse skin, whereas acute or chronic UVB irradiation had no effect on the catalase activities in mice (25).

SOD, CAT, GPX and GSH within cells remove $\text{O}_2^{\bullet-}$ and H_2O_2 before they further react with other species or metal catalysis to generate more reactive species (Figure 3.28).

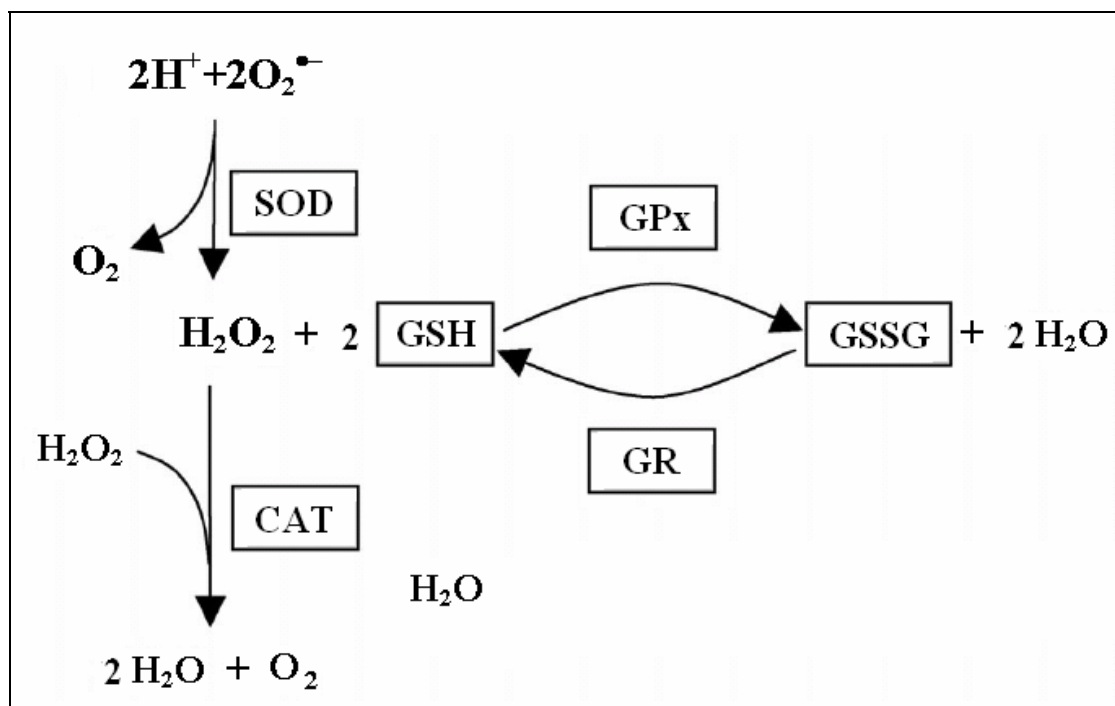


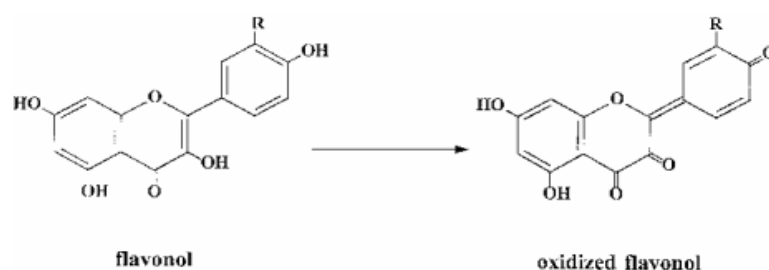
Figure 3.28 Diagrammatic representation of relationship between cellular antioxidants (102).

3.3 Antioxidants as inhibitor of UV- induced melanogenesis: the effects of Thai medicinal plants

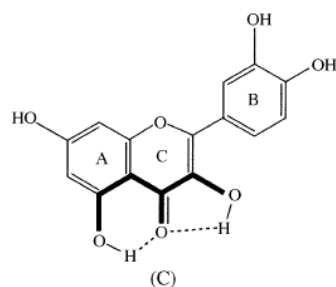
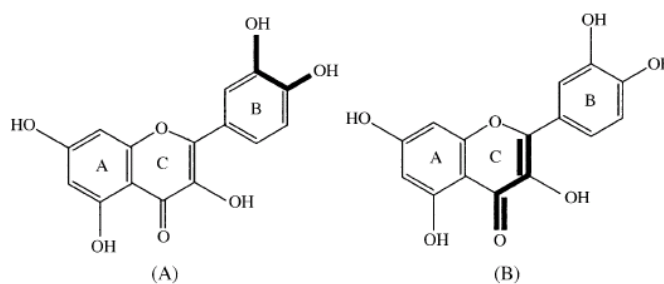
Polyphenolics are diverse group of compounds that are composed of an aromatic benzene ring substituted with hydroxyl groups, including their functional derivatives. Polyphenolics are ubiquitous secondary metabolites of the plant kingdom. The plant phenolic compounds such as flavonoids, tannins and phenolic acids, are widely distributed in various vegetables and fruits and show many physiological and pharmacological functions. Many studies have shown that natural polyphenolic compounds in plants could inhibit lipid oxidation induced by free radicals and protect photooxidation (103).

Several studies have shown the phenolic compounds to act as scavengers of $\text{O}_2^{\bullet-}$, $^1\text{O}_2$, OH^\bullet , and lipid peroxy radicals. In a structure-dependent manner, phenolic compounds are capable of scavenging ROS and chelating transition metal ions such as iron and copper, which play vital roles in the initiation of free radical reactions.

The free radical scavenging and antioxidant activities of phenolics are dependent upon the arrangement of functional groups about the nuclear structure. Both the number and configuration of H-donating hydroxyl groups are the main structural features influencing the antioxidant capacity of phenolics Figure 3.29 (a). In line with literature data the present study corroborates with the view that the following structural features of flavonoid are important for antioxidant and free radical scavenging activities: (A) an *o*-diphenolic group (in ring B), (B) a 2–3 double bond conjugated with 4-oxo function and (C) hydroxyl groups in positions 3 and 5 (Figure 3.29 (b) (103).



(a)



(b)

Figure 3.29 (a) and (b) Structural groups and antioxidant capacity.

In recent years naturally occurring herbal compounds such as phenolic acids, flavonoids, and high molecular weight polyphenols have gained considerable attention as beneficial protective agents of skin damage induced by UV irradiation (Table 3.4).

Table 3.4 Evidence of phenolic compounds as protective agents against skin damage induced by UVR.

Phenolic compounds	Action	Reference
Curcuminoids	Protective effect on the cleavage of DNA by hydroxyl radicals	Ahsan H. <i>et al.</i> , (1999) ²⁹
Tannins	Protect against free radical damage caused by exposure to UV light by reducing H ₂ O ₂ production	Gali-Muhtasib HU, <i>et al.</i> , (1999) ³⁰
Caffeic and ferulic acids	Inhibit propagation of the lipid peroxidative chain reaction and to react with nitrogen oxides	Saija A. <i>et al.</i> , (1999) ³¹
Green tea polyphenol (-)-epigallocatechin-3-gallate	Restore the UV-induced decrease in GSH level and afforded protection to the antioxidant enzyme GPX	Katiyar S.K. <i>et al.</i> , (2001) ³²
Quercetin	Protect skin antioxidant systems, GPx, GR, CAT and SOD activities, against UVA irradiating damage	Inal M.E. <i>et al.</i> , (2001) ³³
<i>Capparis spinosa</i>	Reduce UVB-induced skin erythema	Bonina F <i>et al.</i> , (2002) ³⁴
Ginkgo biloba	Stop lipid peroxidation by quenching the peroxy radical	Ozkur MK, <i>et al.</i> , (2002) ³⁵
Antioxidant complex containing carotenoid: (lycopene, β carotene, α-tocopherol)	Improve any parameters of the epidermal defense against UV-induced cell damage	Cesarini J.P, <i>et al.</i> , (2003) ³⁶

Table 3.4 Evidence of phenolic compounds as protective agents against skin damage induced by UVR. (Continued)

Phenolic compounds	Action	Reference
(+)-Catechin	Protect epidermal cells against UV-induced damage by modulating antioxidant enzyme activities and prevent keratinocyte apoptosis.	Jeon S.E <i>et al.</i> , (2003) ³⁷
Silibinin	Protect ultraviolet apoptosis in HaCaT human immortalized keratinocytes.	Dhanalakshmi I S, <i>et al.</i> , (2004) ³⁸
Grape seed proanthocyanidins	Inhibit UV-radiation-induced oxidative stress and activation of MAPK and NF- κ B signaling in human epidermal keratinocytes.	Mantenea S.K. and Katiyar S.K., (2006) ³⁹
Genistin	Inhibit UV-light-induced plasmid DNA damage and cell growth in human melanoma cells.	Russo A, <i>et al.</i> , (2006) ⁴⁰
<i>Prunella vulgaris</i> and rosmarinic acid	Exhibit ability to reduce the UVA-caused decrease in a cell viability and suppress UVA-induced ROS production.	Psotova, J., <i>et al.</i> , (2006) ⁴¹
Buckwheat herb	Inhibit of the photosensitized lipid peroxidation of linolic acid.	Hinneburg, I., <i>et al.</i> , (2006) ⁴²
Delphinidin	Protects human HaCaT keratinocytes and mouse skin against UVB-mediated oxidative stress and apoptosis.	Afaq, F. <i>et al.</i> , (2007) ⁴³
Eriodictyol	Anti-apoptotic and anti-oxidant effect on UV-induced apoptosis in keratinocytes.	Lee, E. R. <i>et al.</i> , (2007) ⁴⁴
Apigenin	Prevents UVB-induced cyclooxygenase 2 expression: coupled mRNA stabilization and translational inhibition.	Tong, X. <i>et al.</i> , (2007) ⁴⁵

(a) *Alpinia galanga*(b) *Curcuma aromatica***Figure 3.30** (a) and (b) Pictures of *Alpinia galanga* and *Curcuma aromatica*.

Due to biochemical processes occurring in the body, it is normal for free radicals to be present in the body at all times, however when the free radicals increase to an abnormal level the danger begins. Antioxidants are substances with free radical chain reaction breaking properties. Among the numerous antioxidants available, flavonoids are naturally occurring phenolic compounds in plants. The antioxidative effect of flavonoids had long been recognized. They are known to inhibit lipid peroxidation, to scavenge free radicals and active oxygen, to chelate iron ions and to inactivate lipoxygenase. The extracts from various species of Zingiberaceae family showed moderate to good antioxidant properties. It has been interested in Zingiberaceae family species as these could be new source of natural antioxidants because most of these wild rhizomes are used as traditional medicines and spices by the local people. It is known that several species from Zingiberaceae displayed strong antioxidant properties (46-47).

The Zingiberaceae is among the plant families widely distributed throughout the tropics in Southeast Asia. *Alpinia galanga* and *Curcuma aromatica*, in particular, have traditionally been used in skin problems. Screening of rhizomes extracts of Zingiberaceae extracts showed their strong antioxidant activities comparable with or higher than that of α -tocopherol (47). By using sulfur free radical reactivity with curcumin as a reference indicator, the addition of the supernatant from crude extracts to the reaction mixture significantly decreased the depletion of curcumin (104). Hence,

antioxidant properties as the biological activities of potential medicinal plants in the inhibition of oxidative stress-induced skin damage should be investigated.

Galangal, also called galanga, galingale, galangale, and calangall, is a pungent aromatic rhizome produced in eastern Asia. There are two different species of galangal: one is the so-called lesser or smaller galangal (*Alpinia officinarum* Hance Farw.), a perennial herb native to China, with pyramidal racemes of rose-veined white flowers; the other is the so-called greater galangal [*Alpinia galanga* (L.) Swartz. or *Languas galanga* (L.) Stuntz], a stemless perennial herb of southeastern Asia with fragrant short-lived, largely white flowers (105).

Alpinia galanga (*A. galanga*) is widely cultivated in China, India, and Southeast Asian countries such as Thailand, Indonesia, and the Philippines. The rhizomes of this plant are extensively used as spice or ginger substitutes for flavoring foods, and also used in traditional medicine for several purposes, such as stomachic, carminative, antifatulent, antifungal, gastroprotective, antiallergic and anti-itching (105-107). Phenylpropanoids are major components in *A. galanga*. Phenylpropanoids including 1'S-1' Acetoxychavicol acetate, 1'S-1'-acetoxyeugenol acetate, 1'S-1'-hydroxychavicol acetate, *trans-p*-hydroxycinnamaldehyde, *trans-p*-coumaryl alcohol, *trans-p*-hydroxycinnamyl acetate, and *trans-p*-coumaryl diacetate were found from the rhizomes of *A. galanga* SWARTZ (106).

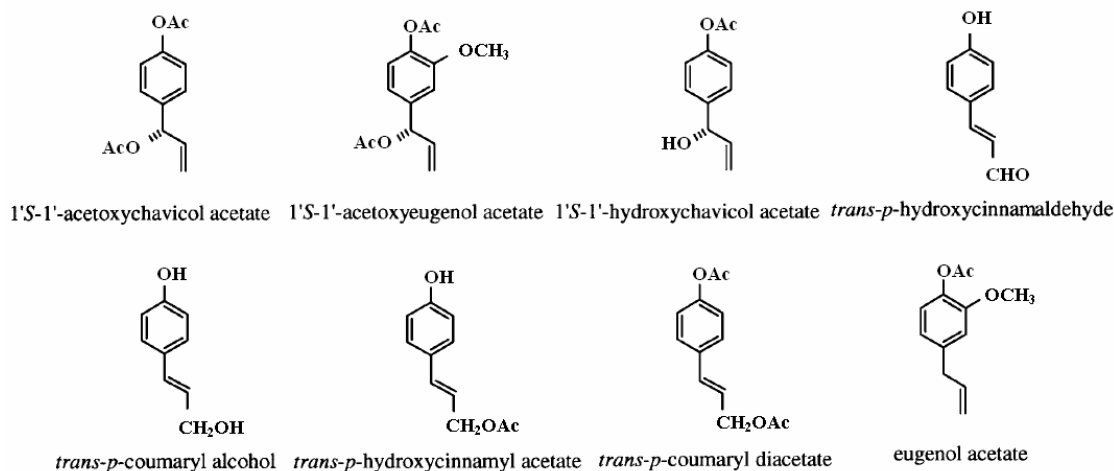


Figure 3.31 Chemical structures of phenylpropanoids from *A. galanga* (106).

The rhizome of *A. galanga* contains up to 1.5% essential oil (1, 8 cineol, α -pinene, eugenol, camphor, methyl cinnamate and sesquiterpenes). In dried galangal, the essential oil has quantitatively different composition from the fresh one. Where as α -pinene, 1, 8-cineol, α -bergamotene, trans- β -farnesene and β -bisabolene seem to contribute to the taste of the fresh galangal equally, the dried rhizome shows galangal variation in aroma components (cineol and farnesene, mostly). The resin causing the pungent taste consists of several diarylheptanoids and phenylalkanones. Furthermore, the rhizome has starch in high contents (108-111).

Extracts of the rhizome of *A. galanga* have been assessed for free radical scavenging activity against 1,1-diphenyl-2-picrylhydrazyl (DPPH) radical and cytotoxic activity against MCF-7 (breast adenocarcinoma) and LS174T (colon adenocarcinoma) cell lines (112). In raw beef, galangal extract at 10% (w/w) was as effective as α -tocopherol at 0.10% (w/w) and butylated hydroxytoluene (BHT) at 0.02% (w/w) in inhibiting/minimising lipid oxidation. However, cooked beef treated with galangal extract or antioxidants had lower a values and total microbial counts than the control. Thus galangal extract may be a possible natural antioxidant source for meat and meat products (113). In minced beef, added galangal extract improved oxidative stability. Galangal extract at higher concentrations of 0.05% and 0.10% (w/w) were also found to extend the shelf-life of minced beef. Addition of α -tocopherol (0.02%, w/w) to galangal extract (0.05%, w/w) were observed to increase the oxidative but not the microbial stability of minced beef during the storage of 7 days (114). Oxygen-derived free radicals and lipid peroxidation are associated with gastrointestinal lesions, and antioxidants prevent the lesions by various ulcerogens. *A. galanga* showed significant increase in the GSH level in the rats gastric mucosa (106). The free radical scavenging and tyrosinase inhibition activities of Lesser Galanga was investigated. Lesser Galanga gave the free radical scavenging activity with % the residual rate of absorbance (%RRA) of about 76.70% comparable to α -tocopherol and ascorbic acid which were 2.7% and 18% respectively and the tyrosinase inhibition activities of about 44.8% of the control while kojic acid was 100% of the control (115).

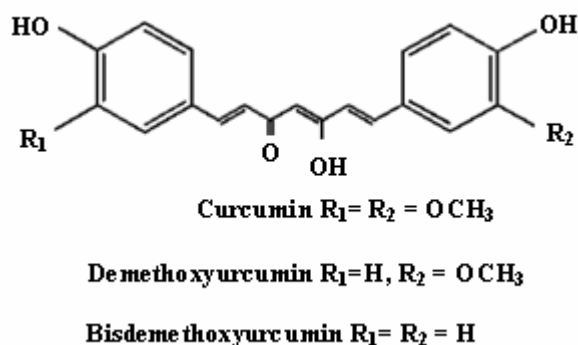


Figure 3.32 Chemical structures of curcuminoids (125).

Acute (24 h) and chronic (90 days) oral toxicity studies on the ethanolic extracts of the rhizomes of *A. galanga* was carried out in mice. Acute dosages were 0.5, 1.0, and 3 g/kg body weight while the chronic dosage was 100 mg/kg/day. All external morphological, hematological, and spermatogenic changes, in addition to body weight and vital organ weights were recorded. During this investigation no significant mortality as compared to the controls was observed. Hematological studies revealed a significant rise in the RBC level, but a significant fall in the WBC and RBC levels of *A. galanga* treated animals (116).

Several frequently used herbal drugs are derived from the *Curcuma* species of the family, Zingiberaceae. *Curcuma* species are medicinal herbs with various pharmacological activities including antioxidative, anticarcinogenic, antiinflammatory and hypocholesterolemic activities (117-124). They have a characteristic yellow color and contain curcuminoids which are natural antioxidants. *Curcuma* species has a characteristic dark yellow color, and it has been found to be a rich source of phenolic compounds. Curcuminoids contain three major yellow pigments; curcumin (diferuloyl methane), demethoxycurcumin (p-hydroxycinnamoyl, feruloylmethane), and bisdemethoxycurcumin (di-p-hydroxycinnamoylmethane). Chemical structures of curcuminoids are shown in figure 3.32. Curcumin, which is the major constituent of curcuminoids, is reported to be a natural antioxidant with inhibition effects for cytotoxicity and cancer. Curcumin has been reported to scavenge superoxide anions, nitric oxide radical and hydroxyl radical (117-124). Curcumin inhibit hydrogen

peroxide induced cell damage in NG108-15 cells (118). *Curcuma longa* has been intensively studied. Pharmacological studies of other *Curcuma* species were very few, because botanical origins of *Curcuma* could not be easily identified due to similarity of morphology, and variety of naming derived from used parts and producing areas (116).

The rhizomes and roots of *Curcuma* (*C. aromatica*) are commonly used as traditional drugs. The rhizome of *Curcuma aromatica* Salisb (*C. aromatica*) has no value as a spice but it used in cosmetic formulation and medicines. It is used as a stomachic carminative, choloretic, analgesic, sedative, hepatitis, menstrual disorder, epilepsy, skin disorder and also used for treatment of cervical cancer. This plant is well known as the source of monoterpenoids, sesquiterpenoids and curcuminoids that have been reported to possess antimicrobial, antifungal, antioxidant and antitumor activities (116-122). *C. aromatica* showed regulatory effect on nitric oxide (NO) levels using sodium nitroprusside as a NO donor by exhibiting a dose-dependent NO scavenging activity *in vitro* (126). Additionally, curcuminoids found in curcuma species were more active than α -tocopherol (Vitamin E) as potent inhibitors of lipid peroxidation (127). Antioxidant activities of demethoxycurcumin and bisdemethoxycurcumin have been reported in the model systems of hydroxyl radical induced DNA damage, DPPH radical scavenging activity and recently in lipid peroxidation (125). Antioxidant property of curcumin acts against the free radicals and thereby reducing the cancer incidences. Curcumin activity is comparable to ascorbic acid, α -tocopherol, and SOD. Very small concentration (100 mg/ml) of curcumin was found to be as effective as butylated hydroxyl anisole (BHA), a potent antioxidant. Antioxidant studies performed with curcuminoids and tetrahydrocurcuminoids showed that they prevent free radical formation and scavenge free radicals already presented in biological system (115). The ethanol-extracted *C. aromatica* did not cause dermal irritation when applied to human skin. No adverse effects on human volunteers were observed 2 months after application (128).

As mentioned above, many of the most popular depigmentating agents in use today exhibit toxicity to melanocytes and are known to produce adverse side effects. The ideal treatment for melasma should allow depigmentation without bleaching of normal skin as well as should not be sensitizing or irritating and be cosmetically acceptable. Hence *A. galanga* and *C. aromatica* were interested in studying the antioxidant effects in inhibition melanogenesis using melanoma cell culture model.

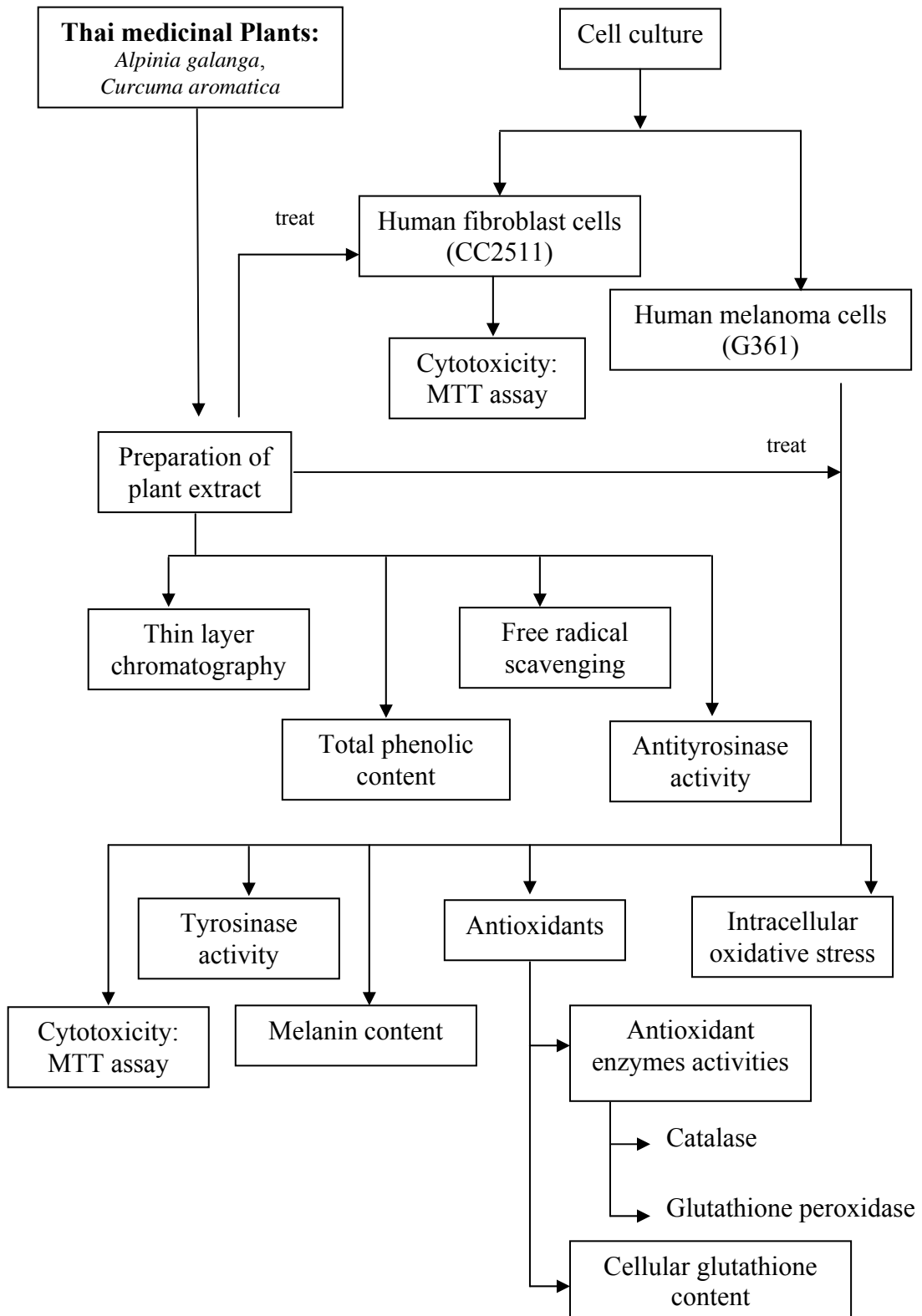


Figure 3.33 Strategy planned for a study on the antioxidant effects of *Alpinia galanga* and *Curcuma aromatica* rhizome extracts on the inhibition of UV-induced cellular melanogenesis.

CHAPTER IV

MATERIALS AND METHODS

4.1 Chemicals, Materials and Instruments

Chemicals and reagents used were of the highest quality available and were purchased from Sigma, Aldrich (USA and Germany), Bio-rad (Germany), BDH Chemical Company (Gillingham, Dorset, UK) or Merck (Darmstadt, Germany) with the following exceptions; streptomycin from General drug house (Thailand), Trypsin 250 from Difco Laboratories and Tyrosinase from Fluka (Germany).

G361 cell line from American Type Culture Collection (ATCC, Rockville, Md, USA) and CC2511 were a kind gift from Assoc. Prof. Parkpoom Tengamnuay, Faculty of Pharmaceutical Sciences, Chulalongkorn University. Dulbecco's modified Eagle medium (DMEM) was obtained from Gibco (USA) or Invitrogen (NY, USA).

Tissue culture plates and flasks were from Corning (USA).

Reagents and materials used with thin layer chromatography (TLC) analysis were from Merck (Darmstadt, Germany). TLC plate imaging to identify the fingerprints of the herbal extracts were performed by TLC combined with video scanning TLC [Camag Video Documentation System connected with Reprostar 3 transilluminator cabinet and used under Video Store 2 (version 2.23) and Video Scan TLC/HPTLC evaluation software (version 1.01.00) (Camag, Muttentz, Switzerland)].

Spectrofluorometric measurements were carried out using a spectrofluorometer Synergy TM from Biotek (Vermont, USA).

4.1.1 Chemicals

- Albumin from bovine serum (BSA) (Sigma, USA)
- Bio-Rad protein assay (Bio-Rad, Germany)
- Catalase from bovine liver (Sigma, USA)
- Diethylenetriaminepentaacetic acid
[[$(\text{HOOCCH}_2)_2\text{NCH}_2\text{CH}_2$] $_2\text{NCH}_2\text{COOH}$], MW 393.35 (Sigma Aldrich, Germany)
- 3,4-Dihydroxy-L-phenylalanine [$\text{C}_9\text{H}_{11}\text{NO}_4$], MW 197.19 (Sigma, USA)
- Diphenylboric acid 2-aminoethyl ester [$(\text{C}_6\text{H}_5)_2\text{BOCH}_2\text{CH}_2\text{NH}_2$], MW 225.09 (Sigma, USA)
- 2,2-Diphenyl-1-(2,4,6-trinitrophenyl)hydrazyl(DPPH) [$\text{C}_{18}\text{H}_{12}\text{N}_5\text{O}_6$] MW 394.32,(Sigma, USA)
- Dimethyl sulfoxide [$(\text{CH}_3)_2\text{SO}$], MW 78.13 (Sigma, USA)
- Dulbecco's modified Eagle's media (DMEM) (GIBCO, USA)
- Ethylenediaminetetraacetic acid disodium salt dihydrate [$\text{C}_{10}\text{H}_{14}\text{N}_2\text{Na}_2\text{O}_8 \cdot 2\text{H}_2\text{O}$], MW 372.24 (Sigma Aldrich, Germany)
- Fast Blue B Salt [$\text{C}_{14}\text{H}_{12}\text{N}_4\text{O}_2\text{Cl}_2 \cdot \text{ZnCl}_2$], MW 475.47 (Sigma-Aldrich, Germany)
- Formaldehyde solution [HCHO], MW 30.03 (Sigma, USA)
- Glutathione Peroxidase from bovine erythrocytes (Sigma, USA)
- L-Glutathione reduced
[$\text{H}_2\text{NCH}(\text{CO}_2\text{H})\text{CH}_2\text{CH}_2\text{CONHCH}(\text{CH}_2\text{SH})\text{CONHCH}_2\text{CO}_2\text{H}$], MW 307.32 (Sigma-Aldrich, Germany)
- Glutathione reductase (Sigma, USA)
- Hydrochloric acid [HCl], MW 36.46 (Sigma, USA)
- Hydrogen peroxide 30 % (w/w) in H_2O [H_2O_2], MW 34.01 (Merck, Germany)
- Hypoxanthine [$\text{C}_5\text{H}_4\text{N}_4\text{O}$], MW 136.11(Sigma, USA)
- Leupeptin (Sigma, USA)
- Melanin (Sigma, USA)

- Methanol [CH₃OH], MW 32.04, (Merck, Germany)
- β-Nicotinamide adenine dinucleotide phosphate, reduced form
MW 833.4 (Sigma, USA)
- Nitrotetrazolium Blue chloride [C₄₀H₃₀N₁₀O₆ · 2Cl], MW 817.64
(Sigma-Aldrich, Germany)
- Penicillin G (General drug house, Thailand)
- Pepstatin A (Isovaleryl-Val-Val-Sta-Ala-Sta) [C₃₄H₆₃N₅O₉], MW
685.9 (Sigma, USA)
- PMSF (phenylmethylsulfonyl fluoride) [C₇H₇FO₂S], MW 174.2
(Sigma, USA)
- Phthaldialdehyde [C₈H₆O₂], MW 134.13 (Sigma-Aldrich, Germany)
- Potassium hydroxide [KOH], MW 56.11 (BDH,UK)
- Potassium periodate [KIO₄], MW 230 (Sigma-Aldrich, Germany)
- Potassium phosphate monobasic [KH₂PO₄], MW 136.09 (Sigma-
Aldrich, Germany)
- Purpald [C₂H₆N₆S], MW 146.17 (Aldrich, USA)
- Sodium hydroxide [NaOH], MW 40.00 (Merck, Germany)
- Streptomycin (General drug house, Thailand)
- Superoxide Dismutase From Bovine Liver MW 32,000 (Sigma, USA)
- Tert-butyl hydroperoxide solution [(CH₃)₃COOH], MW 90.12(Aldrich, USA)
- Trichloroacetic acid [Cl₃CCOOH], MW 163.39(Sigma-Aldrich,
Germany)
- Triton X-100 (t-octylphenoxy polyethoxyethanol) (Sigma, USA)
- TRIS hydrochloride [NH₂C(CH₂OH)₃ · HCl], MW 157.60 (Sigma,
USA)
- Trypsin 250 (Difco Laboratories)
- Tyrosinase (Fluka, Germany)
- Xanthine Oxidase from microbial source (Sigma, USA)

4.1.2 Materials

- Autopipet matrix cellmateII (Matrix Technologies corporation, USA)
- 25-cm² cell culture flasks (Corning, USA)
- 75-cm² cell culture flasks (Corning, USA)
- 24-well cell culture cluster; Flat bottom (Corning, USA)
- 96 well cell culture cluster; Flat bottom (Corning, USA)
- Centrifuge tube 50 ml (Corning, USA)
- Disposable syringe (Nipro, Thailand)
- Hemacytometer (Reichert scientific instruments, USA)
- Hypodermic needle (Nipro, Thailand)
- Syringe filter; Minisart (Sartorius, Germany)
- TLC aluminium sheets; Silica gel 60F₂₅₄ (Merck, Germany)
- Whatman filter paper (Whatman, England)

4.1.3 Instruments

- CAMAG Reprostar3 (Camag, Switzerland)
- CO₂ incubator; MCO-20AIC (Sunyo, Japan)
- Dermalight Ultra1 (Hoenle, Germany)
- Inverted Microscope CKX41SF (Olympus Optical Co. Ltd., Japan)
- Linomat5 (Camag, Switzerland)
- Lyovac lyophilizer (Cologne, Germany)
- Refrigerated centrifuge BR3.11 (Jouan, USA)
- Rotary evaporator; Rotavapor R110 (Buchi, Switzerland)
- Spectrofluorometer; Synergy HT (Bio-Tek®, USA)
- Thermo shaker (Biosan, Latvia)
- TLC plate heater III (Camag, Switzerland)
- TLC tank (Camag, Switzerland)
- Vortex-2 genie (Scientific industries, USA)

4.2 Methods

4.2.1. Quantitative study of plant extracts

4.2.1.1 Preparation of the plant extracts

The dried rhizomes piece of *A. galanga* and *C. aromatica* were obtained from Ms. Chaisri and Dr. Laohapand, Siriraj Ayurved Applied Thai Traditional Medicine Clinic, Center of Applied Thai Traditional Medicine, Siriraj Hospital Medical School, Mahidol University. The dried rhizome pieces were extracted as previously described. The dried rhizome pieces were macerated in 90% ethanol at room temperature for 72 hours. Each extract was passed through Whatman filter paper 110 mm (Whatman, England). The filtrate obtained was concentrated by evaporation under reduced pressure in rotatory evaporator under reduced pressure (Rotavapor R110, BUCHI, Switzerland) and then lyophilized (Lyovac lyofilizer, Cologne, Germany) to dryness for further analysis. Extracts isolated were kept at -80°C until testing.

4.2.1.2 Thin layer chromatography (TLC) analysis

TLC combined with video scanning was performed to analyse herbal extracts as described (Lee et al., 2005). Stock solutions containing 100 mg/ml of each extract and 10 mg/ml of curcuminoids were prepared in 80% ethanol. A drop (1 μl) of each extract and phenolic compounds was loaded on TLC plate and developed in a solvent system to the distance of 90 mm (TLC; silica gel 60 F254, Merck)

Solvent systems used were as the followings:

System 1 *chloroform: ethanol: glacial acetic acid* = 47.5 : 2.5 : 0.5

System 2 *toluene : ethyl acetate* = 46.5 :3.5

Absorbent: TLC silica gel plate (60 F 254, 10 cm x 10 cm)

Spray reagent: Fast blue salt reagent (FBS)

0.5 g fast blue salt B is dissolved in 100 ml water. The plate is sprayed with 6 – 8 ml, dried and inspected in visible light.

To confirm the presence of phenolic, TLC was additionally sprayed with specific reagents (FBS). TLC plate imaging to identify the fingerprints of the herbal extracts were perform by TLC combined with video scanning TLC [Camag Video Documentation System connected with Reprostar 3 transilluminator cabinet and used under Video Store 2 (version 2.23) and Video Scan TLC/HPTLC evaluation software

(version 1.01.00) (Camag, Switzerland)]. The retardation factor (R_f value) and relative retardation factor (rRF value) are used to characterize and compare components of each herbal extracts.

$$\text{Retardation factor (R}_f \text{ value)} = \frac{\text{distance from origin to component spot}}{\text{distance from origin to solvent front}}$$

$$\text{Relative retardation factor (rRF value)} = \frac{\text{R}_f \text{ of component}}{\text{R}_f \text{ of marker}}$$

Following the guidelines for bioequivalence (BE) assessment, coding that a standard BE range for basic pharmacokinetic parameters of 0.8–1.25 (80%-125%) and the percent coefficients of variation (%CV) of less than 15% for the assay precision have been generally accepted. This study applied such guidelines using rRf values as a parameter for qualitative analysis of the plant extracts(129,130).

4.2.2. Determination of total phenolics

The content of total phenolics was determined by using the Folin-Ciocalteu method. Under alkaline conditions, phenolics are oxidised by the Folin-Ciocalteu reagent containing a mixture of phosphotungstic acid (H₃PW₁₂O₄₀) and phosphomolybdic acid (H₃PMO₁₂O₄₀). The reagent becomes partly reduced producing the complex molybden-tungstic blue.

The amount of total phenolics in extracts was determined according to the Folin-Ciocalteu procedure (Singleton and Rossi, 1965). Samples 200μl were added into test tubes; 1.0 mL of Folin-Ciocalteu's reagent and 0.8 mL of sodium carbonate (7.5%) were added. The tubes were mixed and incubate at room temperature allowed to stand for 30 min. Absorption at 765 nm was measured by spectrophotometer. Determination of total phenolic using gallic acid as reference phenolic.

4.2.3 Free radical scavenging activity assay

In detecting free radical scavenging activities of the phenolic compounds of the plant extracts, DPPH (1,1-diphenyl-2-picrylhydrazyl) is a stable free radical with violet color. If DPPH radical are scavenged, violet color will be changed to yellow. This assay uses this character to study free radical scavenging activity of herbs tested.

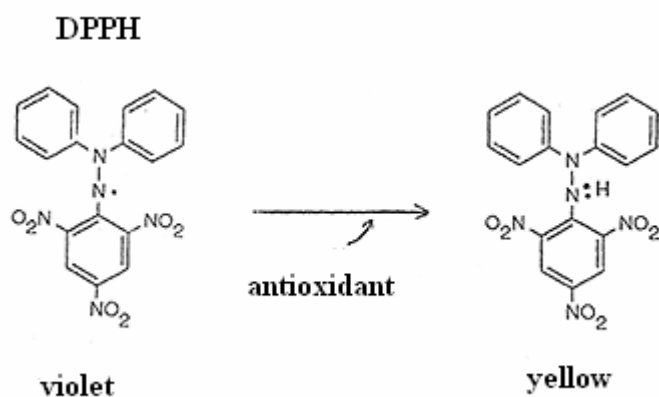


Figure 4.1 DPPH scavenging

Free radical scavenging activity of the herbal extracts were studied by DPPH radical scavenging activity. Samples in ethanol (100 μ l) was added to a solution of DPPH radical in ethanol (0.2mM, 100 μ l) in a 96 well plate. The absorbance at 520 nm was determined at 0 and 30 min.

The scavenging activity of samples was estimated by measuring the absorption of the mixture, which reflects the amount of DPPH radical remaining in the solution. The scavenging activity was calculated by comparing the absorbance of each sample with that of a blank containing only DPPH and the solvent. L-ascorbic acid was used as a reference.

$$\% \text{ scavenging activity} = \frac{(A_0 - A_{30})}{A_C} \times 100\%$$

A_C = absorbance of control at 0 min

A_0 = absorbance of sample at 0 min

A_{30} = absorbance of sample at 30 min

4.2.4 Antityrosinase activity

Table 4.1 Preparation of reagents for antityrosinase activity assay

	20 mM phosphate buffer	Tyrosinase solution (480 units/ml)	Test sample	Methanol
A (control)	120 µl	40 µl	-	20 µl
B (blank of control)	160 µl	-	-	20 µl
C (test sample)	120 µl	40 µl	20 µl	-
D (blank of test sample)	160 µl	-	20 µl	-

Reagents for antityrosinase activity assay were prepared using 20mM phosphate buffer pH 6.8 (NaH₂PO₄.H₂O 0.2839 g and Na₂HPO₄ 0.1320 g in HPLC-grade water 200 ml adjust to pH 6.8), 0.85 mM L-DOPA in 20mM phosphate buffer, tyrosinase solution 480 units/ml in 20mM phosphate buffer, test sample in methanol.

Set up the following reactions in a 96 well plate (per well). Incubate at 25°C 10 min. Initiate the reactions by adding 20 µl of L-DOPA solution to each well using a multichannel pipettor and incubate at 25°C 5 min. Measuring absorbance at 470 nm.

$$\% \text{ tyrosinase inhibition} = \frac{(A - B) - (C - D)}{(A - B)} \times 100$$

4.2.5 Cell culture

4.2.5.1 Cell culture

The human fibroblast cells (CC2511) are cultured in flask with fibroblast growth medium containing 15% fetal bovine serum (FBS), 100 unit/ml penicillin G, 100 µg/ml streptomycin and grown at 37 °C in a humidified atmosphere, in the presence of 5% CO₂. The growth of cells are inspected by using an inverted phase-contrast microscope and fed with the culture medium every 2-3 days until confluence.

The human melanoma cells (G 361) are cultured in flasks with Dulbecco Modified Eagle's medium (DMEM) containing 15% fetal bovine serum (FBS), 100 unit/ml penicillin G, 100 µg/ml streptomycin and grown at 37 °C in a humidified atmosphere, in the presence of 5% CO₂. The growth of cells are inspected by using an

inverted phase-contrast microscope and fed with the culture medium every 2-3 days until confluence.

Cells were cultured in 75 cm² flasks until reaching 80% confluency then harvested. Cells were counted and careful mixing of the cell suspension was needed to ensure uniform plating in the microwells (siphon the cells up and down with a pipette). Cells were plated and left overnight for attachment before the indicated treatments.

Upon different assays used, G361 cells were seeded at 2×10^6 cells/well in a 24-well plate (1 ml/well) and 2×10^5 cells/well in a 96-well plate (200 μ l/well) and CC2511 cells were seeded at 5×10^3 cells/well in a 96-well plate (200 μ l/well).

4.2.5.2 MTT assay

MTT [3-(4,5-dimethylthiazol-2-yl)-2,5-diphenyltetrazolium bromide] assay, first described by Mosmann in 1983, is a colorimetric assay system that based on the ability of a mitochondrial dehydrogenase enzyme from viable cells to cleave the tetrazolium rings of the pale yellow MTT and form a dark blue formazan crystals. The amount of color produced is directly proportional to the number of viable cells. The yellow tetrazolium MTT is reduced by dehydrogenase enzymes from active cells, to generate reducing equivalents such as NADH. The resulting intracellular purple formazan can be solubilized by detergent. Solubilisation of the cells by the addition of a detergent such as DMSO results in the liberation of the crystals which are solubilized and quantified by spectrophotometry.

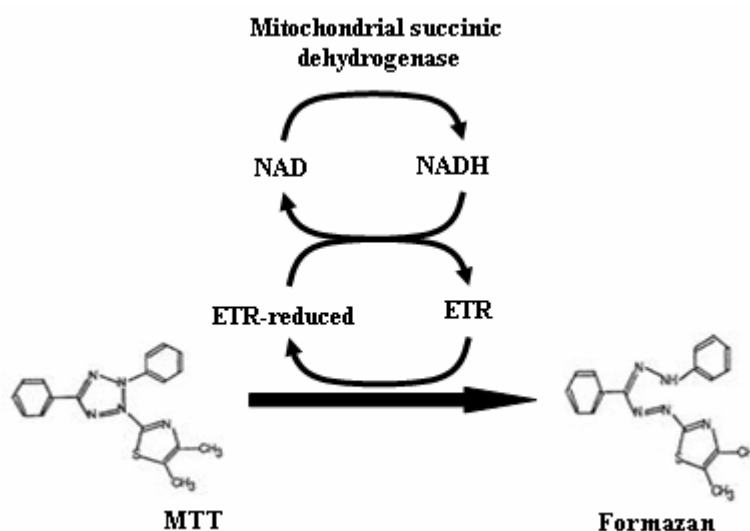


Figure 4.2 Cellular metabolism resulting in the conversion of MTT to formazan.

Human melanoma cells (G361) were cultured on 96 well plates and treated 30 min with different concentrations (0 to 62.5 $\mu\text{g/ml}$) of the plant extracts for 24h or 30 min and then washing with PBS. PBS is added in each well 200 μl and exposed to UVA (64 J/cm^2). After irradiation, MTT is added in each well (0.2 mg/ml final concentrations). The plates are incubated at 37 $^{\circ}\text{C}$ in a 5% CO_2 atmosphere for 1 hour and then washed with 200 μl of PBS. 200 μl of DMSO is added for each well. The plates are shaken for 5-10 min. The optical density is measured at 595 nm by spectrophotometer. The average absorbance of the control wells is regard as 100% and the percentage of cell viability in each well is calculated (% of control).

4.2.5.3 Tyrosinase activity

Human melanoma cells (G361) were cultured on 24 well plates and treated 30 min with different concentrations (0 to 62.5 $\mu\text{g/ml}$) of the plant extracts for 30 min and then washing with PBS. PBS is added in each well 750 μl and exposed to UVA (8 J/cm^2). After irradiation, each well was added cold extracted buffer 100 μl and gentle shaking for 30 sec. Collect cell lysate in microtube. Lysates are kept on ice and enzyme assays are carried out immediately. If not assayed on the same day, freeze the sample was frozen at -80°C . Then 90 μl of each lysate was placed in a well of a 96-well plate. 10 μl of 20mM L-DOPA was added. After incubation at 37 $^{\circ}\text{C}$, absorbance was measured at 475 nm for 1 h by spectrophotometric methods. The tyrosinase activity were calculated by comparing with standard curves produced by the same methods using known concentrations of tyrosinase activity (2034U/mg).

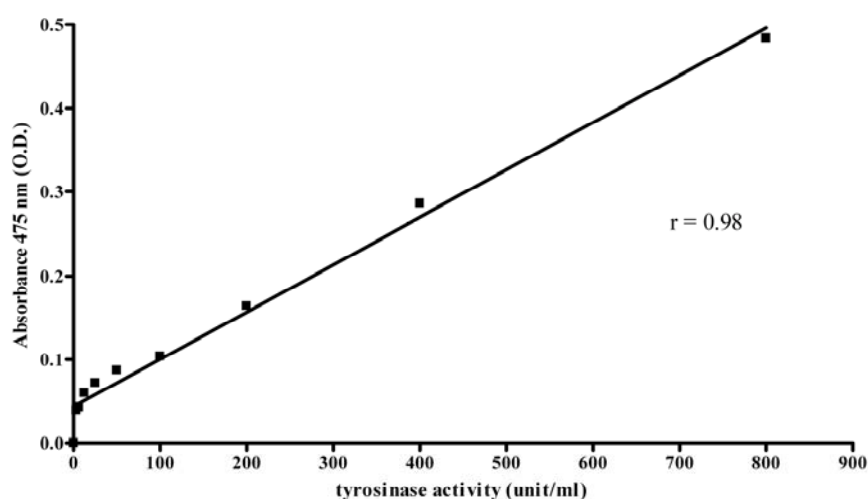


Figure 4.3 Standard curve of tyrosinase activity.

4.2.5.4 Melanin contents

Human melanoma cells (G361) were cultured on 24 well plates and treated 30 min with different concentrations (0 to 62.5 $\mu\text{g/ml}$) of the plant extracts and then washing with PBS. PBS is added in each well 750 μl and exposed to UVA (16 J/cm^2). each well was added 1 N NaOH 300 μl and incubation at room temperature 10 min. Collect cell lysate in microtube. Lysates were kept on ice and melanin contents or protein assay were carried out immediately. If not assayed on the same day, freeze the sample at -80°C . 200 μl of each lysate was placed in a 96-well plate. Absorbance was measured at 475 nm by spectrophotometric methods. Standard curve of synthetic melanin (0-250 $\mu\text{g/ml}$) were prepared.

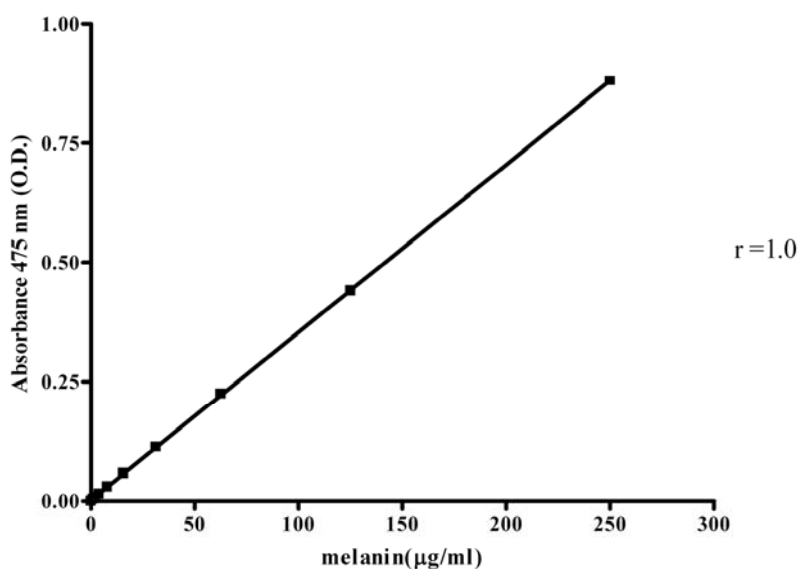


Figure 4.4 Standard curve of melanin content.

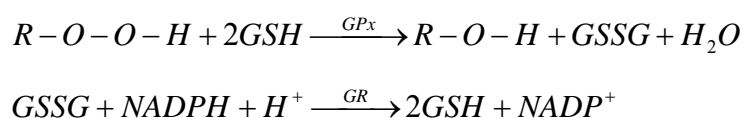
4.2.5.5 Cellular antioxidants

4.2.5.5.1 Antioxidant enzyme activities

Human melanoma cells (G361) were cultured on 24 well plates and treated 30 min with different concentrations (0 to 62.5 $\mu\text{g/ml}$) of the plant extracts and then washing with PBS. PBS is added in each well 750 μl and exposed to UVA (8 J/cm^2). After irradiation, each well was added cold extracted buffer 100 μl and gentle shaking for 30 sec. Collect cell lysate in microtube. Lysates were kept on ice and enzyme assays or protein assay were carried out immediately. If not assayed on the same day, freeze the sample at -80°C . All 96-well plate assays were carried out on a plate reader.

4.2.5.5.1.1 *Glutathione peroxidase (GPx)*

Glutathione peroxidase (GPx) catalyzes the reduction of hydroperoxides, including hydrogen peroxides, by reduced glutathione and functions to protect the cell from oxidative damage. Glutathione peroxidase assay measures GPx activity indirectly by a coupled reaction with glutathione reductase (GR). Oxidized glutathione (GSSG), produced upon reduction of hydroperoxide by GPx, is recycled to its reduced state by GR and NADPH. The oxidation of NADPH to NADP⁺ is accompanied by a decrease in absorbance at 340 nm.



Reagents for GPx assay were prepared using assay buffer (50 mM Tris-HCl and 5 mM EDTA in HPLC-grade water adjust to pH 7.6), glutathione reductase (provided at a concentration of 0.025 unit/ μ l), the mixtures of glutathione and β -NADPH (assay buffer, yields Glutathione and β -NADPH concentrations of 100 mM and 10 mM, respectively, and were used within 4 hours), tert-hydroperoxide (provided at 5 mM in assay buffer). Make a reaction mixture by mixing together. (glutathione reductase 110 μ l, reconstituted GSH + β -NADPH 110 μ l, assay buffer 880 μ l and were used within 4 hours)

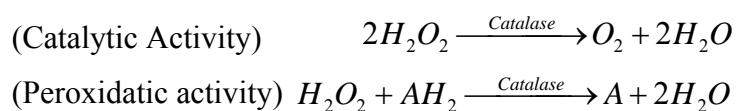
Set up the following reactions in a 96 well plate (per well) containing assay buffer 140 μ l, reaction mixture 20 μ l and GPx or sample 20 μ l. Initiate the reactions by quickly adding 20 μ l of tert-butyl hydroperoxide solution to each well using a multichannel pipettor. Immediately begin measuring absorbance at 340 nm every 30 seconds or 1 minute over a 10-15 minute period. The rate of decrease of absorbance at 340 nm in the background was subtracted from that of the samples or standard to obtain the net rate of decrease of absorbance at 340 nm for the calculation of GPx activity in samples.

Calculate the GPx activity in the samples from the following equations (where Y is the volume of the sample):

$$\begin{aligned}
 \text{Glutathione Peroxidase Activity} &= \frac{\Delta A_{340} / \text{min}}{0.00379 \mu\text{M}^{-1}} \times \frac{0.2 \text{ml}}{Y \text{ml}} \times \text{Sample Dilution} \\
 &= \text{nmole/min/ml} = \text{Units/ml}
 \end{aligned}$$

4.2.5.5.1.2 Catalase (CAT)

Catalase (CAT) is an antioxidant enzyme. CAT is involved in the detoxification of hydrogen peroxide (H_2O_2), a reactive oxygen species (ROS). This enzyme catalyzes the conversion of H_2O_2 to molecular oxygen and water (catalytic activity). CAT also demonstrates peroxidatic activity, in which low molecular weight alcohols can serve as electron donors, while aliphatic alcohols serve as specific substrates for CAT.



Catalase assay utilizes the peroxidatic function of CAT for determination of enzyme activity. The method is based on the reaction of the enzyme with methanol in the presence of an optimal concentration of H_2O_2 . The formaldehyde produced is measured spectrophotometrically with 4-amino-3-hydrazino-5-mercapto-1,2,4-triazole (purpald) as the chromogen. Purpald specifically forms a bicyclic heterocycle with aldehydes, which upon oxidation changes from colorless to a purple color.

Reagents for CAT assay were prepared using assay buffer (100 mM monobasic potassium phosphate, pH 7.0 in HPLC-grade water, stored at 4 °C and were used in two months), sample buffer (25 mM monobasic potassium phosphate, pH 7.5, containing 1mM EDTA), CAT (positive control), CAT samples (stored at 4 °C and used in two months), formaldehyde standard (1 mM formaldehyde stock solution in sample buffer), potassium hydroxide (10 M potassium hydroxide solution in cold HPLC-grade water), hydrogen peroxide (the stock contains 30% solution of hydrogen peroxide. Dilute 40 μl of hydrogen peroxide with 9.96 ml of HPLC-grade water and were used in two hours), purpald (34.2 mM of 4-amino-3-hydrazino-5-mercapto-1,2,4-triazole (Purpald) in 0.5 M hydrochloric acid.) and potassium periodate (65.2 mM potassium periodate in 0.5 M potassium hydroxide).

Formaldehyde standards (final concentration 0-120 μM) were made by dilution with sample buffer to obtain a 1 mM formaldehyde stock solution as described in Table 4.2.(dilution 1:1)

Table 4.2 Preparation of formaldehyde standards.

Tube	Formaldehyde stock (μl)	Add solution from previous tube	Sample buffer (μl)	Final concentration (μM formaldehyde)*
1	1000	-	-	120
2	-	500	500	60
3	-	500	500	30
4	-	500	500	15
5	-	500	500	7.5
6	-	500	500	3.7
7	-	-	1000	0

* Final formaldehyde concentration in the 170 μl reaction.

Add 100 μl of assay buffer, 30 μl of methanol, and 20 μl of standard, CAT or sample to well. Initiate reactions by adding 20 μl of hydrogen peroxide to all the wells. Cover the plate with the plate cover and incubate on a shaker for 20 minutes at room temperature. Add 30 μl of potassium hydroxide to each well to terminate the reaction and then add 30 μl of purpald to each well. Cover the plate with the plate cover and incubate on a shaker for 10 minutes at room temperature. Add 10 μl of potassium periodate to each well. Cover the plate with the plate cover and incubate 5 minutes at room temperature on a shaker. Read the absorbance at 540 nm using a plate reader. Add the amount of substances to each well as described in table 4.3.

Table 4.3 Amount of substances to each well for CAT assay.

	Formaldehyde Standard Wells (μl)	Positive Control Wells (μl)	Sample Wells (μl)
Assay buffer	100	100	100
Methanol	30	30	30
Standard	20	-	-
Catalase	-	20	-
Sample	-	-	20
H ₂ O ₂	20	20	20
KOH	30	30	30
Purpald	30	30	30
Potassium periodate	10	10	10

Calculate the formaldehyde concentration of the samples using the equation obtained from the linear regression of the standard curve substituting corrected absorbance values for each sample.

$$\text{Formaldehyde } (\mu\text{M}) = \left[\frac{\text{Sample absorbance} - y \text{ intercept}}{\text{slope}} \right] \times \frac{0.17 \text{ ml}}{0.02 \text{ ml}}$$

Calculate the catalase activity of the sample using the following equation. One unit is defined as the amount of enzyme that will cause the formation of 1.0 nmol of formaldehyde per minute at 25 °C.

$$\text{CAT Activity} = \frac{\mu\text{M of sample}}{20 \text{ min.}} \times \text{Sample dilution} = \text{nmol/min/ml}$$

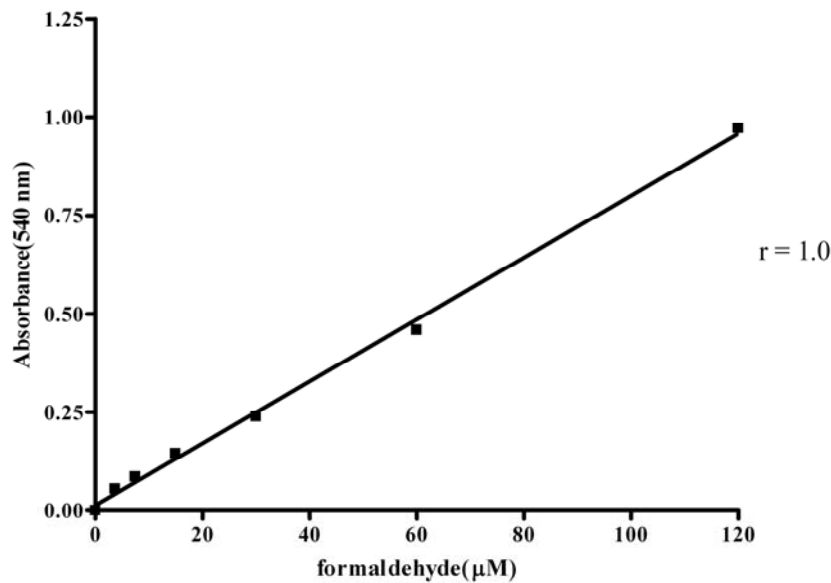


Figure 4.5 Standard curve of formaldehyde.

4.2.5.5.2 Cellular glutathione contents in melanoma exposed to UV

In healthy cells, the glutathione acts as antioxidant by constantly removing ROS. GSH assay is based on the specificity of the reaction between GSH and the fluorescent probe, which can determine GSH levels (Figure 4.6). GSH content was assayed using a modified method of Hissin and Hilf (1976), using the fluorescent reagent *o*-phthalaldehyde (OPA), which reacts specifically with GSH at pH 8.

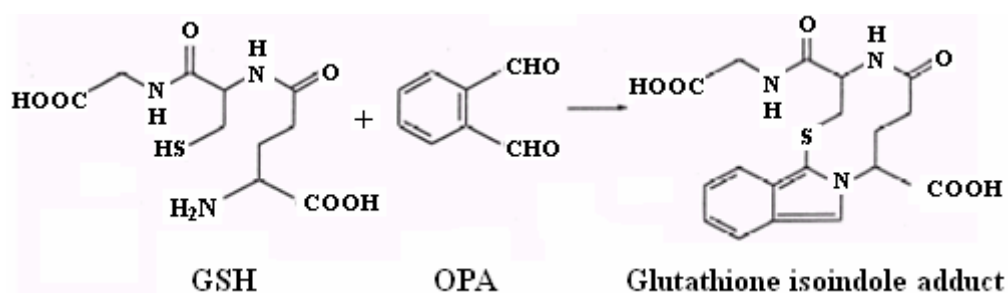


Figure 4.6 The reaction of GSH with OPA.

Human melanoma cells (G361) were cultured on 24 well plates and treated 30 min with different concentrations (0 to 62.5 μg/ml) of the plant extracts and then washing with PBS. PBS is added in each well 750 μl and exposed to UVA (8 J/cm²). After irradiation, each well was added 100 μl ice cold TCA (6.5% trichloroacetic acid)

and the plates were left on ice for 10 min collect cell lysate to detected GSH contents and then added 100 μ l extract buffer for each well to determination protein. Collect cell lysate in microtube. Lysates were kept on ice and GSH contents or protein assay were carried out immediately. If not assayed on the same day, freeze the sample at -80°C .

GSH content assay, white 96-well plates were used; 10 μ l of standard or sample, 175 μ l of phosphate/EDTA buffer (5.45 ml of 1 M NaOH with 500 ml of 13.6 g KH_2PO_4 , 1.86 g EDTA in 900 ml H_2O , pH 8.0 with 1 M NaOH) and 15 μ l of *o*-phthaldialdehyde (OPA) solution (1mg/ml in MeOH) were added, respectively. The plates were left in the dark for 25 mins and fluorescence was measured at 350 nm excitation and 420 nm emission using a spectrofluorimeter. The GSH levels were calculated by comparing with standard curves produced by the same methods using known concentrations of GSH.

Reagents for GSH assay were prepared using buffer 1(13.6 g KH_2PO_4 and 1.86 g EDTA in 900 ml water then adjust to pH 8.0 with 1 M NaOH), buffer 2 (500 ml Buffer 1 and added 5.45 ml NaOH (1M)), OPA (fresh 10 mg OPA in 10 ml methanol) and TCA (6.5% TCA in water) Preparation GSH standard to 32 nmol/ml GSH stock solution by diluted with 6.5% TCA.

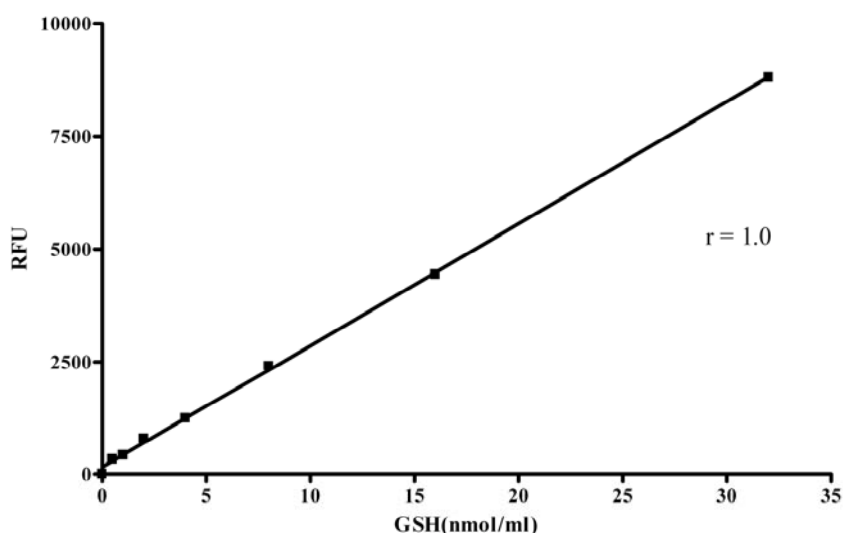


Figure 4.7 Standard curve of GSH.

4.2.5.6 Dichlorofluorescein Diacetate Assay

The generation processes of reactive oxygen species can be monitored by using the fluorescence methods. 2', 7'-Dichlorofluorescein diacetate (DCFH-DA), a stable and non-fluorescent dye, is widely used to measure oxidative stress in cells. The conversion of the nonfluorescent DCFH-DA to the highly fluorescent compound 2',7'-dichlorofluorescein (DCF⁻) happens in several steps. First, DCFH-DA, readily crosses cell membranes and then undergoes deacetylation by intracellular esterases to yield the dichlorofluorescein (DCFH). The probe DCFH trapped within the cells is susceptible to ROS-mediated oxidation to DCF⁻ (Fig.4.10). The fluorescence intensity is directly proportional to the level of DCF⁻ formed intracellularly.

DCFH was stored protected from the light. Sample preparation and experiments were performed in the dark. Human melanoma cells (G361) were cultured on 24 well plates and treated 30 minute with different concentrations (0 to 62.5 $\mu\text{g/ml}$) of the plant extracts. And then medium was removed and washed twice with PBS. The cells were preincubated for 45 min at 37 °C in DMEM (serum free) containing 10 μM DCFH-DA (from a stock solution of 0.05 M DCFH-DA in DMSO). After the preincubation, medium was removed and washed twice with PBS. PBS 750 μl was

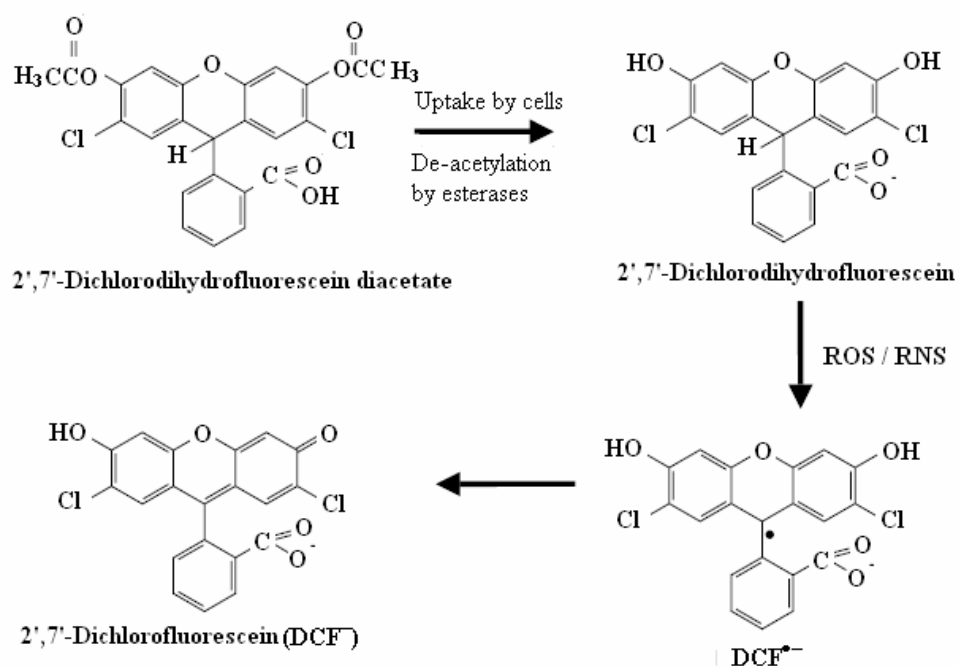


Figure 4.8 The interaction of fluorescent probe with cell and oxidants (72).

added to each well. Cells were then exposed to UVA (16 J/cm^2). The fluorescence intensity was monitored at an interval of 0.5 min for a total period of 20 min with excitation wavelength 485 nm and emission wavelength 530 nm by plate reader. As a positive control, $50 \mu\text{l H}_2\text{O}_2$ was added to induce an increase in DCF fluorescence. The net increase in DCF fluorescence was calculated by taking the difference between the values before and after exposure to UVA. Graphs were plotted on relative fluorescence unit (RFU) with different concentrations of test compounds.

4.2.5.7 Procedure of protein assay

The Bio-Rad protein assay kit was used. This assay is based on the method of Bradford. Addition of an acidic dye, Coomassie Brilliant Blue G-250 dye to protein solution. The binding of Coomassie Brilliant Blue G-250 to protein causes a blue color which is soluble in water. The optical density is measured at 595 nm by spectrophotometer.

Reagents for protein assay were prepared using stock BSA solution (1 mg/ml) by dissolving 0.02 g of BSA in 20 ml of distilled water, aliquot the solution into 10 separate tubes (1 ml/tube) and kept frozen at $-20 \text{ }^\circ\text{C}$. Prepare bovine serum albumin for standard protein at various concentrations ($0, 5, 10, 20, 40, 80, 160, 320, 640 \mu\text{g/ml}$). $10 \mu\text{l}$ standard protein and sample were added to each well of 96 well plate. Bradford reagent was diluted (1:4) with distilled water. Add $190 \mu\text{l}$ of Bradford reagent (diluted) in each well and measured the absorbance at 595 nm and calculation for value of protein in each sample from standard curve fit.

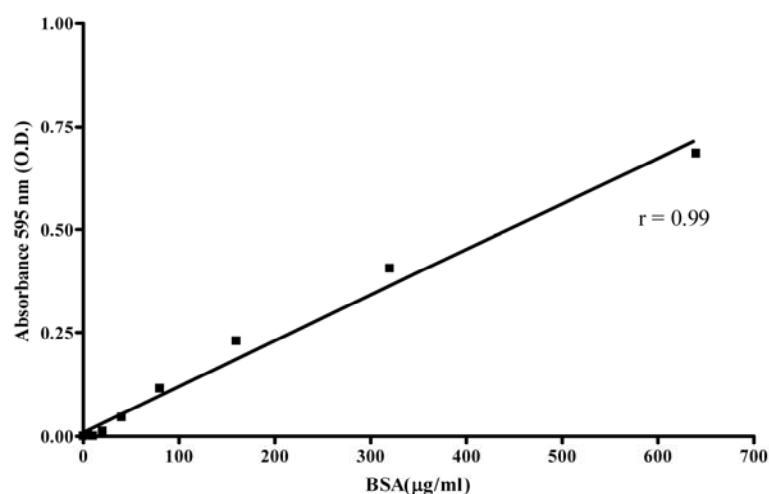


Figure 4.9 Standard curve of protein assay.

CHAPTER V

RESULTS

5.1 Identification of antioxidant activity, the presence of phenolic and antityrosinase activities of the plant extracts

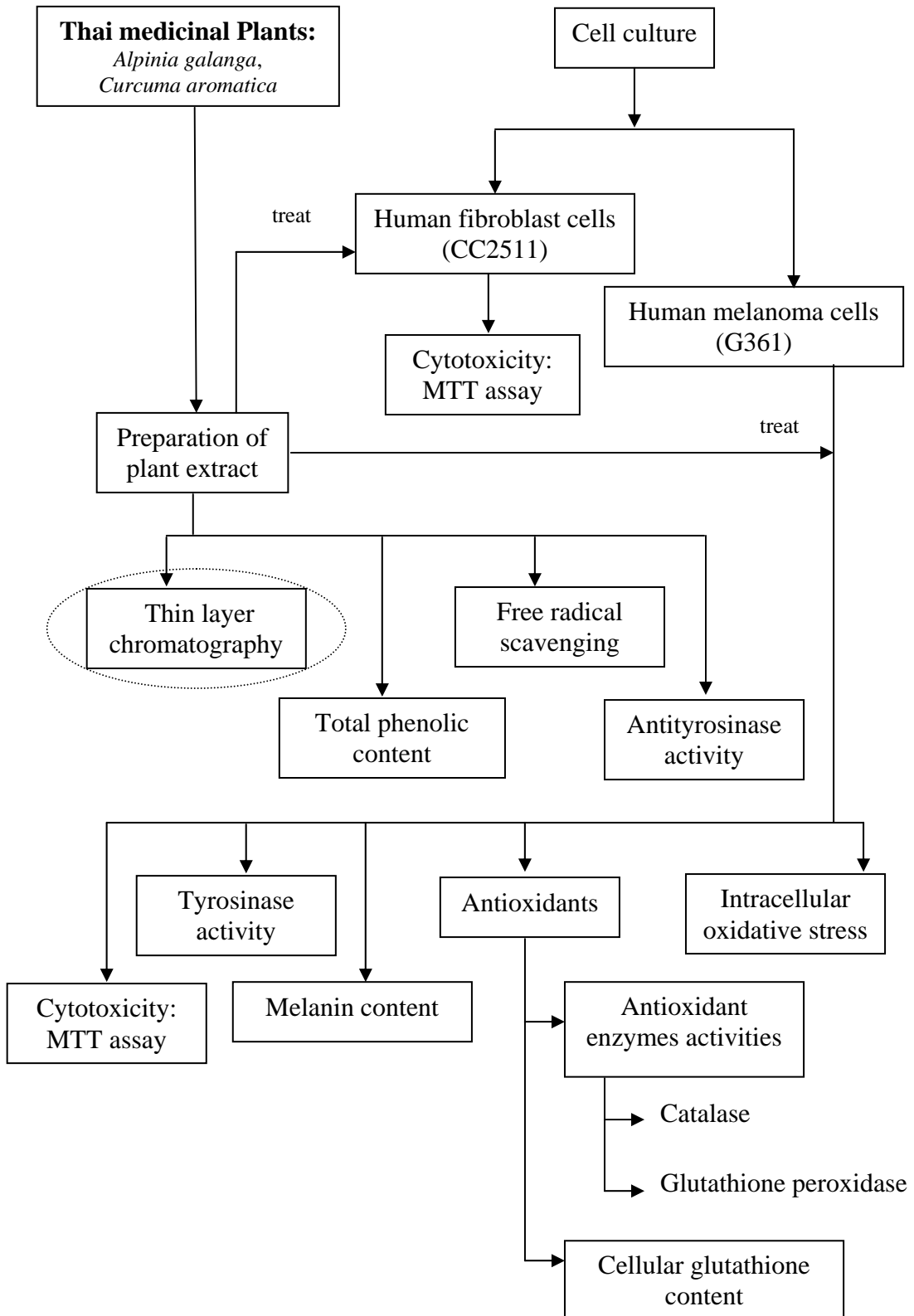
5.1.1 Thin layer chromatography

TLC was a common method for herbal analysis and used for plant extract standardization. The standardization of plant extract was mainly intended to obtain a characteristic fingerprint of a specific plant that represents the presence of a particular quality defining chemical constituents. The advantages of using TLC to construct the fingerprints are its simplicity, versatility, specificity and simple preparation. The fingerprint and parameters of quality assessment of *A. galanga* and *C. aromatica* extracts using the thin layer chromatography (TLC) technique.

Table 5.1 Solvent system of mobile phase to detect phenolic components.

Solvent system	Standard / Sample		Mobile phase		Spray reagent
	Substance	concentration	Solvent	Volume	
1	1. Curcuminoids	10 mg/ ml	1. Chloroform	47.5 ml	FBS
	2. <i>Curcuma aromatica</i>	100 mg/ ml	2. Ethanol	2.5 ml	
	3. <i>Alpinia galanga</i>	100 mg/ ml	3. Acetic acid	0.5 ml	
2	1. Curcuminoids	10 mg/ ml	1. Toluene	46.5 ml	FBS
	2. <i>Curcuma aromatica</i>	100 mg/ ml	2. Ethyl	3.5 ml	
	3. <i>Alpinia galanga</i>	100 mg/ ml	acetate		

Screening of component in *C. aromatica*, Curcuminoid and *A. galanga*. Band were detected by UV 254, 366 nm or visible (FBS for detection). In identifying fingerprints of phenolic compounds of the crude extracts of *A. galanga* and *C. aromatica* by using FBS as a spray reagent for detection. TLC analysis of the extracts showed the presence of phenolics.



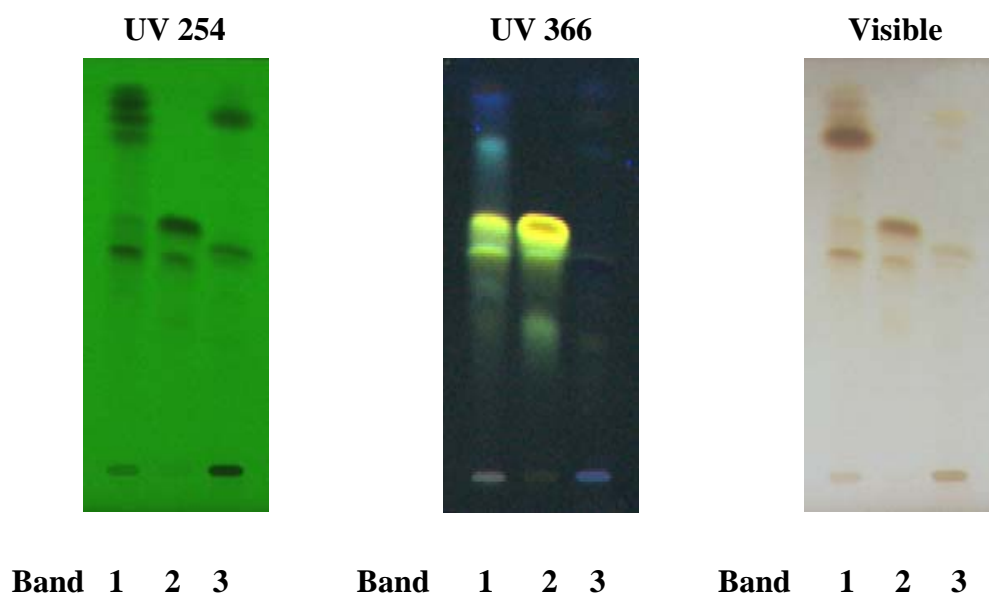


Figure 5.1 Phenolic screening (solvent system 1): Bands were detected by UV 254 nm, UV 366 nm and FBS spray. (band1: *C. aromatica*, band 2: Curcuminoid, band 3: *A. galanga*)

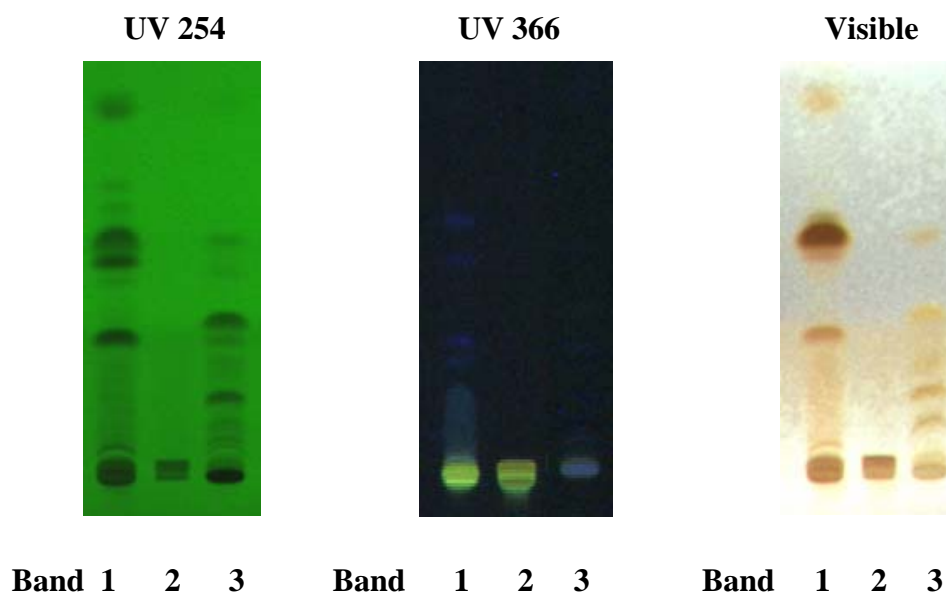


Figure 5.2 Phenolic screening (solvent system 2): Bands were detected by UV 254 nm, UV 366 nm and FBS spray. (band1: *C. aromatica*, band 2: Curcuminoid, band 3: *A. galanga*)

Table 5.2 R_f and rRF value of *Curcuma aromatica* and curcuminoids in solvent system1 (Lot.1).

Lot 1			
Band identified	R_f	rRF	
		M1	M2
1	0.31	0.44	0.38
2	0.72	1.01	0.89
3	0.83	1.17	1.02
4	0.88	1.24	1.09
5	0.93	1.31	1.15
M1(Curcuminoids)	0.71	1.00	-
M2(Curcuminoids)	0.81	-	1.00

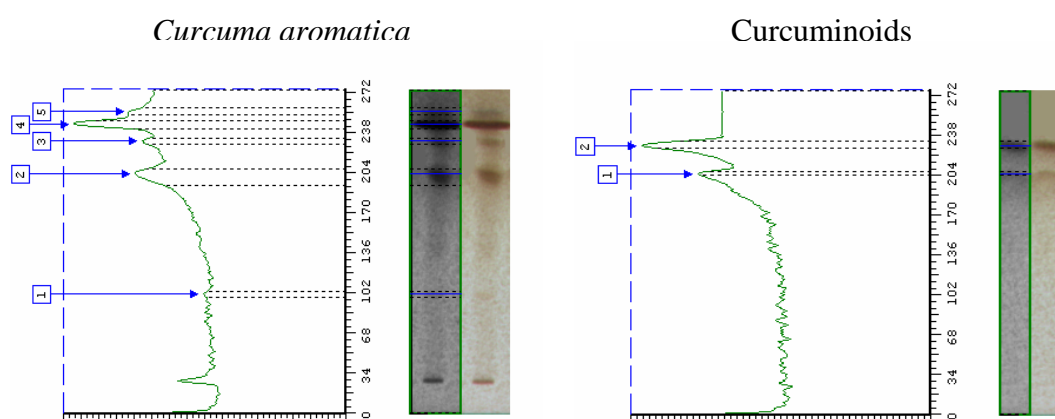


Figure 5.3 Densitometer analysis of *Curcuma aromatica* and curcuminoids in solvent system1 (Lot.1).

Table 5.3 R_f and rRF value of *Curcuma aromatica* and curcuminoids in solvent system1 (Lot.2).

Lot 2			
Band identified	R_f	rRF	
		M1	M2
1	0.27	0.38	0.33
2	0.65	0.92	0.80
3	0.79	1.11	0.98
4	0.87	1.23	1.07
5	0.91	1.28	1.12
M1(Curcuminoids)	0.71	1.00	-
M2(Curcuminoids)	0.81	-	1.00

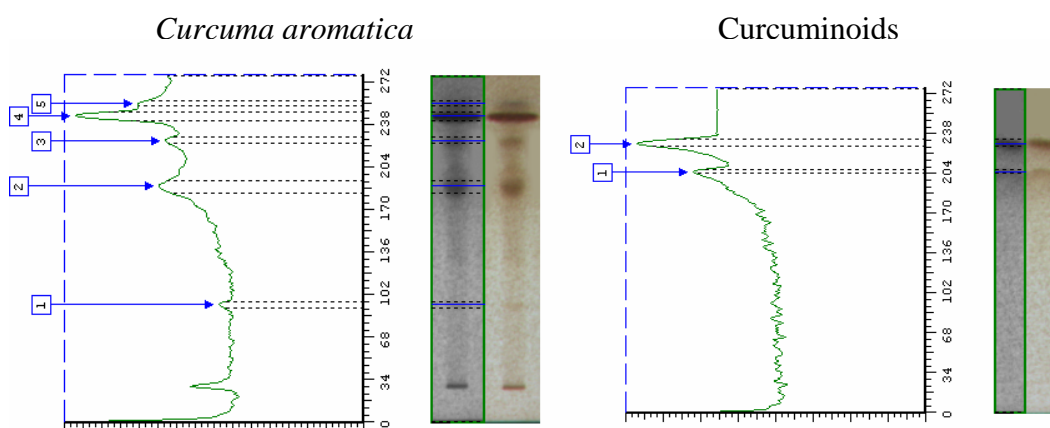


Figure 5.4 Densitometer analysis of *Curcuma aromatica* and curcuminoids in solvent system1 (Lot.2).

Table 5.4 R_f and rRF value of *Curcuma aromatica* and curcuminoids in solvent system1 (Lot.3).

Lot 3			
Band identified	R_f	rRF	
		M1	M2
1	0.32	0.43	0.39
2	0.73	0.97	0.89
3	0.82	1.09	1.00
4	0.87	1.16	1.06
5	0.91	1.21	1.11
M1(Curcuminoids)	0.71	1.00	-
M2(Curcuminoids)	0.81	-	1.00

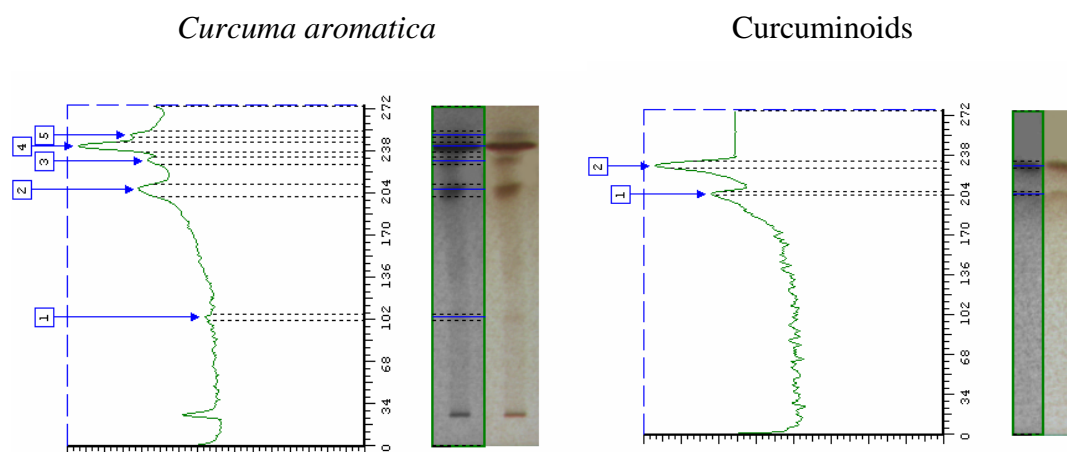


Figure 5.5 Densitometer analysis of *Curcuma aromatica* and curcuminoids in solvent system1 (Lot.3).

Table 5.5 R_f and rRF value of *Curcuma aromatica* 3 lots detected by FBS staining in solvent system 1.

Band identified	R_f / rRF	Lots			mean	Accepted range	% CV
		1	2	3			
1. band 1	R_f	0.31	0.27	0.32	0.30 ± 0.015	0.24 - 0.38	8.82
	rRF (M1)	0.44	0.38	0.43	0.41 ± 0.017	0.33 - 0.52	7.71
	rRF (M2)	0.38	0.33	0.39	0.37 ± 0.018	0.30 - 0.46	8.77
2. band 2	R_f	0.72	0.65	0.73	0.70 ± 0.025	0.56 - 0.88	6.23
	rRF (M1)	1.01	0.92	0.97	0.97 ± 0.029	0.77 - 1.21	4.66
	rRF (M2)	0.89	0.80	0.89	0.86 ± 0.029	0.69 - 1.08	6.04
3. band 3	R_f	0.83	0.79	0.82	0.81 ± 0.012	0.65 - 1.02	2.56
	rRF (M1)	1.17	1.11	1.09	1.13 ± 0.023	0.90 - 1.41	3.71
	rRF (M2)	1.02	0.98	1.00	1.00 ± 0.014	0.80 - 1.25	2.00
4. band 4	R_f	0.88	0.87	0.87	0.87 ± 0.003	0.70 - 1.09	0.66
	rRF (M1)	1.24	1.23	1.16	1.21 ± 0.024	0.97 - 1.51	3.60
	rRF (M2)	1.09	1.07	1.06	1.07 ± 0.007	0.86 - 1.34	1.42
5. band 5	R_f	0.93	0.91	0.91	0.92 ± 0.007	0.73 - 1.15	1.26
	rRF (M1)	1.31	1.28	1.21	1.27 ± 0.029	1.01 - 1.59	4.05
	rRF (M2)	1.15	1.12	1.11	1.13 ± 0.011	0.90 - 1.41	1.85

Table 5.6 R_f and rRF value of *Curcuma aromatica* and curcuminoids in solvent system2 (Lot.1).

Lot 1			
Band identified	R_f	rRF	
		M1	M2
1	0.04	0.80	0.40
2	0.07	1.40	0.70
3	0.10	2.00	1.00
4	0.64	12.80	6.40
M1(Curcuminoids)	0.05	1.00	-
M2(Curcuminoids)	0.10	-	1.00

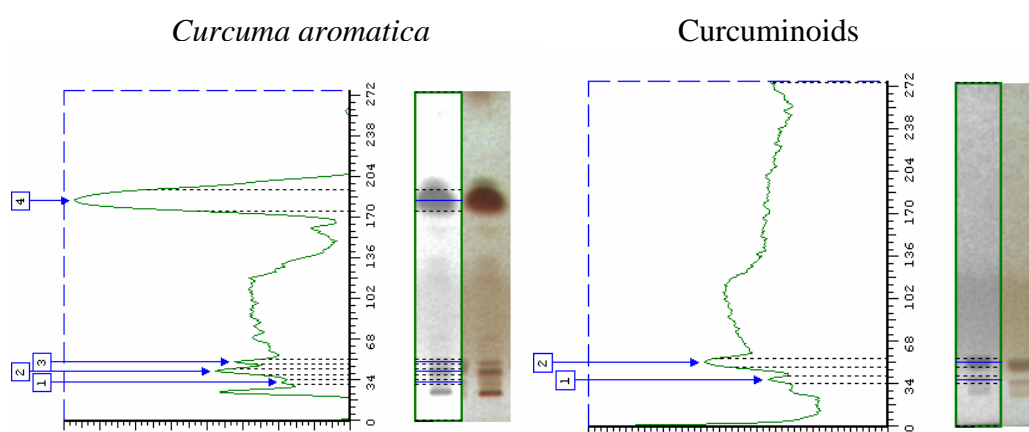


Figure 5.6 Densitometer analysis of *Curcuma aromatica* and curcuminoids in solvent system2 (Lot.1).

Table 5.7 R_f and rRF value of *Curcuma aromatica* and curcuminoids in solvent system2 (Lot.2).

Lot 2			
Band identified	R_f	rRF	
		M1	M2
1	0.04	0.80	0.40
2	0.08	1.60	0.80
3	0.11	2.20	1.10
4	0.64	12.80	6.40
M1(Curcuminoids)	0.05	1.00	-
M2(Curcuminoids)	0.10	-	1.00

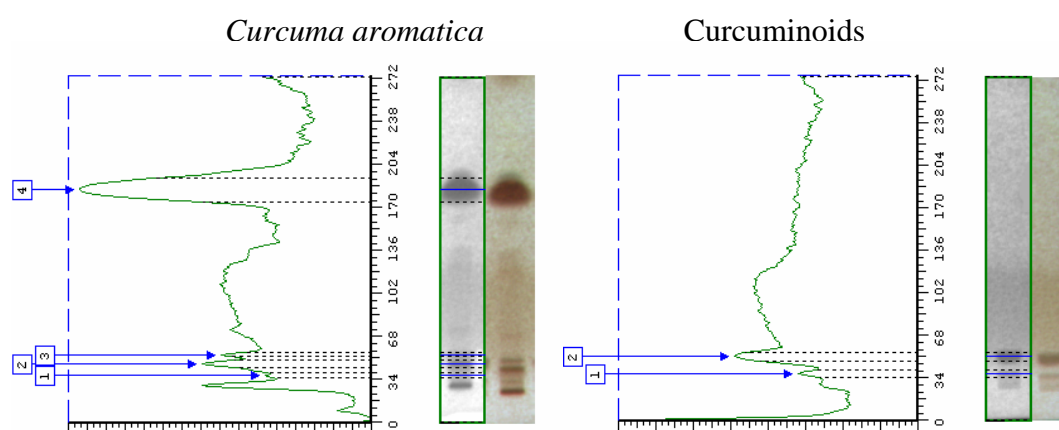


Figure 5.7 Densitometer analysis of *Curcuma aromatica* and curcuminoids in solvent system2 (Lot.2).

Table 5.8 R_f and rRF value of *Curcuma aromatica* and curcuminoids in solvent system2 (Lot.3).

Lot 3			
Band identified	R_f	rRF	
		M1	M2
1	0.04	0.80	0.40
2	0.08	1.60	0.80
3	0.11	2.20	1.10
4	0.63	12.60	6.30
M1(Curcuminoids)	0.05	1.00	-
M2(Curcuminoids)	0.10	-	1.00

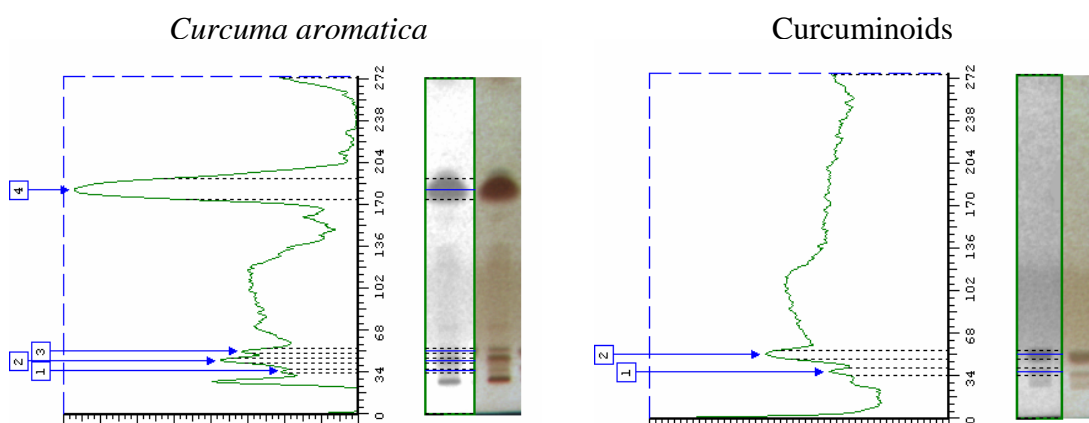


Figure 5.8 Densitometer analysis of *Curcuma aromatica* and curcuminoids in solvent system2 (Lot.3).

Table 5.9 R_f and rRF value of *Curcuma aromatica* 3 lots detected by FBS staining in solvent system 2.

Band identified	R_f / rRF	Lots			mean	Accepted range	% CV
		1	2	3			
1. band 1	R_f	0.04	0.04	0.04	0.04 ± 0.000	0.03 - 0.05	0
	rRF (M1)	0.80	0.80	0.80	0.08 ± 0.000	0.64 - 1.00	0
	rRF (M2)	0.40	0.40	0.40	0.40 ± 0.000	0.32 - 0.50	0
2. band 2	R_f	0.07	0.08	0.08	0.08 ± 0.003	0.06 - 0.10	7.53
	rRF (M1)	1.40	1.60	1.60	1.53 ± 0.067	1.23 - 1.92	7.53
	rRF (M2)	0.70	0.80	0.80	0.77 ± 0.033	0.61 - 0.96	7.53
3. band 3	R_f	0.10	0.11	0.11	0.11 ± 0.003	0.09 - 0.13	5.41
	rRF (M1)	2.00	2.20	2.20	2.13 ± 0.067	1.71 - 2.67	5.41
	rRF (M2)	1.00	1.10	1.10	1.07 ± 0.033	0.85 - 1.33	5.41
4. band 4	R_f	0.64	0.64	0.63	0.64 ± 0.003	0.51 - 0.80	0.91
	rRF (M1)	12.80	12.80	12.60	12.73 ± 0.067	10.19 - 15.92	0.91
	rRF (M2)	6.40	6.40	6.30	6.37 ± 0.033	5.09 - 7.96	0.91

Table 5.10 R_f and rRF value of *Alpinia galanga* and curcuminoids in solvent system1 (Lot.1).

Lot 1			
Band identified	R_f	rRF	
		M1	M2
1	0.59	0.83	0.73
2	0.80	1.13	0.99
M1(Curcuminoids)	0.71	1.00	-
M2(Curcuminoids)	0.81	-	1.00

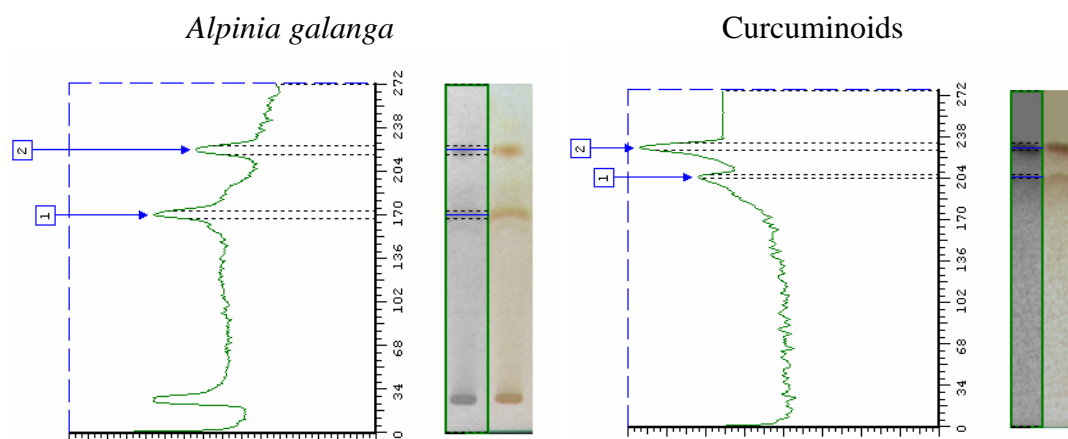


Figure 5.9 Densitometer analysis of *Alpinia galanga* and curcuminoids in solvent system1 (Lot.1).

Table 5.11 R_f and rRF value of *Alpinia galanga* and curcuminoids in solvent system1 (Lot.2).

Lot 2			
Band identified	R_f	rRF	
		M1	M2
1	0.59	0.83	0.73
2	0.79	1.11	0.98
M1(Curcuminoids)	0.71	1.00	-
M2(Curcuminoids)	0.81	-	1.00

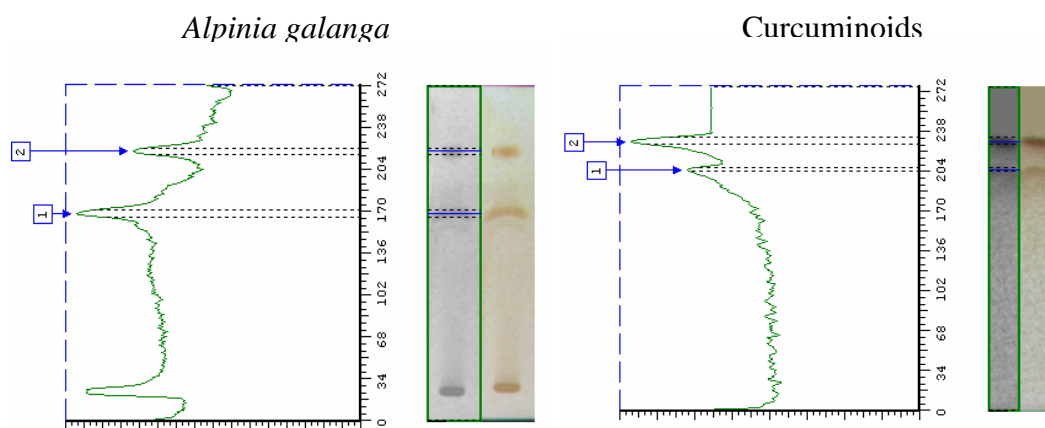


Figure 5.10 Densitometer analysis of *Alpinia galanga* and curcuminoids in solvent system1 (Lot.2).

Table 5.12 R_f and rRF value of *Alpinia galanga* and curcuminoids in solvent system1 (Lot.3).

Lot 3			
Band identified	R_f	rRF	
		M1	M2
1	0.61	0.86	0.75
2	0.80	1.13	0.99
M1(Curcuminoids)	0.71	1.00	-
M2(Curcuminoids)	0.81	-	1.00

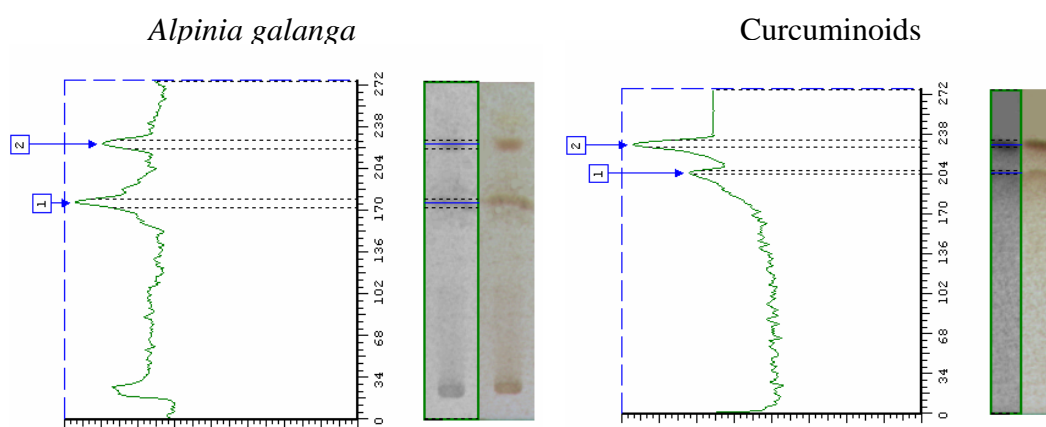


Figure 5.11 Densitometer analysis of *Alpinia galanga* and curcuminoids in solvent system1 (Lot.3).

Table 5.13 R_f and rRF value of *Alpinia galanga* 3 lots detected by FBS staining in solvent system 1.

Band identified	R_f / rRF	Lots			mean	Accepted range	% CV
		1	2	3			
1. band 1	R_f	0.59	0.59	0.61	0.60 ± 0.007	0.48 - 0.75	1.94
	rRF (M1)	0.83	0.83	0.86	0.84 ± 0.010	0.67 - 1.05	2.06
	rRF (M2)	0.73	0.73	0.75	0.74 ± 0.007	0.59 - 0.92	1.57
2. band 2	R_f	0.80	0.79	0.80	0.80 ± 0.003	0.64 - 1.00	0.72
	rRF (M1)	1.13	1.11	1.13	1.12 ± 0.007	0.90 - 1.40	1.03
	rRF (M2)	0.99	0.98	0.99	0.99 ± 0.003	0.79 - 1.23	0.59

Table 5.14 R_f and rRF value of *Alpinia galanga* and curcuminoids in solvent system2 (Lot.1).

Lot 1			
Band identified	R_f	rRF	
		M1	M2
1	0.05	1.00	0.50
2	0.11	2.20	1.10
3	0.19	3.80	1.90
4	0.25	5.00	2.50
5	0.40	8.00	4.00
6	0.58	11.60	5.80
M1(Curcuminoids)	0.05	1.00	-
M2(Curcuminoids)	0.10	-	1.00

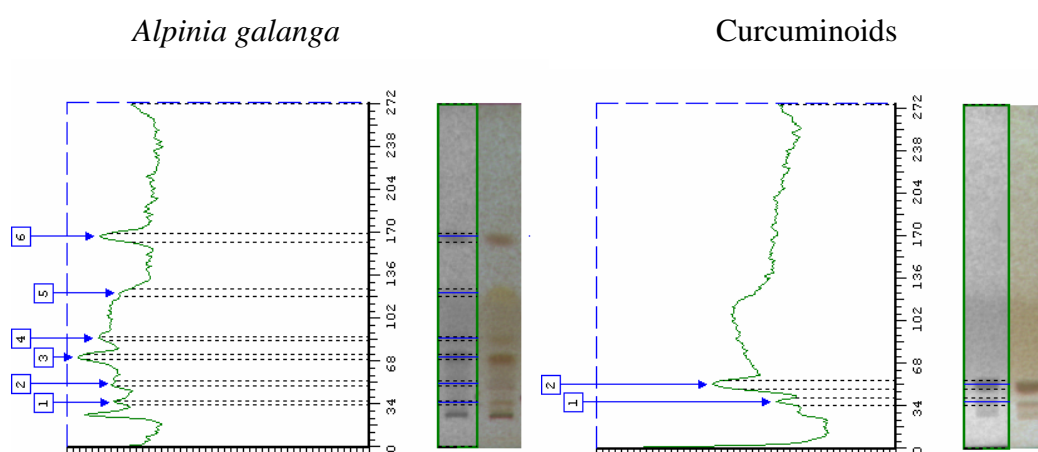


Figure 5.12 Densitometer analysis of *Alpinia galanga* and curcuminoids in solvent system2 (Lot.1).

Table 5.15 R_f and rRF value of *Alpinia galanga* and curcuminoids in solvent system2 (Lot.2).

Lot 2			
Band identified	R_f	rRF	
		M1	M2
1	0.05	1.00	0.50
2	0.10	2.00	1.00
3	0.18	3.60	1.80
4	0.24	4.80	2.40
5	0.37	7.40	3.70
6	0.56	11.20	5.60
M1(Curcuminoids)	0.05	1.00	-
M2(Curcuminoids)	0.10	-	1.00

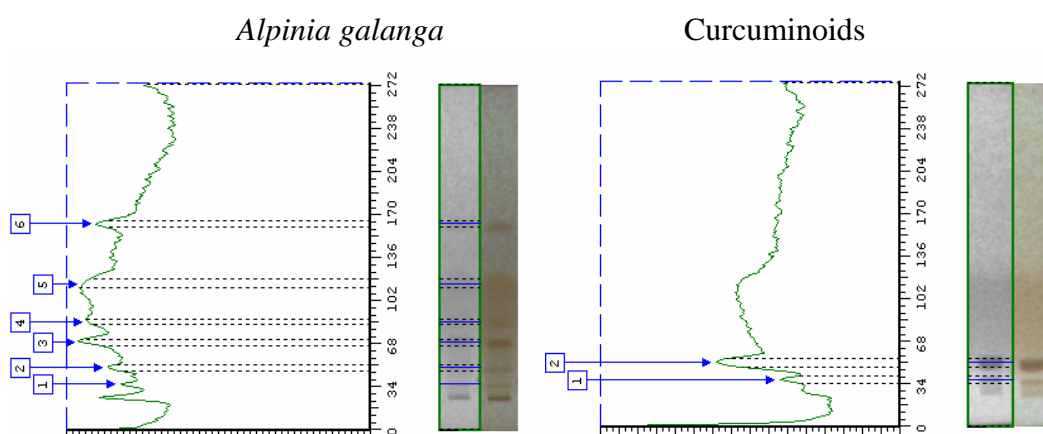


Figure 5.13 Densitometer analysis of *Alpinia galanga* and curcuminoids in solvent system2 (Lot.2).

Table 5.16 R_f and rRF value of *Alpinia galanga* and curcuminoids in solvent system2 (Lot.3).

Lot 3			
Band identified	R_f	rRF	
		M1	M2
1	0.05	1.00	0.50
2	0.10	2.00	1.00
3	0.18	3.60	1.80
4	0.26	5.20	2.60
5	0.37	7.40	3.70
6	0.56	11.20	5.60
M1(Curcuminoids)	0.05	1.00	-
M2(Curcuminoids)	0.10	-	1.00

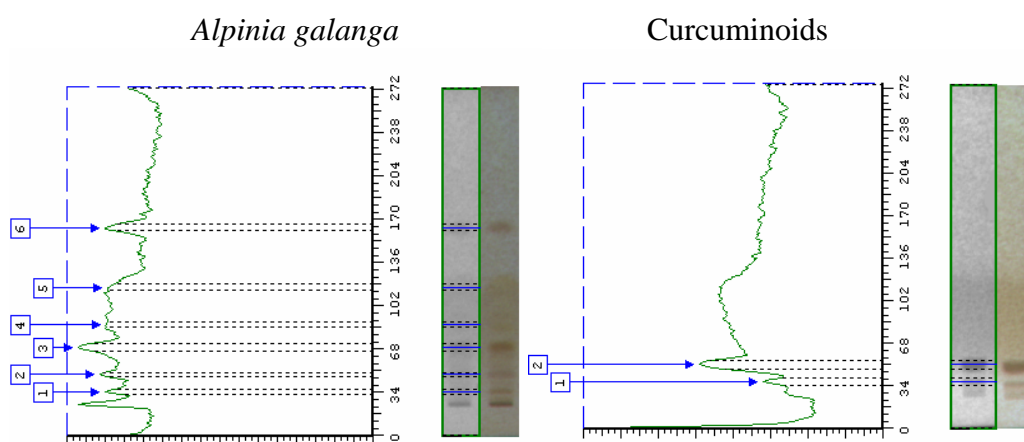
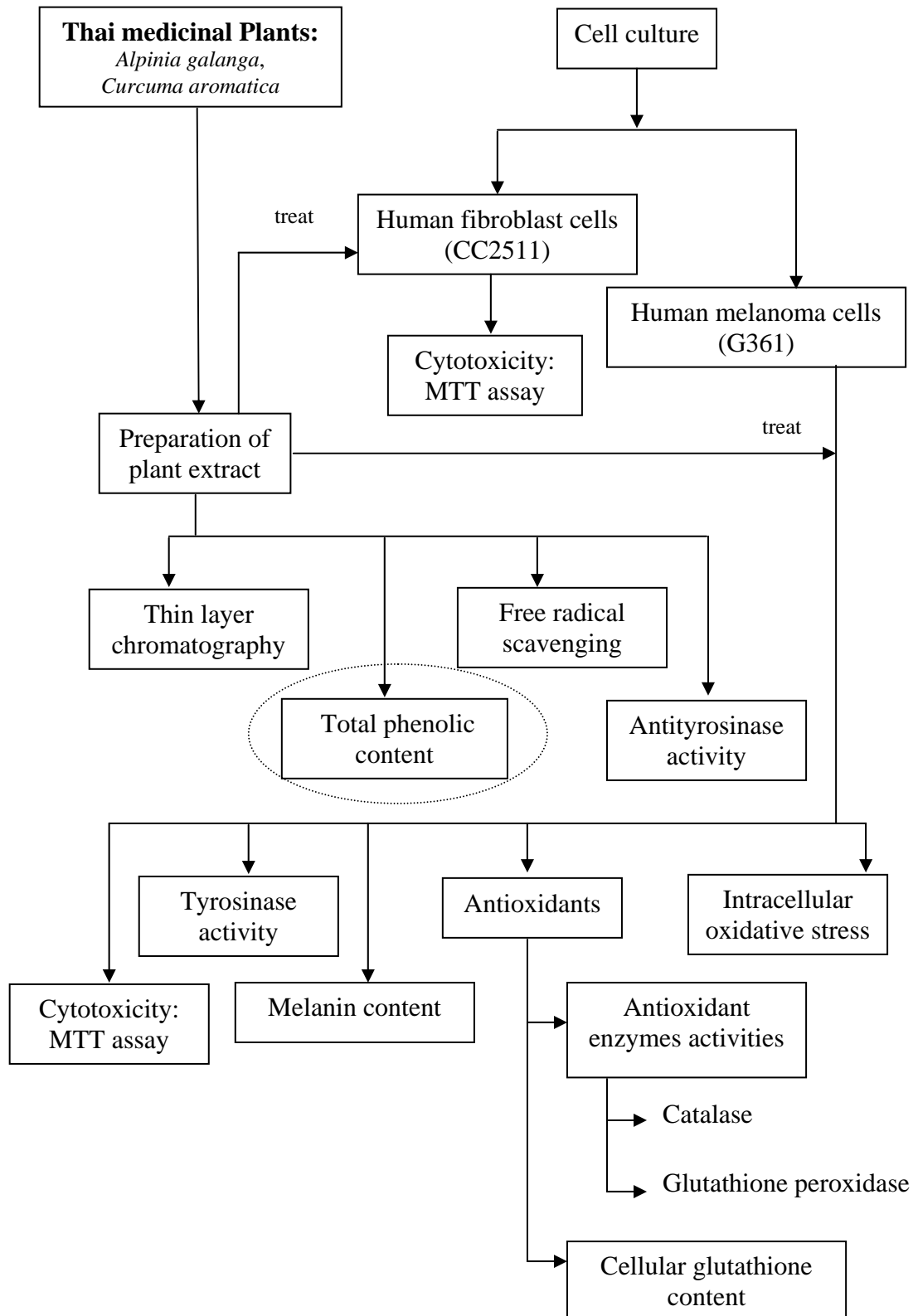


Figure 5.14 Densitometer analysis of *Alpinia galanga* and curcuminoids in solvent system2 (Lot.3).

Table 5.17 R_f and rRF value of *Alpinia galanga* 3 lots detected by FBS staining in solvent system 2.

Band identified	R_f / rRF	Lots			mean	Accepted range	% CV
		1	2	3			
1. band 1	R_f	0.05	0.05	0.05	0.05 ± 0.000	0.04 - 0.06	0
	rRF (M1)	1.00	1.00	1.00	1.00 ± 0.000	0.80 - 1.25	0
	rRF (M2)	0.50	0.50	0.50	0.50 ± 0.000	0.40 - 0.63	0
2. band 2	R_f	0.11	0.10	0.10	0.10 ± 0.003	0.08 - 0.13	5.59
	rRF (M1)	2.20	2.00	2.00	2.07 ± 0.067	1.65 - 2.58	5.59
	rRF (M2)	1.10	1.00	1.00	1.03 ± 0.033	0.83 - 1.29	5.59
3. band 3	R_f	0.19	0.18	0.18	0.18 ± 0.033	0.15 - 0.23	3.15
	rRF (M1)	3.80	3.60	3.60	3.67 ± 0.067	2.93 - 4.58	3.15
	rRF (M2)	1.90	1.80	1.80	1.83 ± 0.033	1.47 - 2.29	3.15
4. band 4	R_f	0.25	0.24	0.26	0.25 ± 0.006	0.20 - 0.31	4.00
	rRF (M1)	5.00	4.80	5.20	5.00 ± 0.115	4.00 - 6.25	4.00
	rRF (M2)	2.50	2.40	2.60	2.50 ± 0.058	2.00 - 3.13	4.00
5. band 5	R_f	0.40	0.37	0.37	0.38 ± 0.010	0.30 - 0.48	4.56
	rRF (M1)	8.00	7.40	7.40	7.60 ± 0.200	6.08 - 9.50	4.56
	rRF (M2)	4.00	3.70	3.70	3.80 ± 0.100	3.04 - 4.75	4.56
6. band 6	R_f	0.58	0.56	0.56	0.57 ± 0.007	0.45 - 0.71	2.04
	rRF (M1)	11.60	11.20	11.20	11.33 ± 0.133	9.07 - 14.71	2.04
	rRF (M2)	5.80	5.60	5.60	5.67 ± 0.067	4.53 - 7.08	2.04



5.1.2 Determination of total phenolics

The total phenolic contents of *A. galanga* and *C. aromatica* extracts were determined according to the Folin-Ciocalteu method (Waterman and Mole, 1994). The phenolic contents were found to be a significantly greater in *C. aromatica* than *A. galanga*, approximately 2.8 times, Gallic acid equivalence (GAE) was used to compare phenolic contents of the extracts and was calculated from standard curve of gallic acid (Figure 5.15).

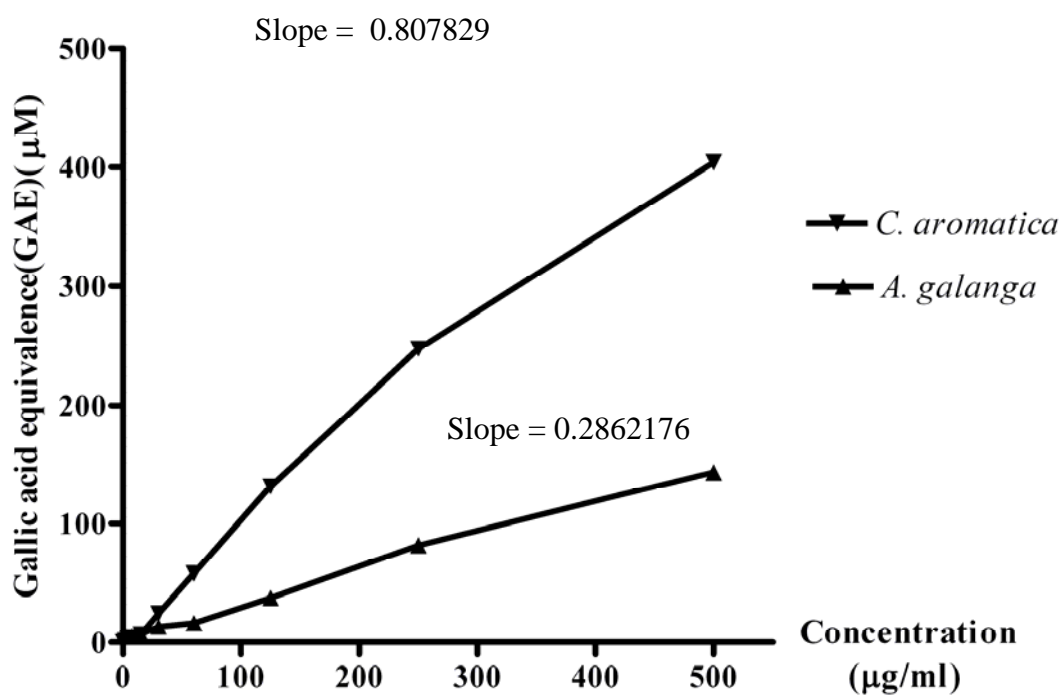
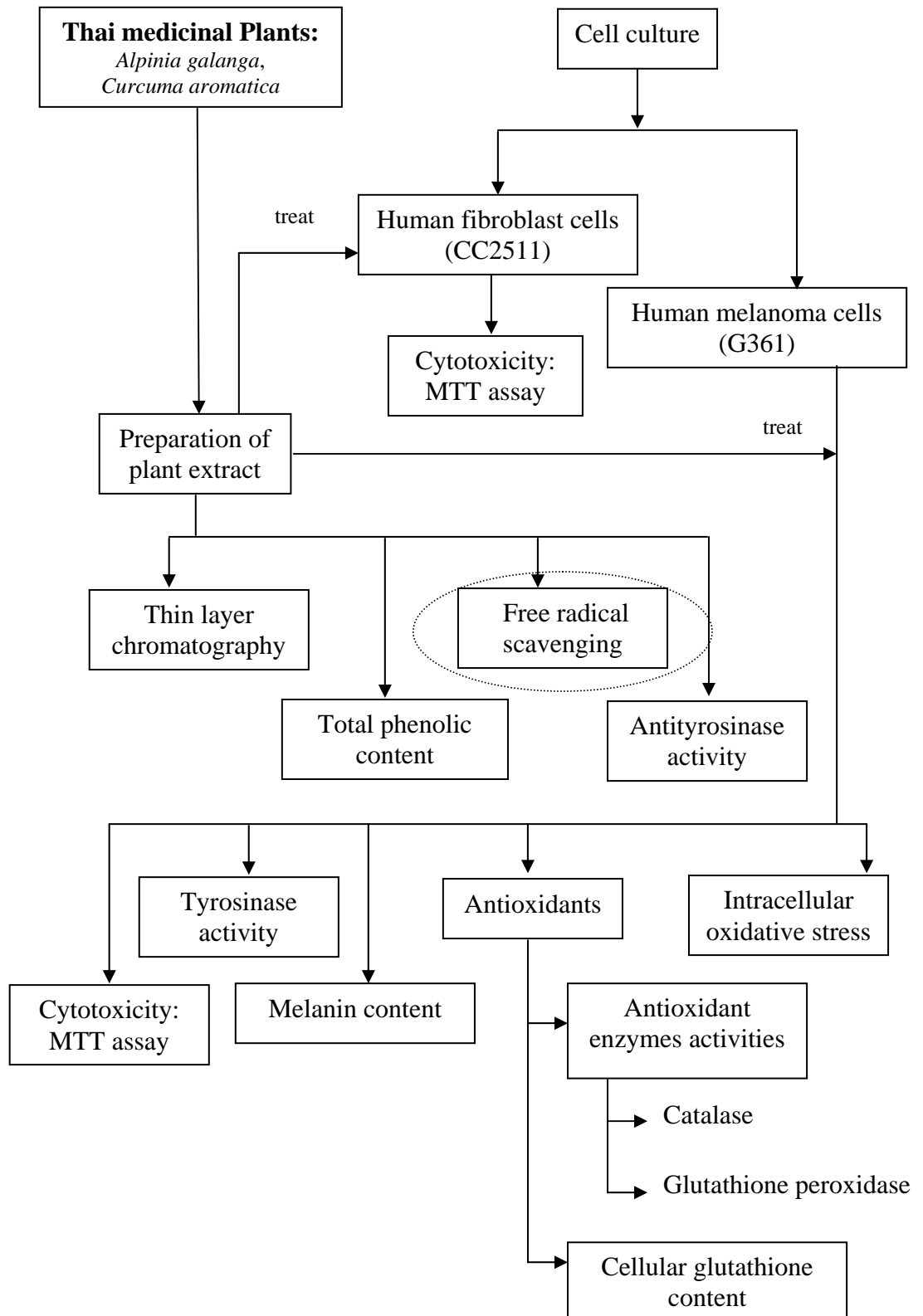


Figure 5.15 Determination of total phenolics contents in extracts of *A. galanga* and *C. aromatica* by Folin-Ciocalteu method. Statistical significance was evaluated using student's unpaired t test. Results were measured spectrophotometrically at 760 nm. Results are expressed as Mean \pm SD of 3 experiments and reported at Gallic Acid Equivalent, GAE.



5.1.3 Free radical scavenging activity assay

The free radical scavenging activity of *A. galanga* and *C. aromatica* extracts were assessed by 1,1-Diphenyl-2-picrylhydrazyl (DPPH) assay. The result in figure 5.16 demonstrates that *A. galanga* and *C. aromatica* extracts exerted hydrogen-donating capacity and have radical scavenging activity in a concentration-dependent manner. In addition, the free radical scavenging activity were greater in *C. aromatica* than *A. galanga* extracts.

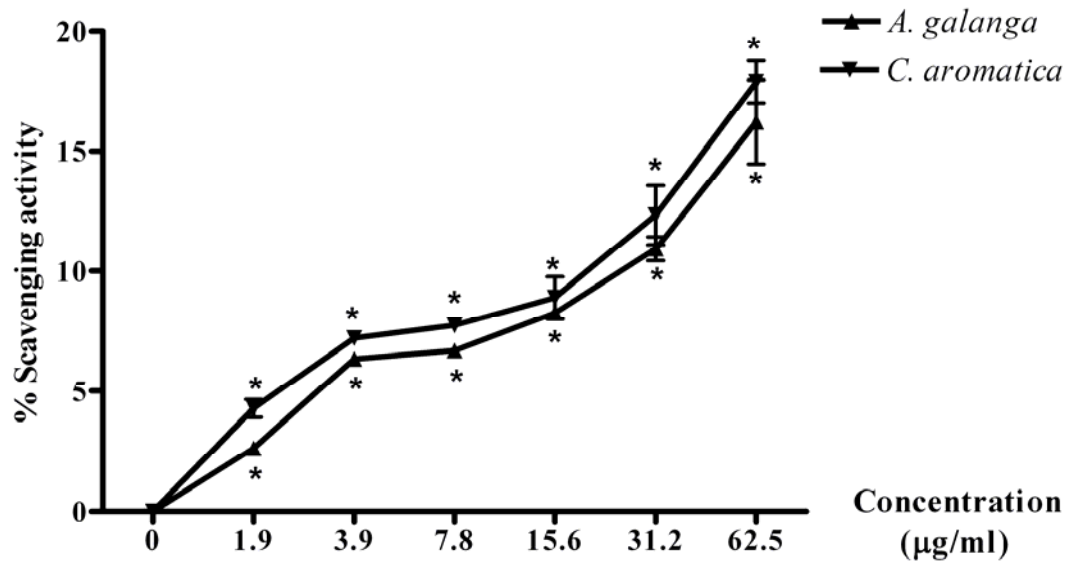
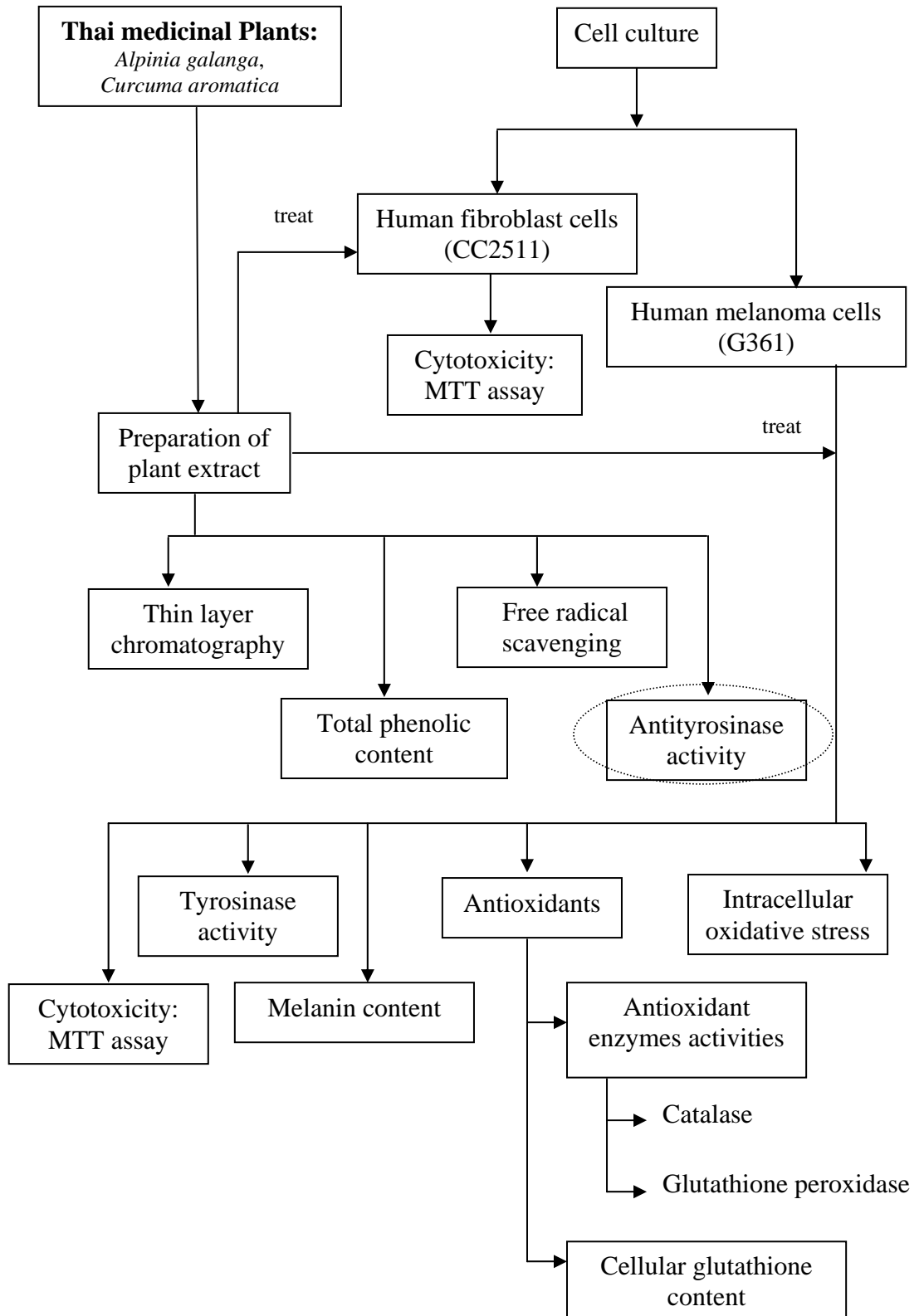


Figure 5.16 The effect of *A. galanga* and *C. aromatica* extracts on free radical scavenging activity. Free radical scavenging activity was measured spectrophotometrically at 520 nm. Results are expressed as Mean \pm SD of 3 experiments. Statistical significance was evaluated using student's unpaired t test. * $P < 0.05$ when compared with each other.



5.1.4 Antityrosinase activities

The effects of *A. galanga* and *C. aromatica* extracts in inhibition of tyrosinase activities were determined according to dopachrome method. The data showed that both extracts were able to inhibit tyrosinase enzyme activities in a concentration-dependent manner and antityrosinase activities were markedly greater in *C. aromatica* than *A. galanga* extracts (Figure 5.17).

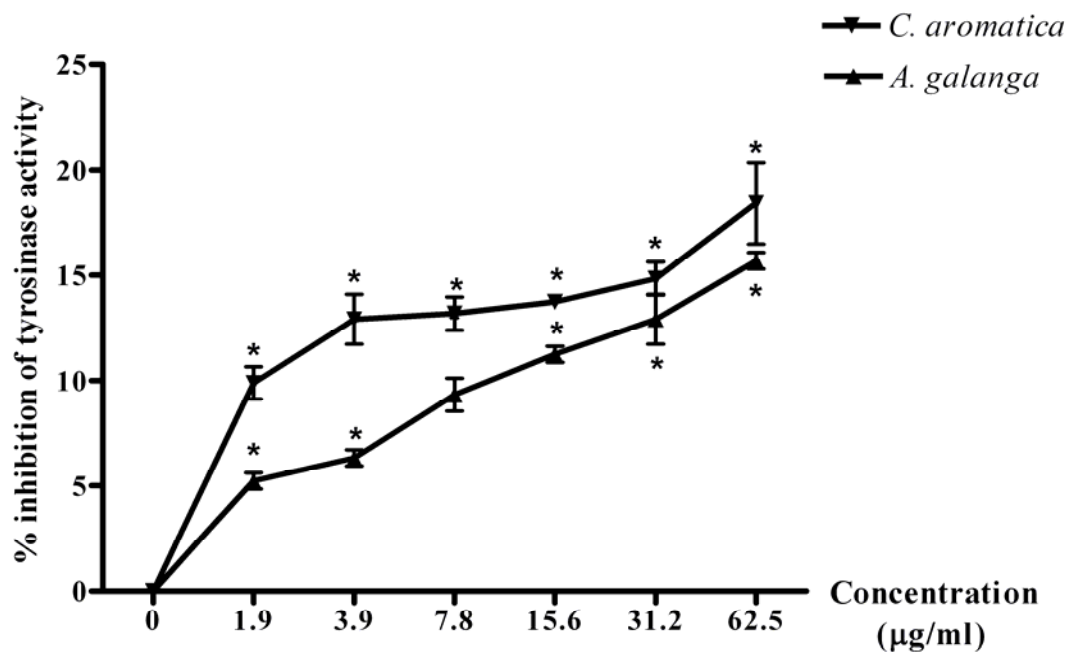
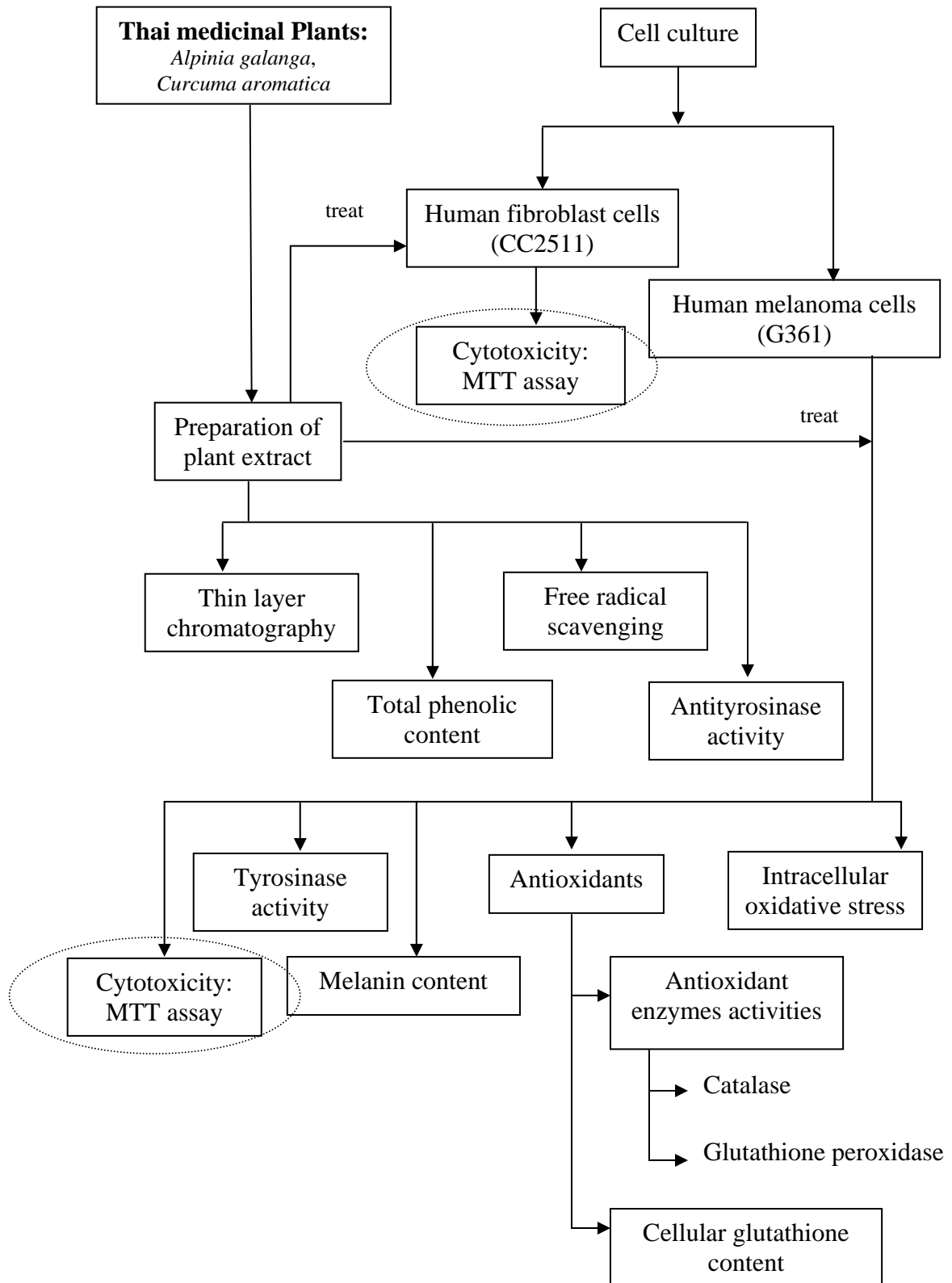


Figure 5.17 Inhibitory effect of *A. galanga* and *C. aromatica* extracts on tyrosinase activities. Antityrosinase activities were measured spectrophotometrically at 475 nm. Results are expressed as Mean \pm SD of 3 experiments. Statistical significance was evaluated using student's unpaired t test. * $P < 0.05$ when compared with the control.



5.2 Cellular study of the effects *A. galanga* and *C. aromatica* extracts in inhibiting UVR-induced melanogenesis.

5.2.1 Assessment of cell viability by MTT reduction assay

5.2.1.1 Cytotoxic effect on CC2511 and G361

In this study, I choosed CC2511 and G361 cells to study the cytotoxic effect of *A. galanga* and *C. aromatica*. While I selected G361 melanoma cells to studied melanogenesis pathway but normal skin cells to confirm cytotoxic effect of plant extracts is important. CC2511, normal human fibroblast is represented a normal skin cells for this study.

The cytotoxic effects of *A. galanga* and *C. aromatic* extracts were examined in CC2511 and G361 cells. When cells were pre-incubated for 24 hr with various concentration of *A. galanga* and *C. aromatica* extracts (0-500 $\mu\text{g/ml}$), the data showed that both extracts were cytotoxic CC2511 cells at high concentrations, higher than 31.25 $\mu\text{g/ml}$ for *A. galanga* extract and higher than 62.5 $\mu\text{g/ml}$ for *C. aromatica* extract (Figure 5.18).

A. galanga and *C. aromatica* extracts have cytotoxicity to G361 cells at high concentrations, higher than 62.5 $\mu\text{g/ml}$ for *A. galanga* extract and higher than 125 $\mu\text{g/ml}$ for *C. aromatica* extract (Figure 5.19).

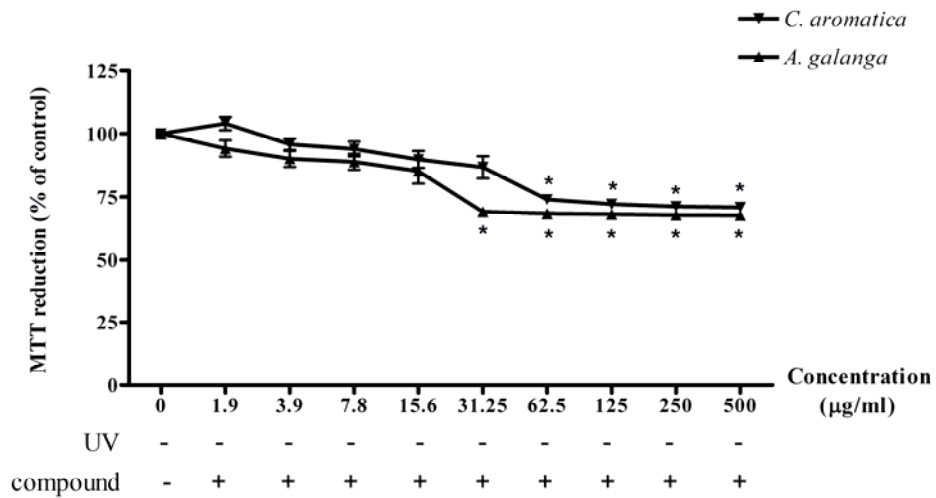


Figure 5.18 Cytotoxicity of *A. galanga* and *C. aromatica* extracts on CC2511 cells. CC2511 cells were pre-incubated with various concentrations of extracts for 24 hr. The cell viability rate was determined by MTT reduction. Results are expressed as Mean \pm sem of 9 experiments. Statistical significance was evaluated using student's unpaired t test. * $P < 0.05$ when compared with the control (Cells in the absence of plant extracts and UV exposed.).

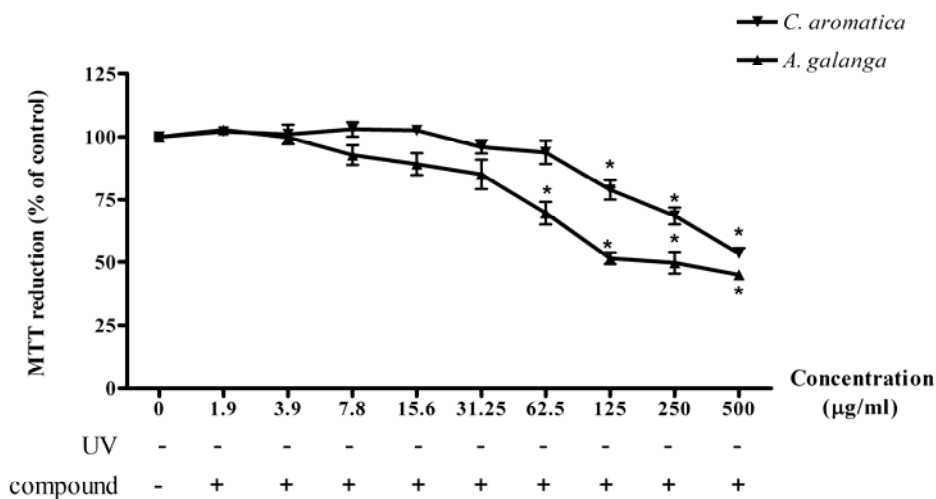


Figure 5.19 Cytotoxicity of *A. galanga* and *C. aromatica* extracts on G361 cells. G361 cells were pre-incubated with various concentrations of extracts for 24 hr. The cell viability rate was determined by MTT reduction. Results are expressed as Mean \pm sem of 9 experiments. Statistical significance was evaluated using student's unpaired t test. * $P < 0.05$ when compared with the control (Cells in the absence of plant extracts and UV exposed.).

5.2.1.2 Assessment of cell viability by MTT reduction assay on G361 cells exposed to UVR.

The effect of UVA (0-64 J/cm²) on cell viability were determined by MTT assay. All dose of UVA (1-64 J/cm²) was shown to provide cytytoxic effect on G361. Figure 5.20 showed that UVA was able to induce cells cytotoxicity in a dose-dependent manner.

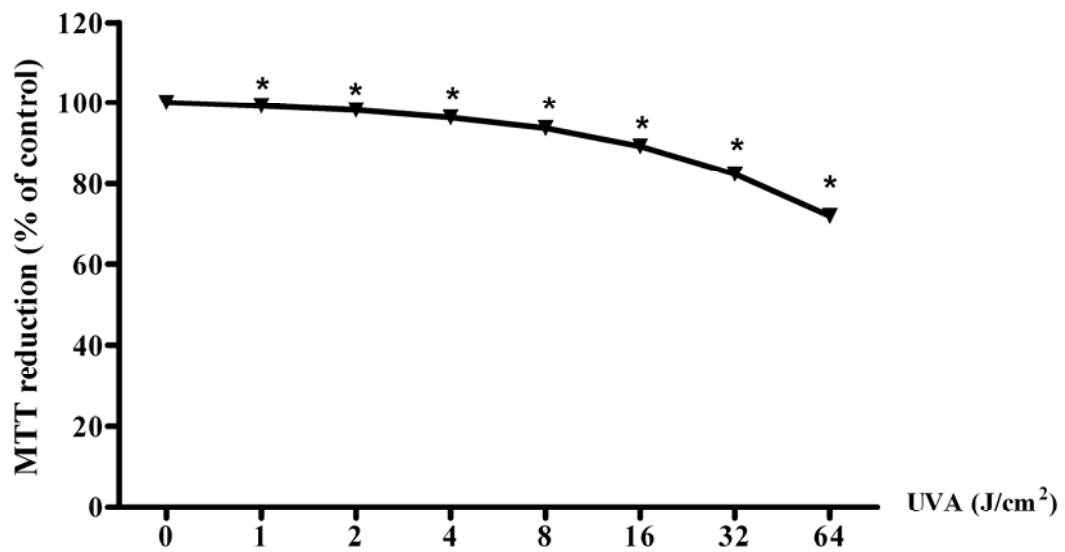


Figure 5.20 Effect of dose of UVA on viability of G361 cells. G361 cells were exposed with various dose of UVA. The cell viability rate was determined by MTT reduction. Results are expressed as Mean \pm sem of 9 experiments. Statistical significance was evaluated using analysis of variance. * $P < 0.05$ when compared with the control (Cells in the absence of UV exposed.).

5.2.1.3 Effects of *A. galanga* and *C. aromatica* extracts on G361 and CC2511 cells exposed to UVR

UVA (64 J/cm²) was shown to provide cytotoxic effect on G361 and CC2511 cells. However, pre-incubation of the cells with *A. galanga* and *C. aromatica* extracts for 30 min before UVR, both extracts were able to inhibit cells cytotoxicity.

Figure 5.21 showed that *A. galanga* and *C. aromatica* extracts have cytotoxicity to CC2511 cells at high concentrations, higher than 125 µg/ml for *A. galanga* extract and higher than 250 µg/ml for *C. aromatica* extract.

Figure 5.22 showed that *A. galanga* and *C. aromatica* extracts have cytotoxicity to G361 cells at high concentrations, higher than 62.5 µg/ml for *A. galanga* extract and higher than 125 µg/ml for *C. aromatica* extract.

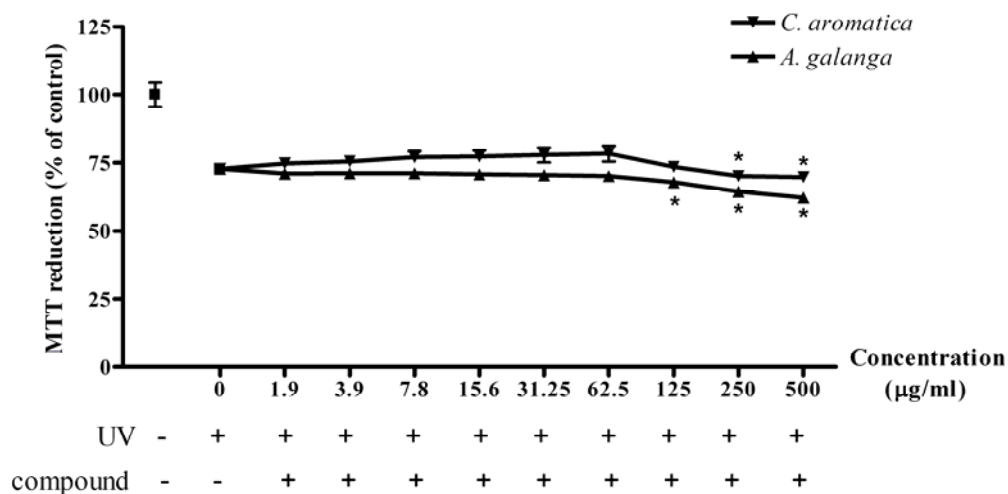


Figure 5.21 The effect of *A. galanga* and *C. aromatica* extracts on CC2511 cells exposed with UVA. CC2511 cells were pre-incubated with various concentrations of extracts for 30 min and exposed to UVA (64 J/cm²). The cell viability was determined by MTT reduction. Results are expressed as Mean ± sem of 9 experiments. Statistical significance was evaluated using analysis of variance. **P*<0.05 when compared with the control (Cells exposed to UVA in the absence of plant extracts.) .

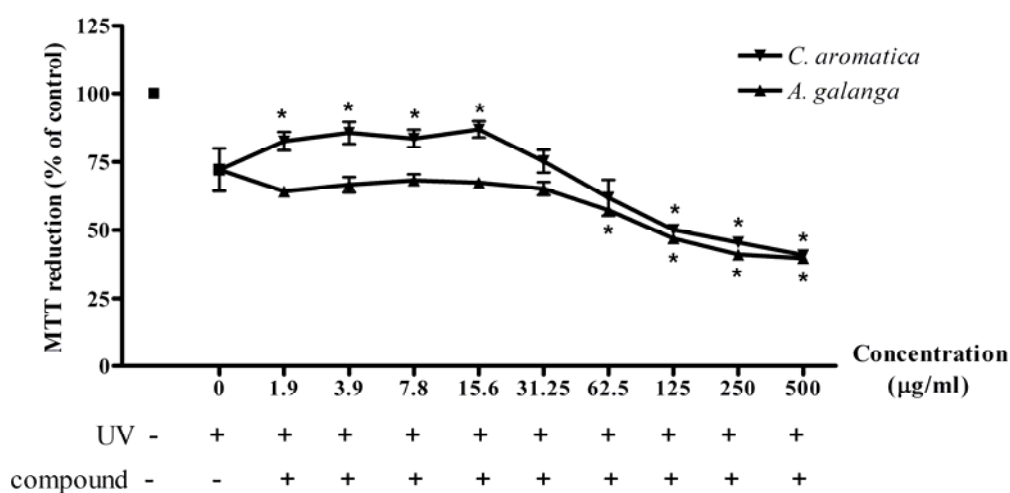
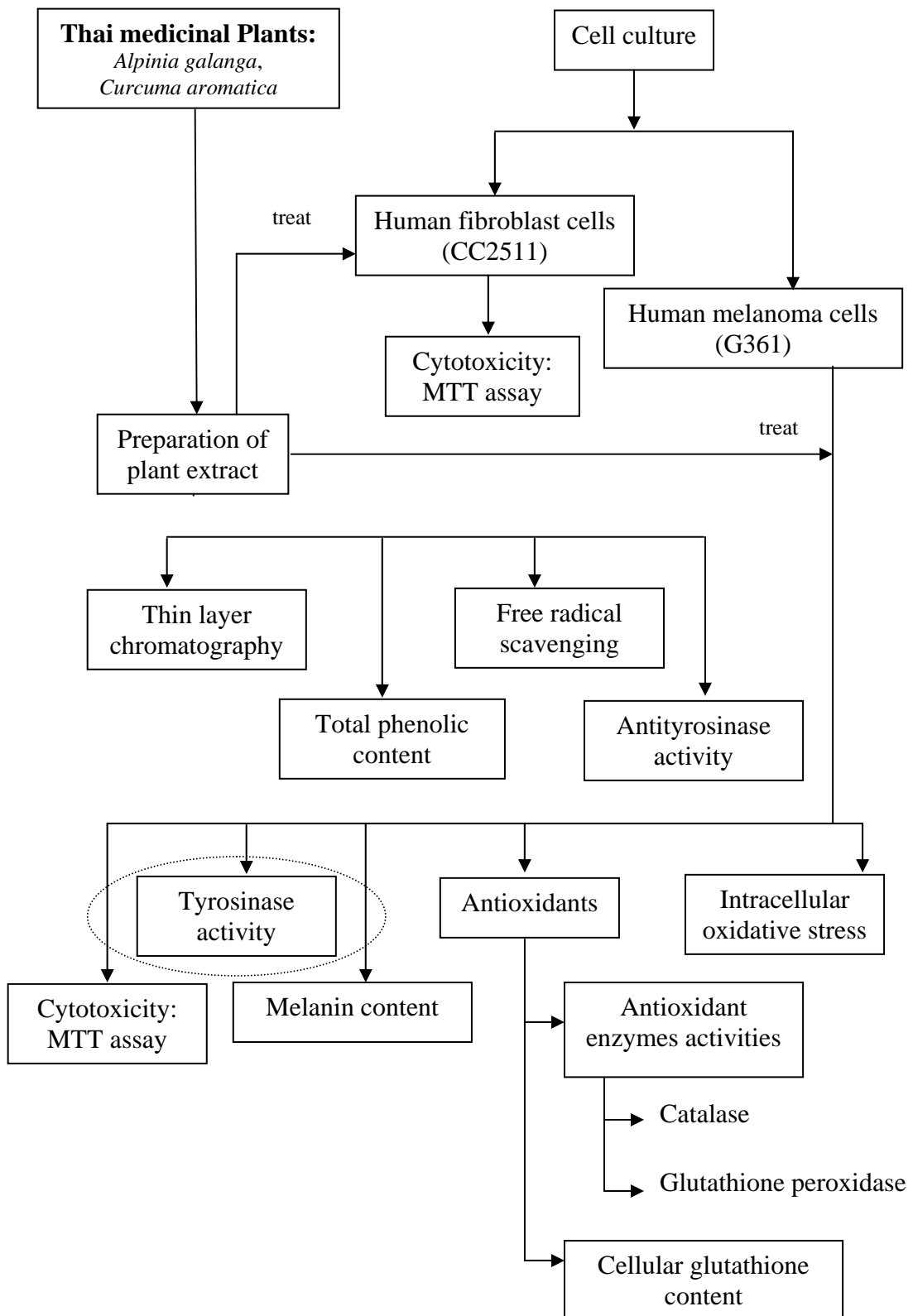


Figure 5.22 The effect of *A. galanga* and *C. aromatica* extracts on G361 cells exposed with UVA. G361 cells were pre-incubated with various concentrations of extracts for 30 min and exposed to UVA (64 J/cm²). The cell viability was determined by MTT reduction. Results are expressed as Mean ± sem of 9 experiments. Statistical significance was evaluated using analysis of variance. **P*<0.05 when compared with the control (Cells exposed to UVA in the absence of plant extracts.) .



5.2.2 Effect on tyrosinase activity

The effect of *A. galanga* and *C. aromatica* extracts on tyrosinase activity was examined in G361 cells. Pre-incubation of the cells with *A. galanga* and *C. aromatica* extracts for 30 min. The data showed that *A. galanga* extract at concentrations 1.9-31.2 µg/ml and *C. aromatica* extract at all concentrations decreased tyrosinase activity (Figure 5.23).

In studying the effects of the extracts on tyrosinase activity in cells exposed to UVA at 8 J/cm², UVA was able to increase tyrosinase activity in G361 cells (Table 5.18, Figure 5.27). However, *A. galanga* extract at concentrations 3.9 - 62.5 µg/ml and *C. aromatica* extract at all concentrations were able to inhibit induction of tyrosinase activity (Figure 5.24).

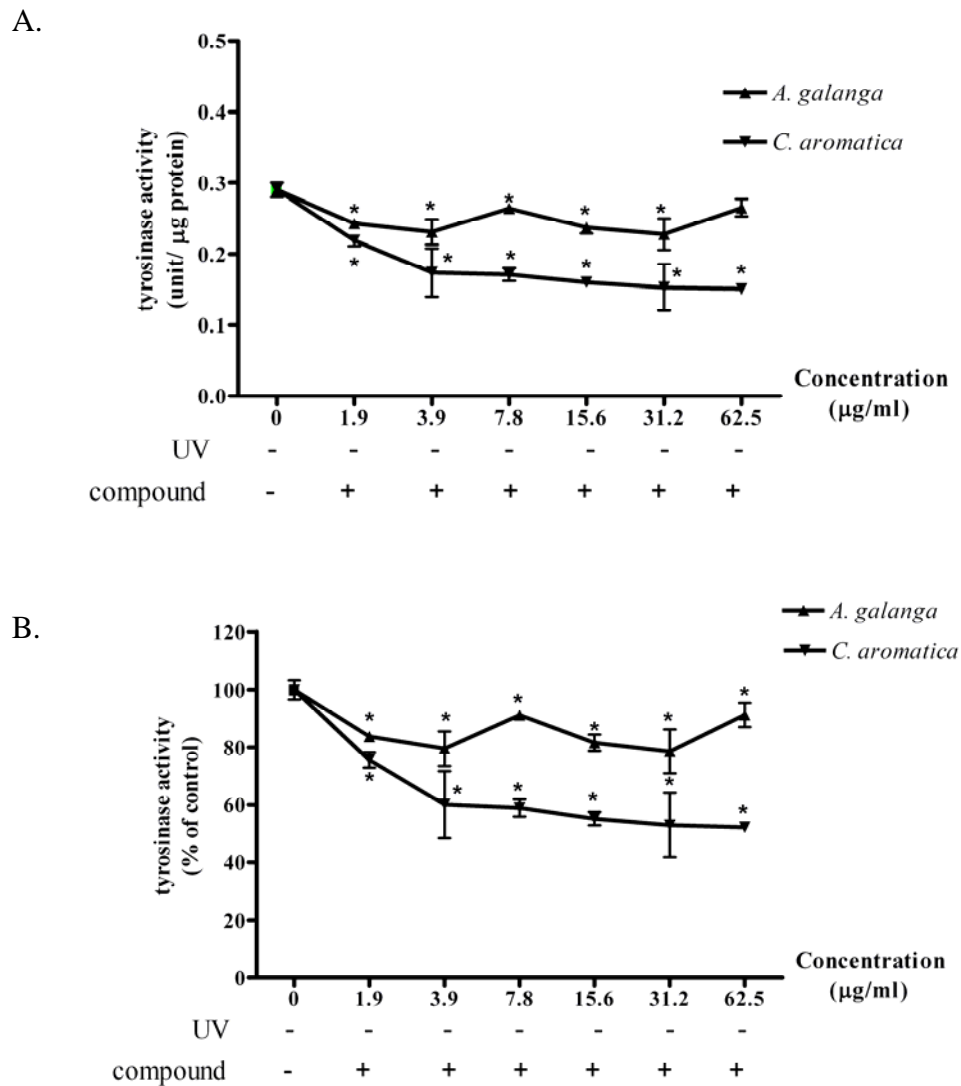
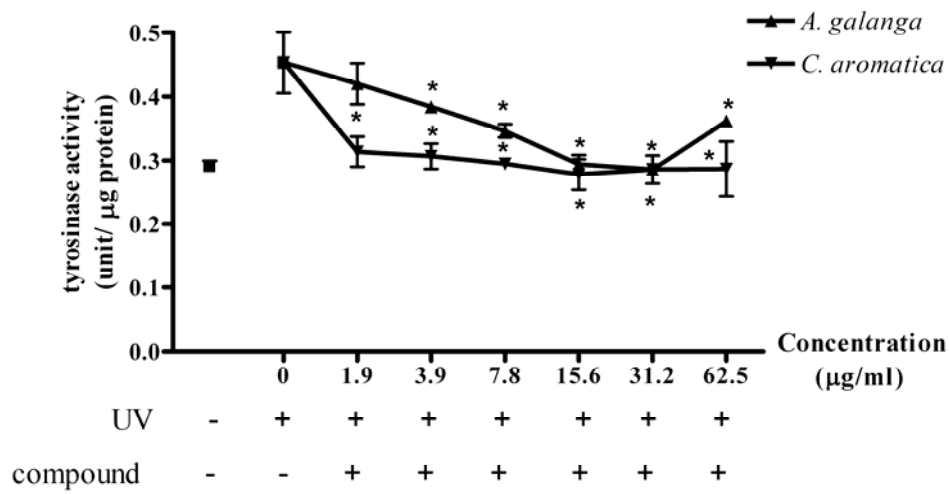


Figure 5.23 The effect of *A. galanga* and *C. aromatica* extracts on tyrosinase activity in G361 cells. Cells were pre-treated with each plant extract for 30 min. Results are expressed as Mean \pm sem of 9 experiments. Statistical significance was evaluated using analysis of variance. * $P < 0.05$ when compared with the control (Cells in the absence of plant extracts and UV exposed.).

A.



B.

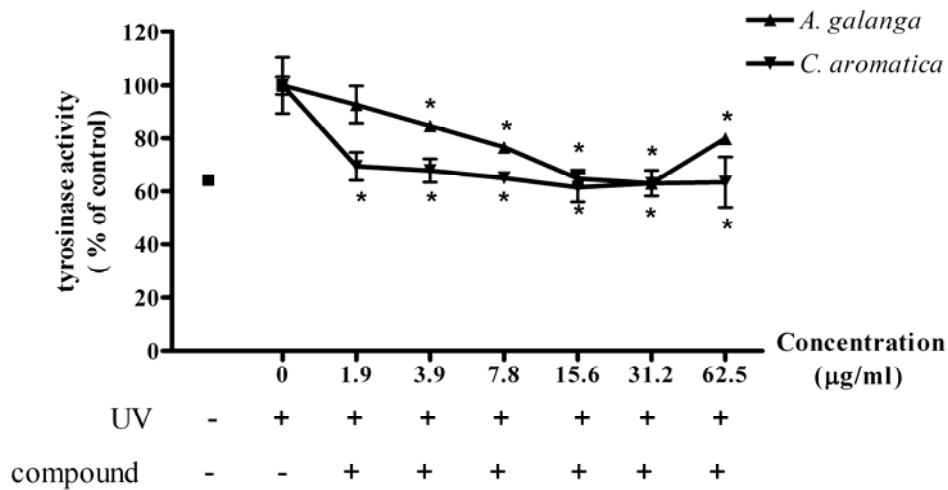
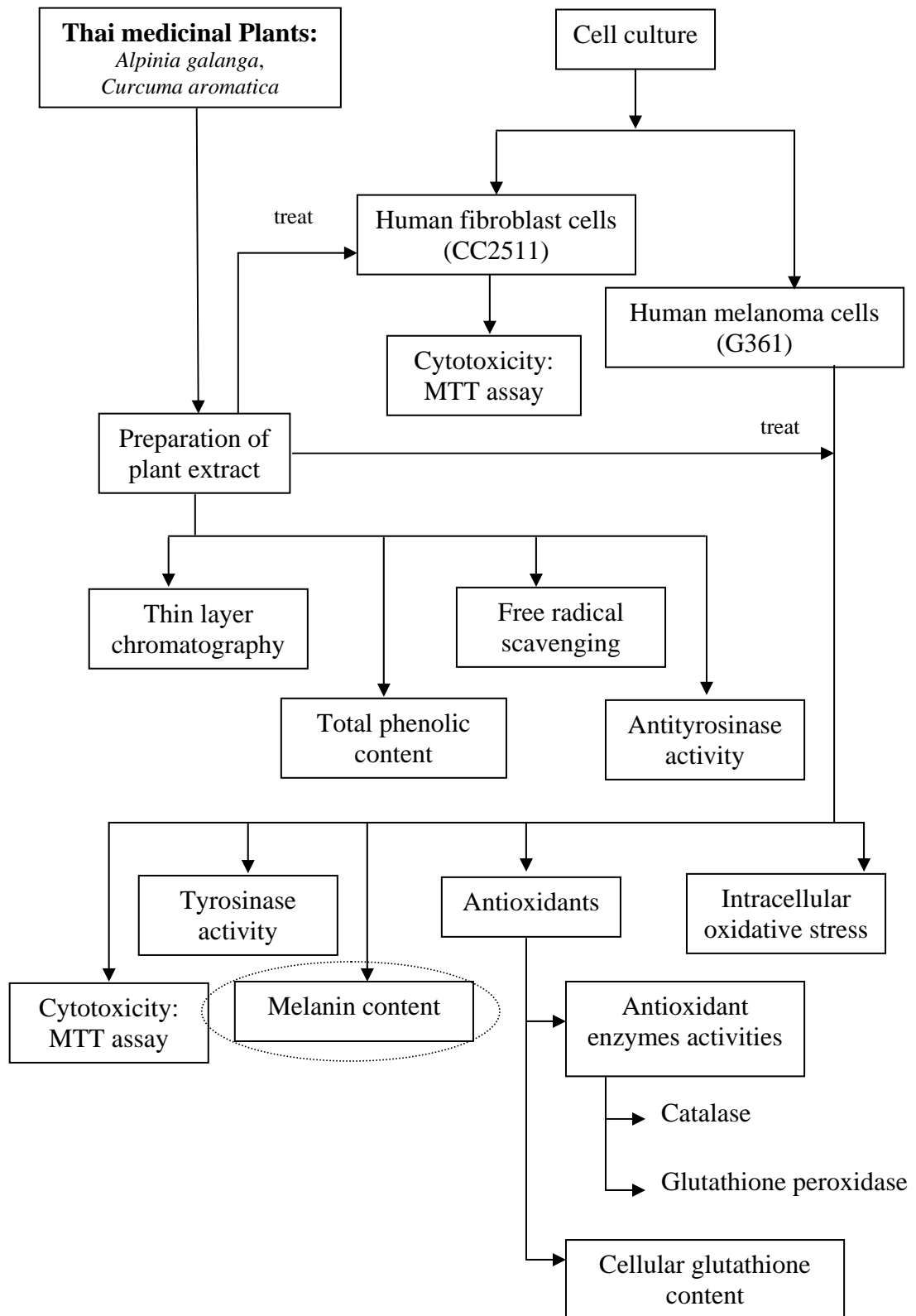


Figure 5.24 The effect of *A. galanga* and *C. aromatica* extracts on tyrosinase activity in G361 cells exposed with UVA. Cells were pre-treated with each plant extract for 30 min and exposed to UVA (8 J/cm²). Results are expressed as Mean ± sem of 9 experiments. Statistical significance was evaluated using analysis of variance. **P*<0.05 when compared with the control (Cells-exposed UVA in the absence of plant extracts.).



5.2.3 Effect on melanin contents

The effects of *A. galanga* and *C. aromatica* extracts on melanin contents were examined in G361 cells. Without UVA exposed, pre-incubation of the cells with *A. galanga* and *C. aromatica* extracts for 30 min. The data showed that melanin contents were not significantly different in the cells treated with both plant extracts (Figure 5.25).

In studying the effects of the extracts on melanin contents in cells exposed to UVA at 8 J/cm², UVA was able to increase melanin content in G361 cells (Table 5.18, Figure 5.27). Nevertheless *A. galanga* extract at concentrations of 15.6 – 31.2 µg/ml and *C. aromatica* extract at all concentrations were capable to inhibit induction of melanin contents (Figure 5.26).

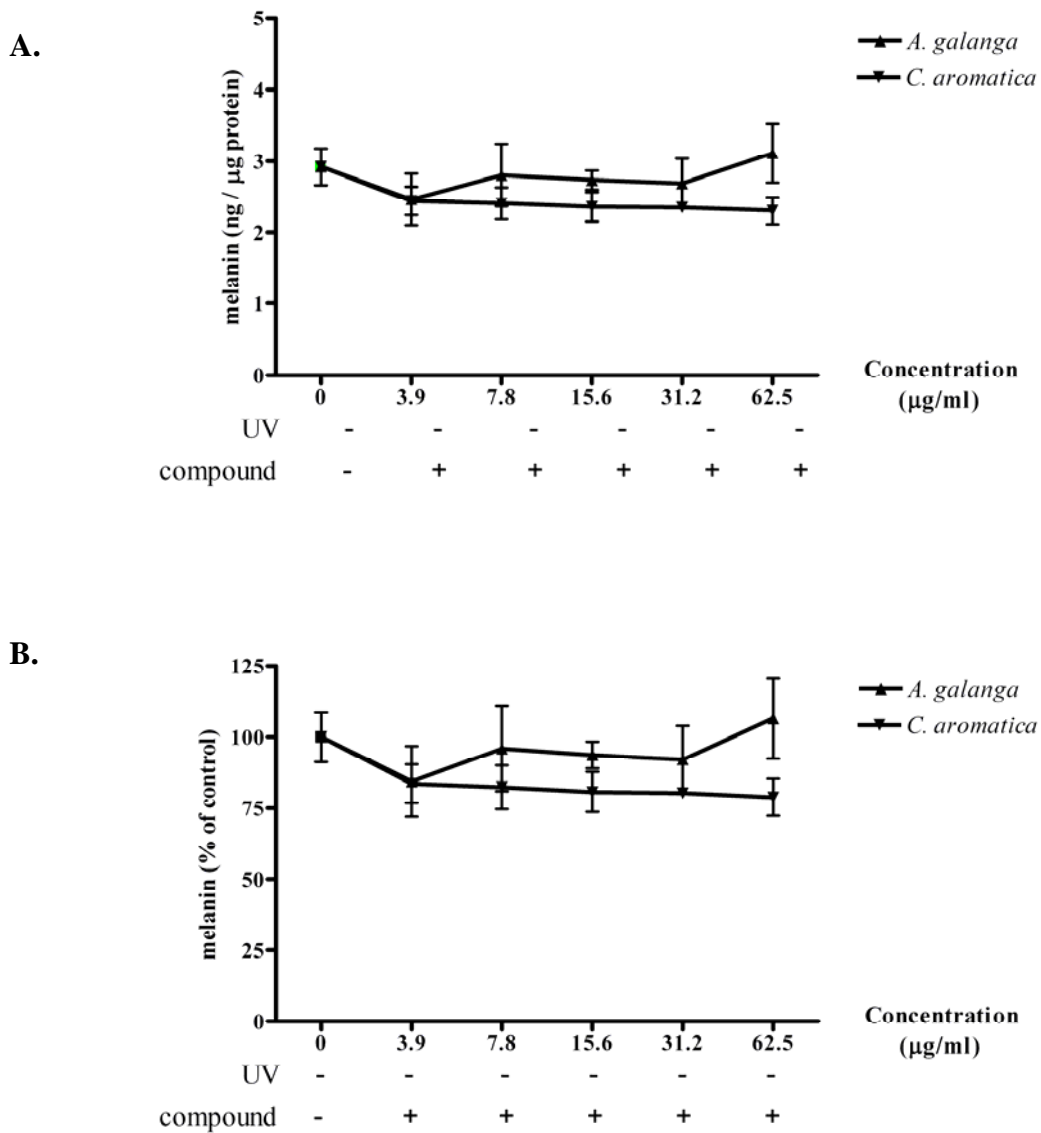


Figure 5.25 The effect of *A. galanga* and *C. aromatica* extracts on melanin contents in G361 cells. Cells were pre-treated with each plant extract for 30 min. Melanin contents were measured spectrophotometrically at 475 nm and using synthetic melanin as a standard. Results are expressed as Mean \pm sem of 3 experiments. Statistical significance was evaluated using analysis of variance. * $P < 0.05$ when compared with the control (Cells in the absence of plant extracts and UV exposed.).

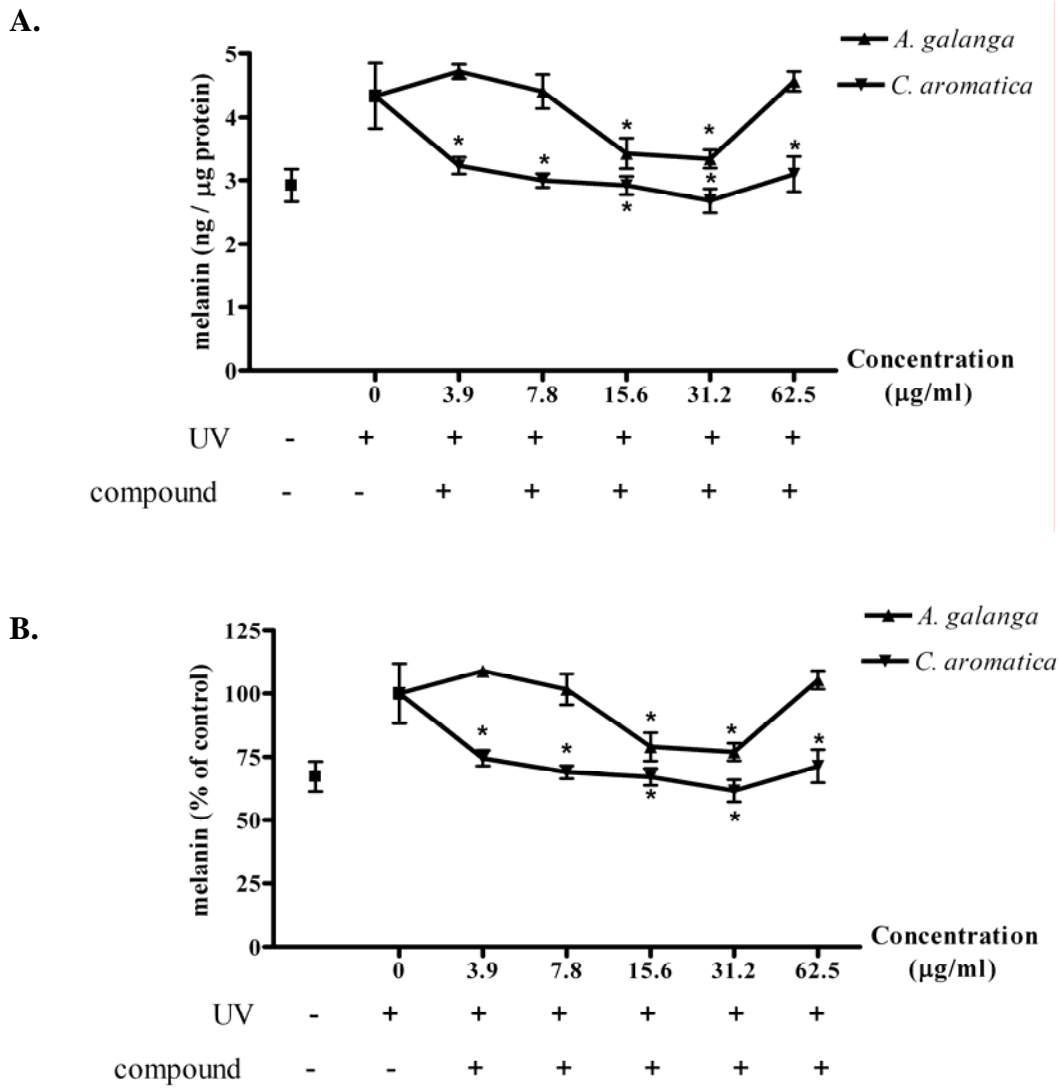


Figure 5.26 The effect of *A. galanga* and *C. aromatica* extracts on melanin contents in G361 cells exposed with UVA. Cells were pre-treated with each plant extract for 30 min and exposed to UVA (8 J/cm²). Melanin contents were measured spectrophotometrically at 475 nm and using synthetic melanin as a standard. Results are expressed as Mean ± sem of 9 experiments. Statistical significance was evaluated using analysis of variance. **P*<0.05 when compared with the control (Cells exposed to UVA in the absence of plant extracts.).

Table 5.18 The effects of UVA on tyrosinase activity and melanin content in G361 cells. The result is compared in % increase (8 J/cm² on tyrosinase activity and 16 J/cm² on melanin content).

% increase	
Tyrosinase activity	Melanin content
35.98 %	32.68 %

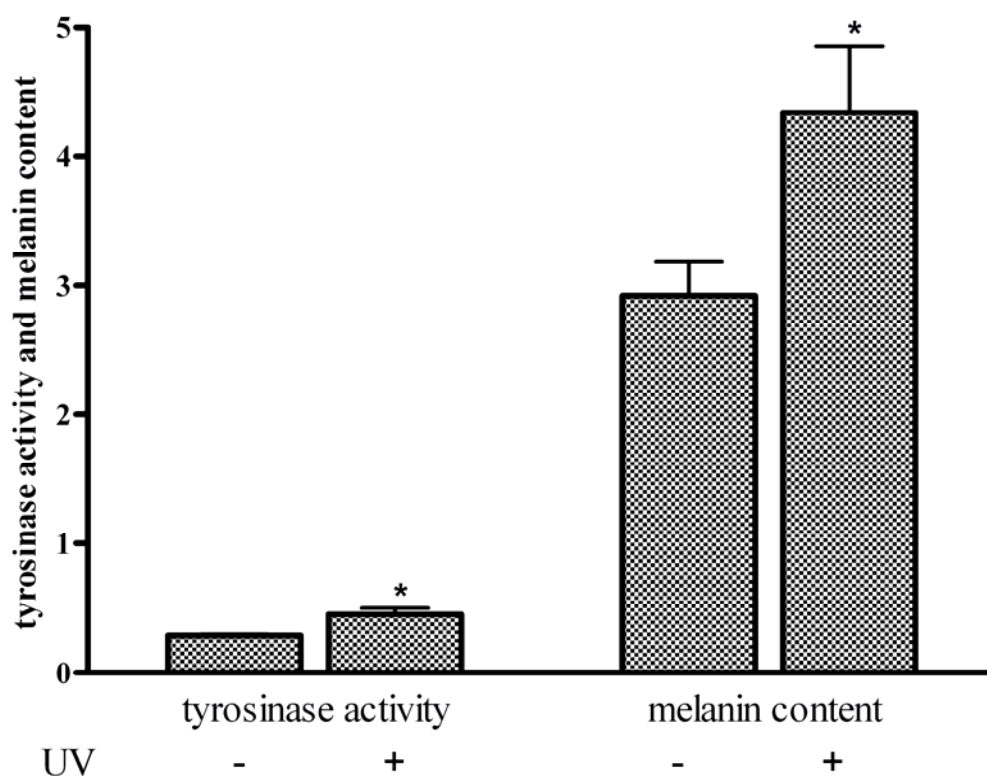
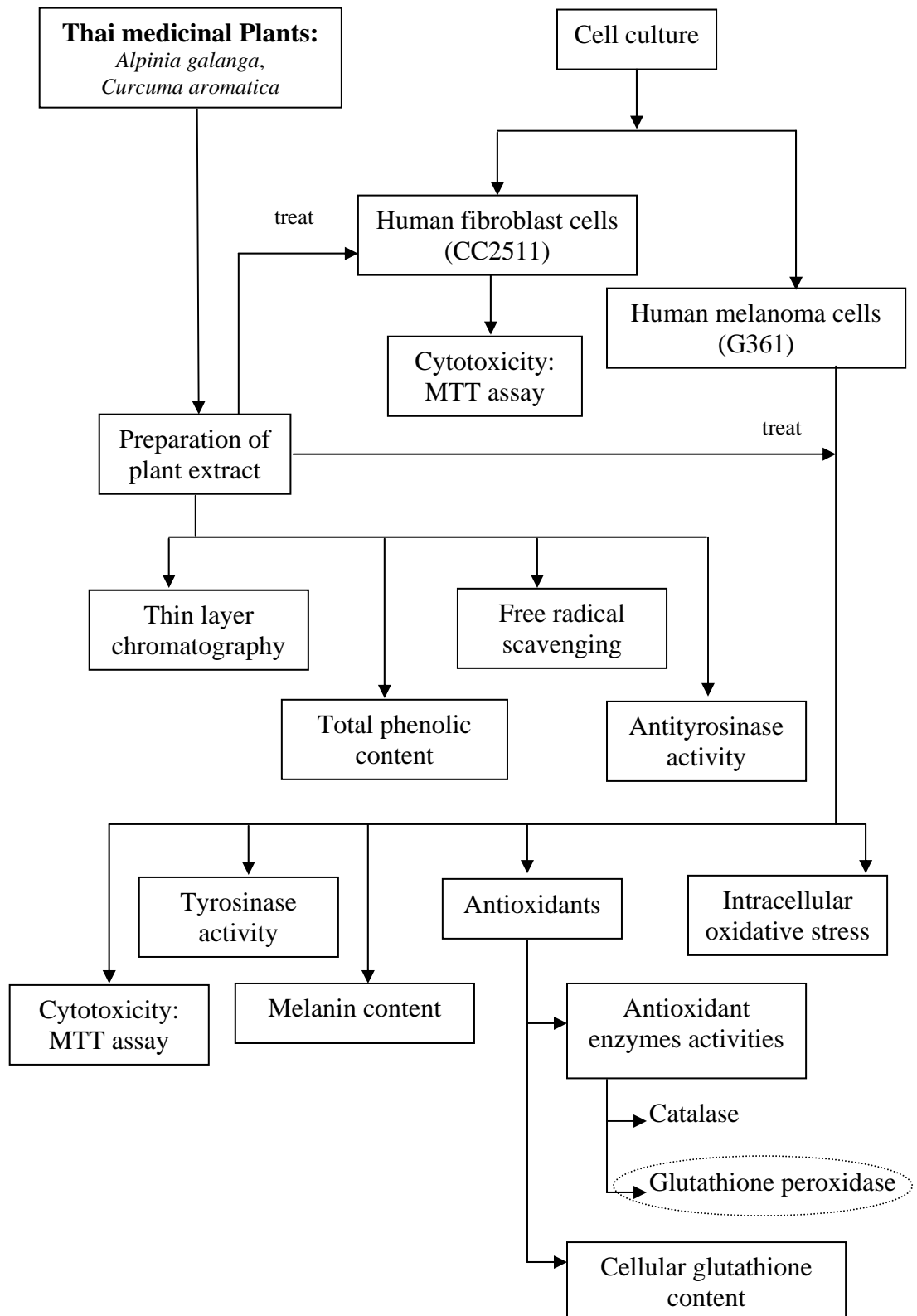


Figure 5.27 The effects of UVA on tyrosinase activity and melanin content in G361 cells. (8 J/cm² on tyrosinase activity and 16 J/cm² on melanin content) The tyrosinase activity is expressed as units per μg of protein and melanin content is expressed as ng per μg of protein. Results are expressed as Mean \pm sem of 9 experiments. Statistical significance was evaluated using analysis of variance. $P < 0.05$ when compared with the control (Cells in the absence of plant extracts).



5.2.4 Assessment of cellular antioxidants

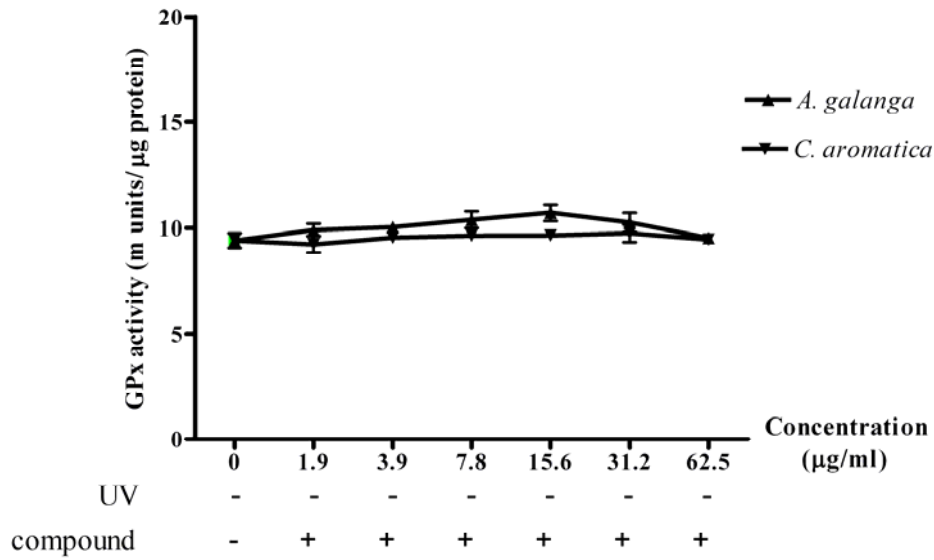
5.2.4.1 Antioxidant enzyme activities

5.2.4.1.1 Glutathione peroxidase (GPx) activity

The effect of *A. galanga* and *C. aromatica* extracts on GPx activity was examined in G361 cells. Pre-incubation of the cells with *A. galanga* and *C. aromatica* extracts for 30 min. The data showed that GPx activity was not significantly different in the cells treated with both plant extracts (Figure 5.28).

In studying activities of GPX in G361 cells exposed to UVA at 8 J/cm², UVR caused a significant decrease in GPX activity in the cells (Table 5.20, Figure 5.32). However, both extracts were able to inhibit UV-induced reduction of the enzyme activity in a concentration-dependent manner (Table 5.19, Figure 5.29).

A.



B.

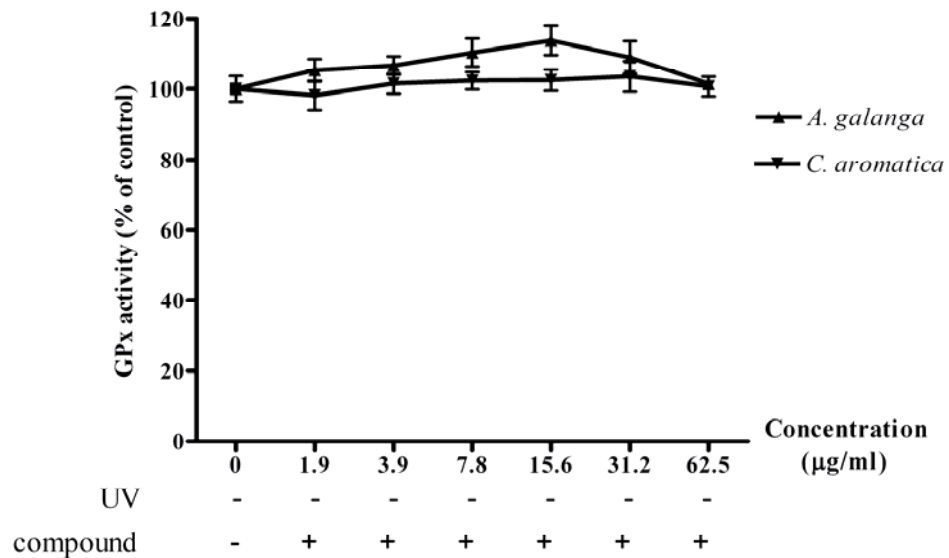
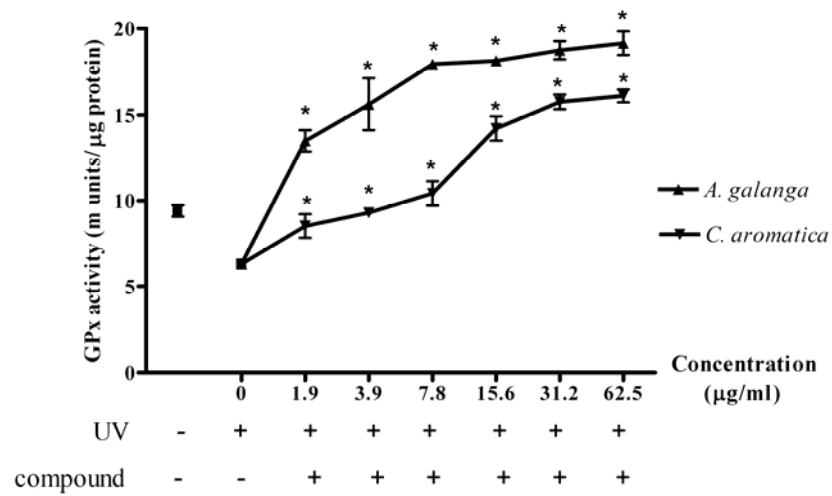


Figure 5.28 The effect of *A. galanga* and *C. aromatica* extracts on GPx activity in G361 cells. Cells were pre-treated with each plant extract for 30 min and GPx activity was measured spectrophotometrically at 340 nm. Results are expressed as Mean \pm sem of 3 experiments. Statistical significance was evaluated using analysis of variance. * $P < 0.05$ when compared with the control (Cells in the absence of plant extracts and UV exposed.).

Table 5.19 EC₅₀ values of herbal extracts on GPx activity in G361 cells exposed with UVA. (8 J/cm²). Values given are means (µg/ml) ± sem.

Herbal extracts	(Means) EC₅₀ (µg/ml) ± SEM	<i>p</i>-value
<i>A. galanga</i>	< 1.9	< 0.05
<i>C. aromatica</i>	4.3545 ± 0.2954	< 0.05

A.



B.

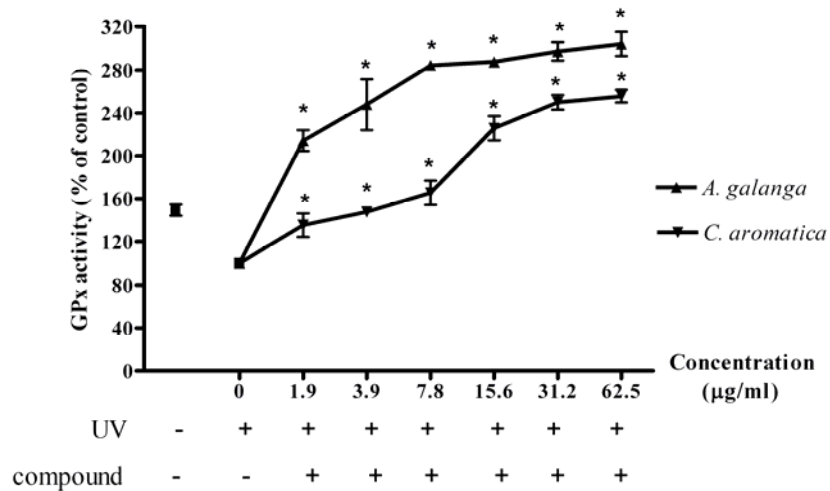
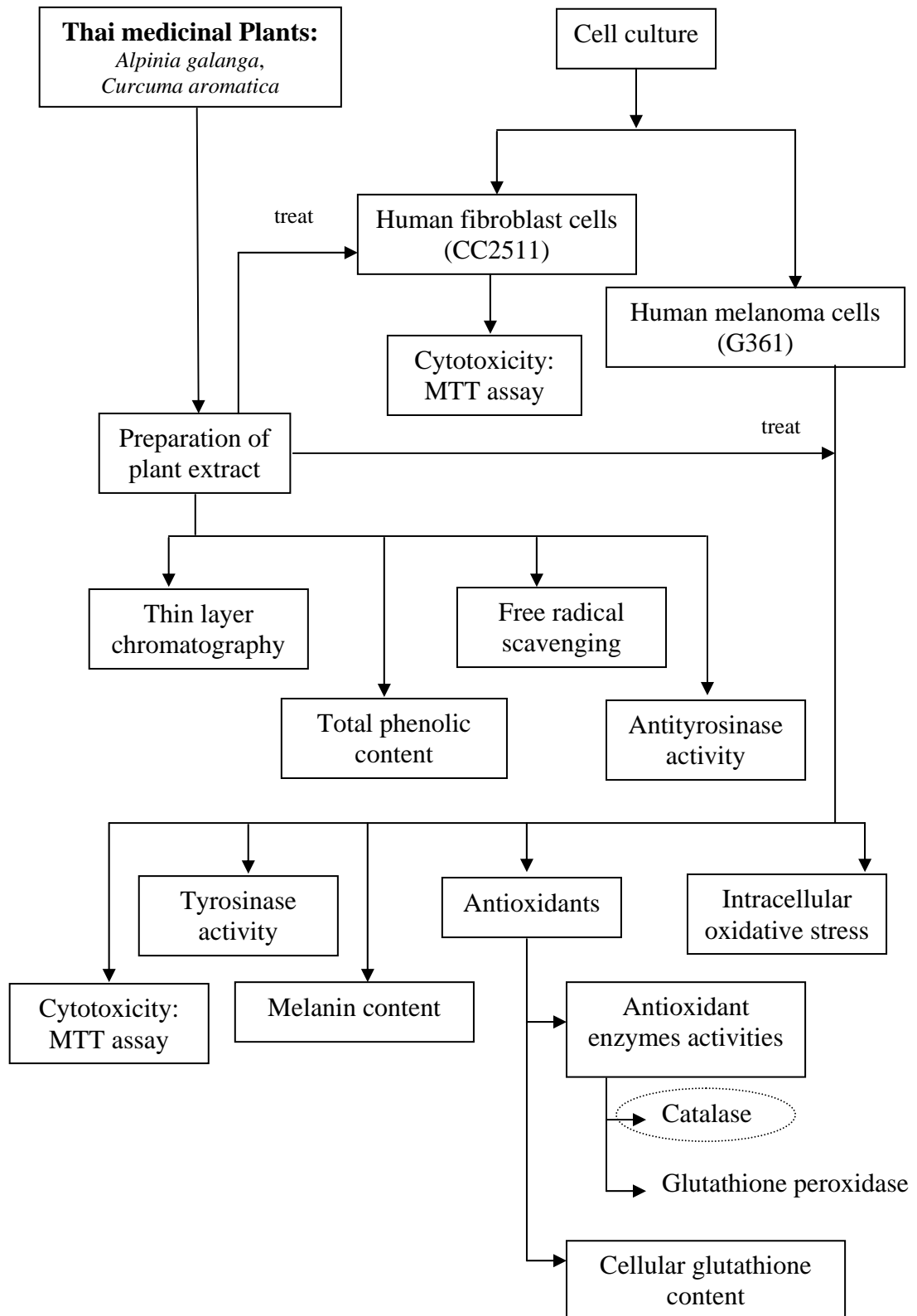


Figure 5.29 The effect of *A. galanga* and *C. aromatica* extracts on GPx activity in G361 cells exposed with UVA. Cells were pre-treated with each plant extract for 30 min and exposed to UVA (8 J/cm²). GPx activity was measured spectrophotometrically at 340 nm. Results are expressed as Mean ± sem of 9 experiments. Statistical significance was evaluated using analysis of variance. **P*<0.05 when compared with the control (Cells exposed to UVA in the absence of plant extracts).

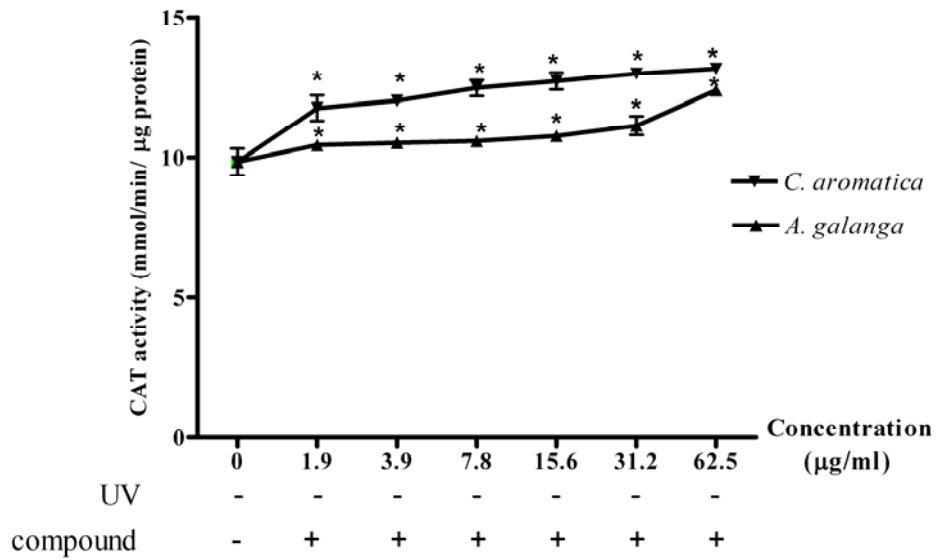


5.2.4.1.2 Catalase (CAT) activity

The effect of *A. galanga* and *C. aromatica* extracts on CAT activity was examined in G361 cells. Pre-incubation of the cells with *A. galanga* and *C. aromatica* extracts for 30 min. The data showed that both extracts were able to increase the enzyme activity in a concentration-dependent manner (Figure 5.30).

In studying of the effects of the extracts on CAT activity in cells exposed to UVA at 8 J/cm², UVR could reduce CAT activity in the cells (Table 5.20, Figure 5.32). However, the extracts of *C. aromatica* at all concentrations, but not *A. galanga* extracts were able to inhibit reduction of the enzyme activity in the cells exposed with UVA (Figure 5.31).

A



B.

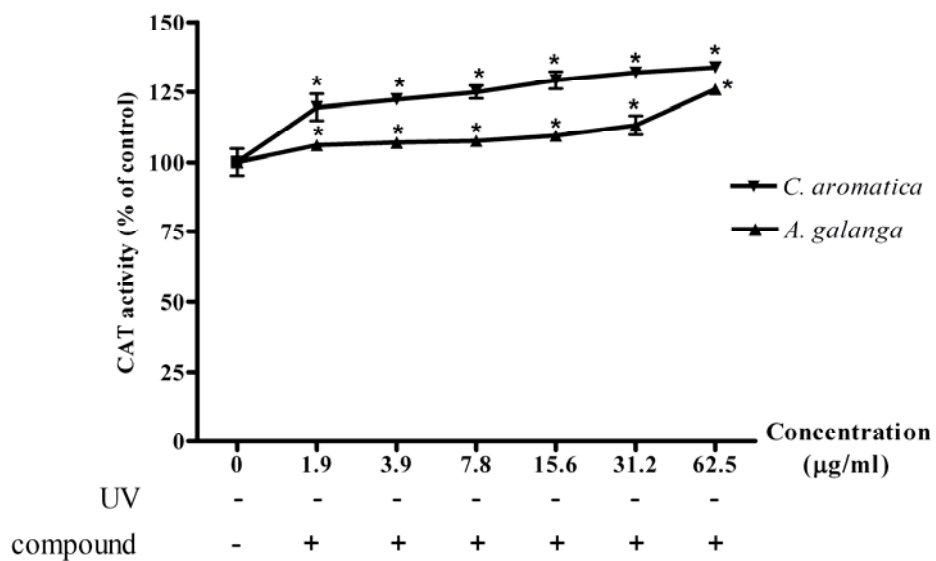


Figure 5.30 The effect of *A. galanga* and *C. aromatica* extracts on CAT activity in G361 cells. Cells were pre-treated with each plant extract for 30 min and CAT activity was measured spectrophotometrically at 540 nm. Results are expressed as Mean \pm sem of 9 experiments. Statistical significance was evaluated using analysis of variance. * $P < 0.05$ when compared with the control (Cells in the absence of plant extracts and UV exposed.).

A.

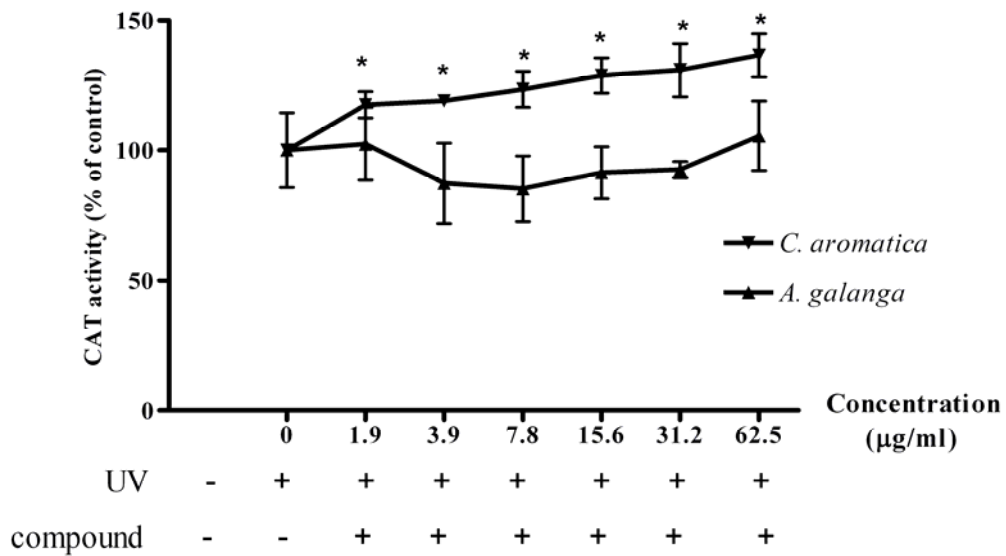
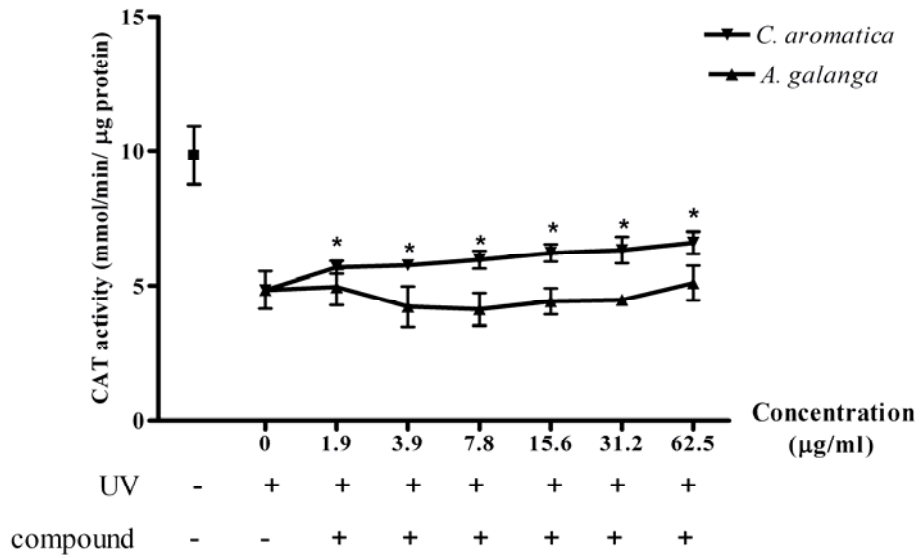


Figure 5.31 The effect of *A. galanga* and *C. aromatica* extracts on CAT activity in G361 cells exposed with UVA. Cells were pre-treated with each plant extract for 30 min and exposed to UVA (8 J/cm²). CAT activity was measured spectrophotometrically at 540 nm. Results are expressed as Mean ± sem of 9 experiments. Statistical significance was evaluated using analysis of variance. *P<0.05 when compared with the control (Cells exposed to UVA in the absence of plant extracts).

Table 5.20 The effects of UVA on CAT and GPx activities in G361 cells (8 J/cm^2). The result is compared in % decrease of enzyme activity.

% decrease of enzyme activity	
CAT	GPx
50.74 %	33.10 %

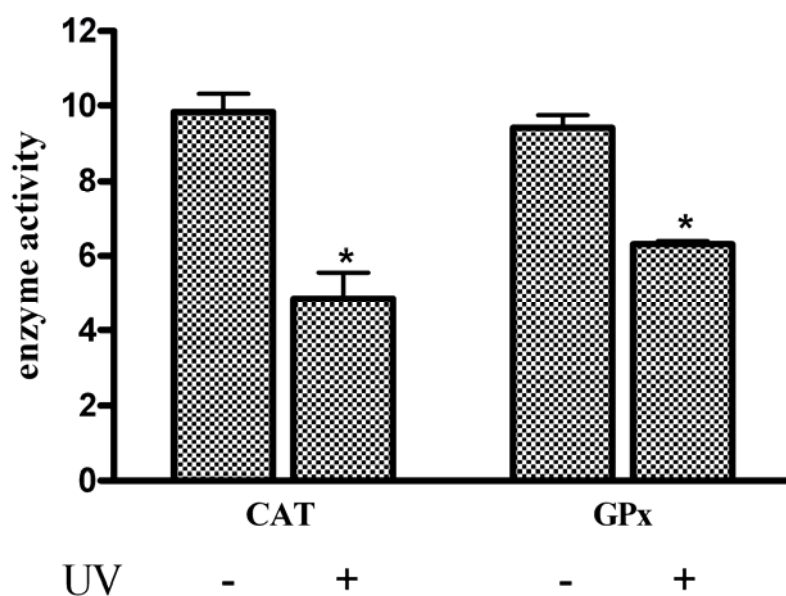


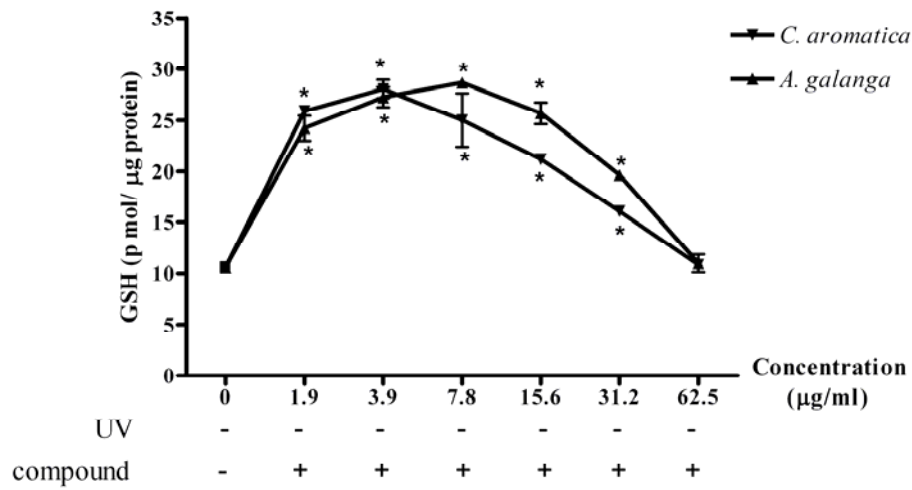
Figure 5.32 The effects of UVA on CAT and GPx activities in G361 cells (8 J/cm^2). The GPx activity is expressed as average enzyme m units per μg of protein and CAT activity is expressed as average enzyme mmol per min per μg of protein. Results are expressed as Mean \pm sem of 9 experiments. Statistical significance was evaluated using analysis of variance. * $P < 0.05$ when compared with the control (Cells-exposed UVA in the absence of plant extracts.).

5.2.4.2 Cellular glutathione contents

The effect of *A. galanga* and *C. aromatica* extracts on glutathione contents was examined in G361 cells. Pre-incubation of the cells with *A. galanga* and *C. aromatica* extracts for 24 h. *A. galanga* and *C. aromatica* extracts at concentration 1.9-31.2 µg/ml increased intracellular GSH contents (Figure 5.33).

In studying the effects of the extracts on GSH content in cells exposed to UVA at 8 J/cm², UVA was able to decrease the contents of GSH in melanoma cells (Table 5.21, Figure 5.35). However both extracts at concentration 1.9-15.6 µg/ml could protect GSH depletion from UVR. Nevertheless, a decrease in GSH content was found in cells pre-incubated with *A. galanga* extract at concentration 62.5 µg/ml (Figure 5.34).

A.



B.

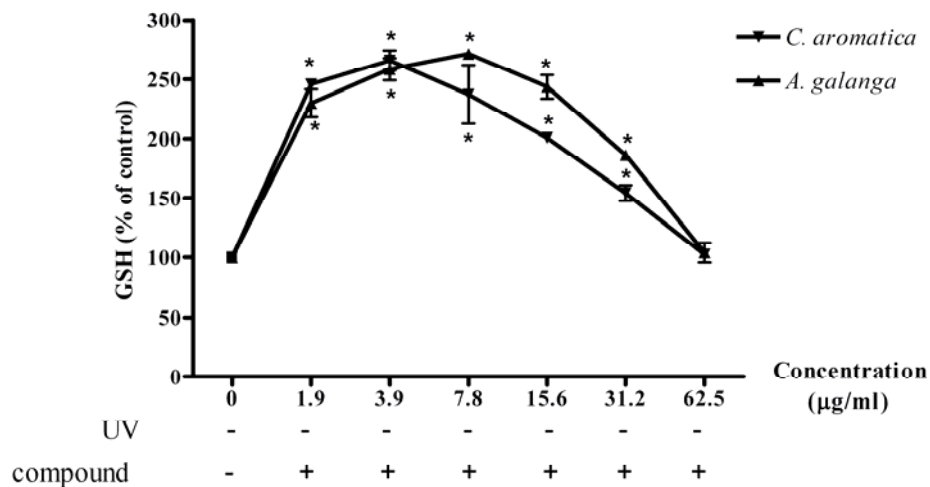
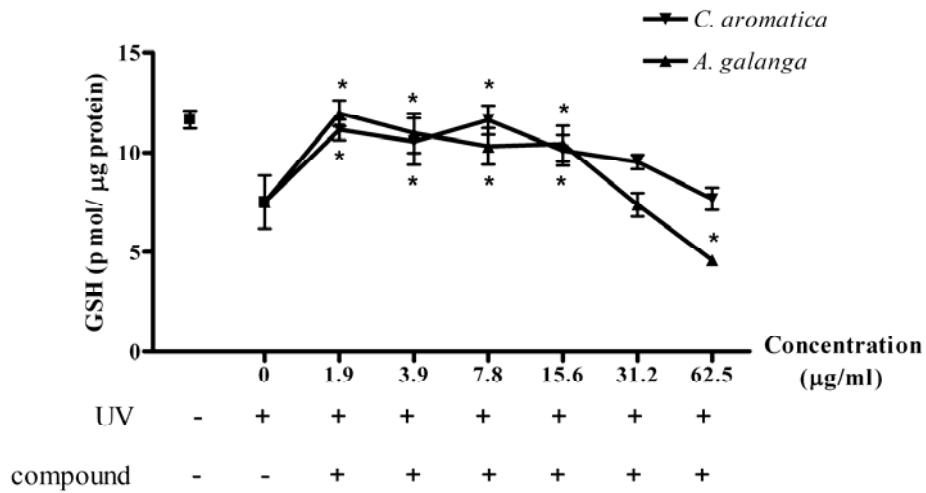


Figure 5.33 The effect of *A. galanga* and *C. aromatica* extracts on intracellular GSH contents in G361 cells. Cells were pre-treated with each plant extract for 24 h. Intracellular GSH contents were measured using OPA probe reacting specifically with GSH. The GSH content is expressed as pmole per µg of protein. Results are expressed as Mean ± sem of 9 experiments. Statistical significance was evaluated using analysis of variance. * $P < 0.05$ when compared with the control (Cells in the absence of plant extracts and UV exposed.)

A.



B.

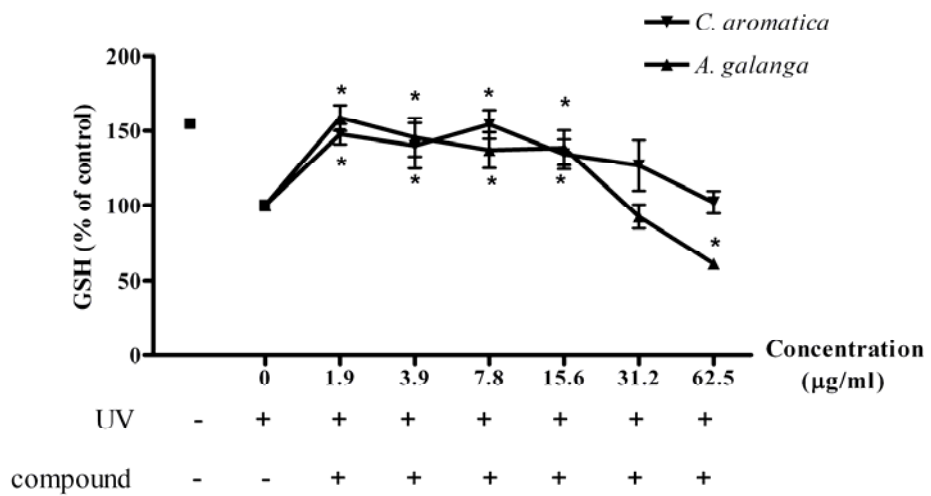


Figure 5.34 The effect of *A. galanga* and *C. aromatica* extracts on intracellular GSH contents in G361 cells exposed with UVA. Cells were pre-treated with each plant extract for 30 min and exposed to UVA (8 J/cm²). Intracellular GSH contents were measured using OPA probe reacting specifically with GSH. Results are expressed as Mean ± sem of 9 experiments. Statistical significance was evaluated using analysis of variance. **P*<0.05 when compared with the control (Cells exposed to UVA in the absence of plant extracts)

Table 5.21 The effects of UVA on GSH contents in G361 cells. The result is compared in % decrease of GSH contents (8 J/cm²).

% decrease of GSH contents
35.31 %

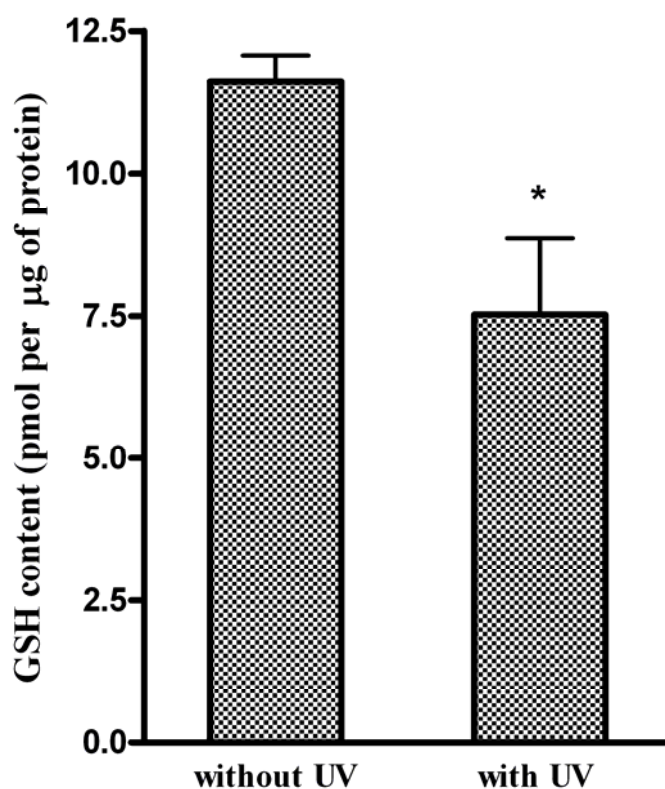
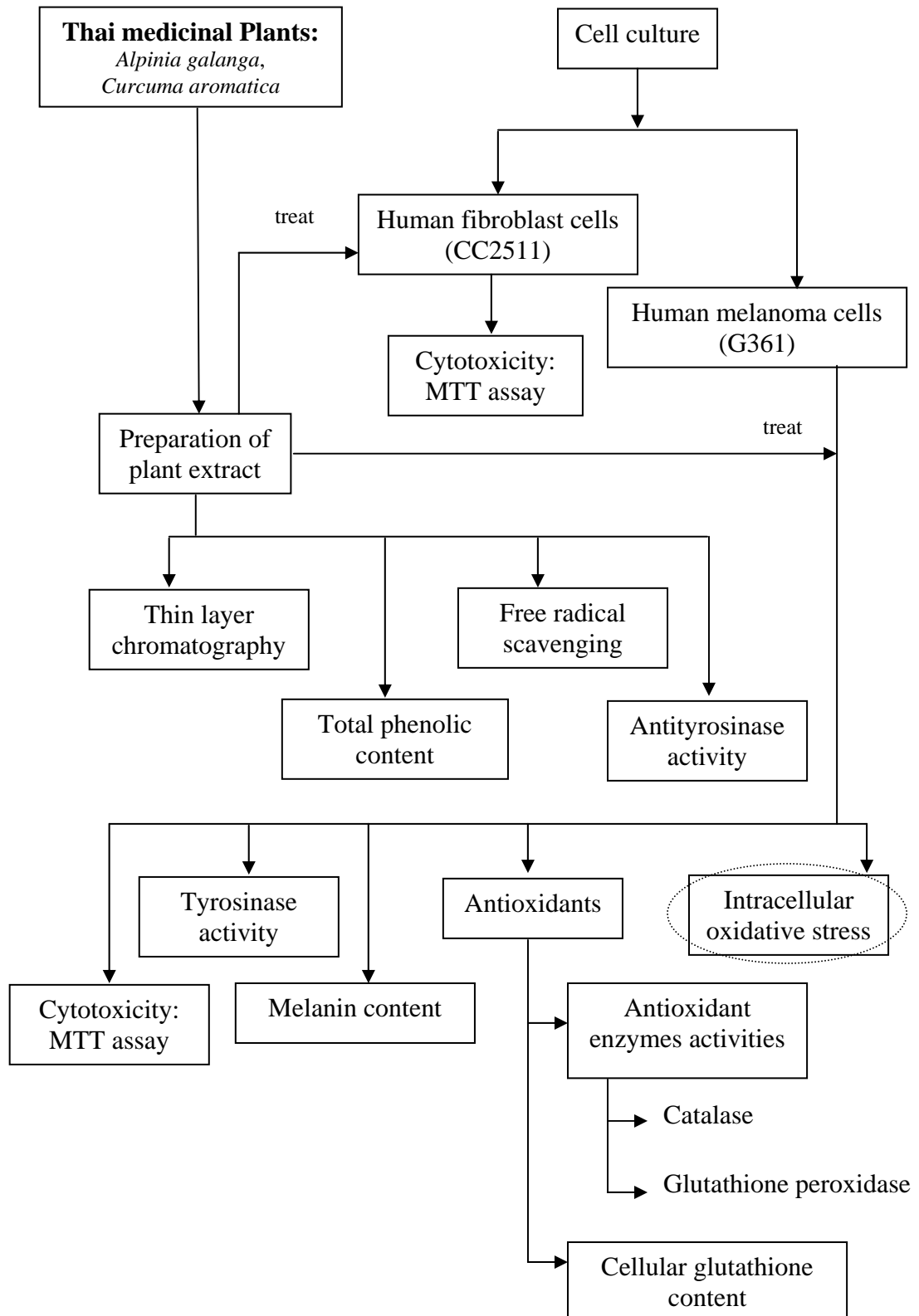


Figure 5.35 The effects of UVA on GSH content in G361 cells (8 J/cm²). Results are expressed as Mean ± sem of 9 experiments. Statistical significance was evaluated using analysis of variance. **P*<0.05 when compared with the control (Cells-exposed UVA in the absence of plant extracts).



5.2.5 Effect on intracellular oxidative stress

The generation processes of reactive oxygen species in G361 cells, as assessed by using DCF fluorescence intensity (excitation 485 nm/emission 530 nm). Cells were pre-treated with each plant extract for 30 min. The data showed that both extracts were able to decrease ROS production in a concentration-dependent manner (Figure 5.36).

In studying of the effects of the extracts on ROS production in cells exposed to UVA at 16 J/cm^2 , UVR could induce ROS production in the cells. The data showed that both extracts were able to decrease ROS production in a concentration-dependent manner in the cells exposed with UVA (Figure 5.37).

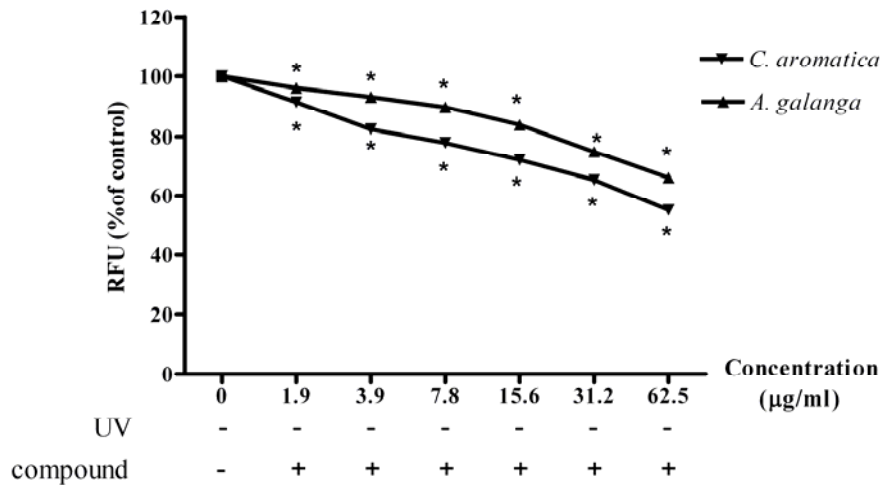


Figure 5.36 The effects of *A. galanga* and *C. aromatica* extracts on the inhibition of ROS in G361 cells. Cells were pre-treated with each plant extract for 30 min. Results are expressed as Mean \pm sem of 9 experiments. Statistical significance was evaluated using analysis of variance. * $P < 0.05$ when compared with the control (Cells in the absence of plant extracts and UV exposed.).

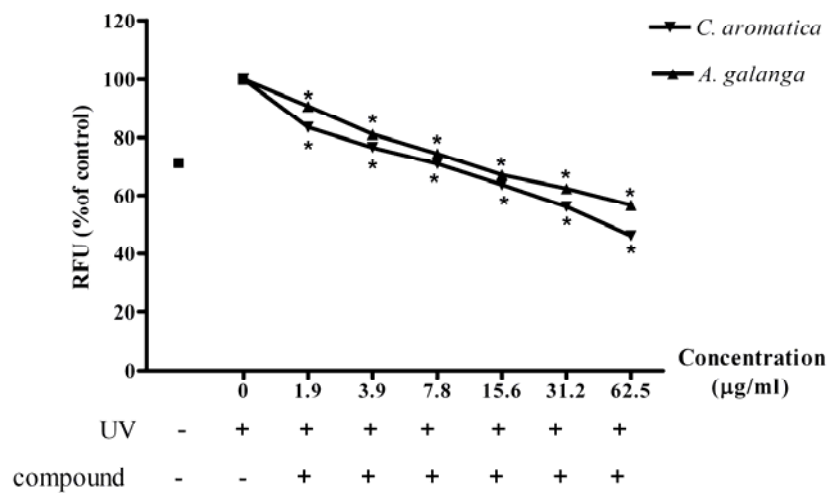


Figure 5.37 The effects of *A. galanga* and *C. aromatica* extracts on the inhibition of ROS in G361 cells exposed with UVA. Cells were pre-treated with each plant extract for 30 min and exposed to UVA (16 J/cm²). Results are expressed as Mean \pm sem of 9 experiments. Statistical significance was evaluated using analysis of variance. * $P < 0.05$ when compared with the control (Cells-exposed UVA in the absence of plant extracts).

CHAPTER VI

DISCUSSION

Skin is the largest and first line of defense in protecting the internal organs from various chemical and physical environment. UV is a major environmental factor which affects the skin and leads to skin photodamage including melasma. Most of the solar UV energy incident on the skin is from the UVA region (>95%) while the UVB content of total solar UV on skin can be well below 2% (20). Compared to UVB, UVA is about 1000 times more effective in the production of an immediate tanning effect which is caused by darkening of the melanin in the epidermis (17). UVA can pass through the epidermal layers of human skin to the basal layer and can readily reach the melanocytes residing on the epidermal-dermal junction, and possibly lead to oxidative DNA damage and mutagenesis (18). Several studies support a causative role of UVA on skin photodamage by photooxidative mechanism mediated by ROS (17-20, 70-72, 131-132). H₂O₂ has been identified as the primary mediator of UVA-induced photosensitization of skin cells (20). Irradiation of melanocyte with UV results in dose-dependent generation of H₂O₂ (18). DCF fluorescence is an assay detecting generalized oxidative stress and ROS formation (72).

The redox state of the skin is regulated by the balance between a variety of endogenous antioxidants, and oxidants. Depletion of antioxidants or an increase in the formation of ROS will alter the balance and make the skin more oxidative. Since UV-mediated oxidative stress is believed to be involved in skin damage including melanogenesis, it is of great interest to study and develop exogenous antioxidant to promote antioxidant defense against oxidative stress capable of damaging skin cells.

Phenolic compounds are diverse group of compounds that are composed of an aromatic benzene ring substituted with hydroxyl groups. There are widely distributed in various vegetables and fruits and show many physiological and pharmacological

functions including antioxidant properties. Polyphenols have been widely studied as beneficial protective agents of skin damage induced by UVR. Traditionally, extracts of plant in Zingiberaceae including *C. aromatica* and *A. galanga* gave high antioxidant activities.

The identification of antioxidant activities, the presence and contents of phenolic and antityrosinase activities of the plant extracts

Phenolic compounds, which may be responsible for the biological activity of *C. aromatica* and *A. galanga* were identified by assessing their presence and contents using TLC analysis and folin assay. In addition, both TLC-DPPH analysis and DPPH assay indicated that both plant extracts-derived phenolics possessed free radical scavenging activities. In agreement with previous report, both extracts appeared to contain curcuminoid (115,117), a powerful antioxidant phenolic, although further investigation using analytical methods (such as HPLC or LC-MS) with better accuracy and precision is needed to evaluate whether it is the active constituent of the plant extracts. Moreover, antioxidant and antityrosinase properties of the plant extracts investigated were found to be greater in *C. aromatica* than *A. galanga*, which contained less phenolic contents than *C. aromatica*.

The antioxidant capacity of phenolic compounds is determined by their structure, in particular the ease with which a hydrogen atom from an aromatic hydroxyl group can be donated to a free radical and the ability of an aromatic compound to support an unpaired electron as the result of delocalization around the M-electron system to form stable product (133,134). It was reported that some phenolic compounds including flavonoids inhibited tyrosinase activity by active site chelation and other acted as cofactor and/or substrate of tyrosinase. Some flavonols possessing a 3-hydroxy-4-keto moiety, such as kaempferol and quercetin, competitively inhibit tyrosinase activity by their ability to chelate the copper in the active site, leading to irreversible inactivation of tyrosinase. Gallic acid inhibits the oxidation of L-DOPA catalyzed by tyrosinase and act as a substrate, being oxidized prior to L-DOPA, which accelerates the oxidation of gallic acid. (48,135)

CAT activity increases depending on the structure of antioxidative flavonoids and their derivatives. Combination of many factors such as the position of functional

groups on the flavonoid structure and their interaction with CAT, including that of the ferriprotoporphyrin group, also contribute to this effect. In particular, the substitutions at C-3 in flavonoids are regarded to be important in terms of the antioxidative potency against H_2O_2 , the enhancing effect on CAT activity, or binding of flavonoids to the heme moiety or a protein region of CAT contributes to the enhancement of CAT activity (136).

Before testing biological activities of the plant extracts in cell culture model, qualitative studies of *C. aromatica* and *A. galanga* using TLC analysis were performed to assure the stability of the phenolic compounds present in the plant extracts that they would not change over time (about 1 year).

Cellular study of the effects of *C. aromatica* and *A. galanga* extracts in inhibiting UVR-induced melanogenesis

In assessing the cytotoxicity of the plant extracts using MTT reduction and GSH content assay after 24-h incubation, they were shown to be non-cytotoxic except at high concentrations as shown in Table 6.1.

Table 6.1 Comparative effects of *C. aromatica* and *A. galanga* extracts on G361 cell cytotoxicity using MTT reduction and intracellular GSH content assays.

Assays	Cytotoxic dose ($\mu\text{g/ml}$)	
	<i>C. aromatica</i>	<i>A. galanga</i>
MTT reduction	125	62.5
GSH content	>62.5	>62.5

The role of H_2O_2 in melanogenesis has not been clearly defined, with some reports indicating it functions to enhance pigment formation by regulating level of tyrosinase. The polymerization reactions involving quinonic melanogenic intermediates are spontaneous and lead to the H_2O_2 formation of as a by product during the tyrosinase-mediated conversion of tyrosine to dopaquinone. Tyrosinase mediated diphenolase activity was enhanced by the endogenously generated H_2O_2 (later stages), and by at least one other reactive intermediate of oxygen (137,138). In

addition, others also indicated that H_2O_2 induced tyrosinase/DOPA oxidase activity including induction of 60 and 55 kDA DOPA oxidase in melanoma cells since exogenous agents that increase H_2O_2 elevated tyrosinase, in reaction prevented by CAT but not SOD (138).

A well-documented feature of isolated human melanoma cells is that their antioxidant capacity is altered when compared with normal melanocytes. It was shown previously in vitro that melanoma cells reveal a decreased CAT activity and low levels of ubiquinone but a higher SOD activity and increased levels of vitamin E. In vitro, human melanoma cells exhibit low levels of antioxidants such as ferritin and GSH but are resistant to oxidative stress. Intracellular superoxide anion concentration is markedly elevated in melanoma compared with melanocytes while H_2O_2 concentration in both cell types is similar (139).

UVR-induced skin pigmentation have a direct effect on melanocytes to cause melanogenesis (83). In addition, it has been shown that the basal layer of the human epidermis, where the melanocytes are situated, harbours more UVA than UVB. Several studies had shown increased melanogenesis by UVA. However, melanin synthesis may also under some conditions enhance induction of oxidative DNA damage in melanocytes in vitro by UVA. Melanocytes or melanoma cells in culture may be sensitized to UVA-induced oxidative DNA damage by stimulated melanin synthesis (140).

The results in this thesis are in agreement with previous investigations showing that UVA irradiation on G361 cells increased tyrosinase activities and melanin synthesis (51,76). UVA was able to increase melanogenesis including induce ROS lead to induction of higher tyrosinase level (141). In addition, it has been found that UVA induced photochemical alteration in skin pigment by changed spectral range. After UVA irradiation pheomelanin absorbance decreases both in the visible and the UVA range. UVA induces significant photochemical alterations in the skin witnessed by increased photoprotection in the visible spectral range and reduced protection in the UVA range. The decrease of absorbance in the UV wavelength range following UVA exposure offers a direct explanation on the lack of any UV photoprotection of UVA-induced pigment (62). This study found that UVA (8 and 16 J/cm^2) caused increase in tyrosinase activities ($\geq 8 J/cm^2$) and melanin contents ($\geq 16 J/cm^2$). Hence, the UVA

doses of 8 and 16 J/cm² were used to study the antioxidant effects of plant extracts on inhibiting cellular melanogenesis. This study also showed that *A. galanga* and *C. aromatica* extracts were able to inhibit induction of the tyrosinase activity and melanin contents by UVR.

UVR-induced cellular oxidative stress and damage is proposed to play a crucial role in melanogenesis as previously discussed. This study showed that UVA could induce G361 cell damage and ROS production-induced intracellular oxidative stress as detected by MTT reduction and DCF-DA assay, respectively. Only *C. aromatica* was shown to inhibit UVA-dependent G361 cell damage and both *C. aromatica* and *A. galanga* could protect cellular oxidative stress against UVA exposure.

It has also been reported on the effect of UV on antioxidant enzyme activity. However, activity of each antioxidant enzyme provides different responses in various conditions including cell types and UV dose. Murine epidermal and dermal CAT showed a marked drop in activity after acute UVA and UVB irradiation (133). In the hairless mouse system, a single UV dose rapidly decreases the activities of catalase and total SOD, but hardly affects GPx. Single exposure of fibroblast to UVA induces SOD activity in a time and dose dependent manner. GPx activity in fibroblasts is unaffected by UVA (23). Thus, decreased cutaneous catalase activity appears to be a consistent finding regardless of the model system or spectrum and dose of UV irradiation studied; while the effect of UV irradiation on SOD and GPx appears to depend on the experimental system (23).

In order to study the roles of the plant extracts in the inhibition of cellular melanogenesis induced by UVA, their effects on activity of endogenous antioxidant enzymes, glutathione contents, melanin contents and tyrosinase activity in G361 cells exposed to UVA were determined. In the study on the antioxidant enzyme activity, UVR deteriorated both CAT and GPx activity in the cells and CAT activity was reduced to a greater extent than that of GPx. It may be because GPx is recycled back to the reduced form more rapidly than CAT. In addition, previous study reported that CAT became a more important antioxidant defense at higher rates of the generation of H₂O₂, a major oxidant associated with UVR (22, 26). Thus, CAT activity might be considered as a very sensitive marker for the increased susceptibility of skin to

external stimuli including an acute and high dose of UVA. In the antioxidant enzyme defense system, SOD converts $O_2^{\bullet-}$ into H_2O_2 and then CAT and GPx convert intermediates into harmless product water. Therefore, CAT and GPx activities were decreased as a result of scavenging ROS after UVR. CAT was probably inactivated directly due to the destruction of the heme ring, which was the active site of the enzyme (36) and because ROS created as a result of UVR destroyed the enzyme indirectly (28). It is known that GPx has a higher affinity to H_2O_2 than CAT. CAT has extremely high maximum catalytic rates but low substrate affinities, since the reaction requires the simultaneous access of two H_2O_2 molecules to the active site (142).

In addition, it is important to study the UV effect on contents of cellular GSH because it acts as a major cellular antioxidant maintaining the intracellular redox balance and involves in regulation of melanin synthesis by inhibit tyrosinase activity. Depletion of skin GSH by UVR might lead to the accumulation of H_2O_2 as a result of insufficient detoxification. The reaction leading to melanogenesis pigments are enhanced by H_2O_2 as well as by other forms of ROS. High levels of intracellular thiols including GSH led to a low tyrosinase activity but a high GPx activity. Thus, melanogenesis could be a mechanism compensating a deficit in GSH-dependent antioxidant defences (143). GSH is very likely to be altered by the UVA-induced oxidative stress such as ROS (144). In the same way as the response of antioxidant enzyme activity to UV exposure, there was a significant depletion of GSH contents in G361 cells exposed to UVA. Hence, UV exposure in this study caused an imbalance of intracellular redox in G361 as shown by GSH depletion. This study showed that UVA was able to decrease the contents of GSH in melanoma cells, although the plant extracts increased intracellular GSH contents at low concentrations of herbal extracts. In addition, there was a tendency in GSH content decrease when treating cells with herbal extracts at concentrations up to 31.25 $\mu\text{g/ml}$. It has some evidence support that GSH depletion may be lead to apoptosis at least by DNA fragmentation (96-97). In addition, antioxidant compounds including phenolics or flavonoids capable of scavenging free radicals often involve radical formation of the flavonoid itself. The chemical properties of some antioxidants may also give them prooxidant properties which can auto oxidize and products of auto-oxidation can possibly react with otherwise reduce cellular concentrations of glutathione (145).

This study as demonstrated in table 6.2 found that *C. aromatica* was able to increase activity of both CAT, GPx and contents of GSH but *A. galanga* was able to inhibit reduction of GPx activity and of GSH content but not CAT activities in the G361 cells exposed with UVA. This could be due to different effect of each plant on antioxidant defense systems responding to UV-induced oxidative stress. Thus, combination of different antioxidant compounds may yield a greater benefit than using single compound.

Table 6.2 Comparative effects of *C. aromatica* and *A. galanga* on the inhibition of UVR-induced reduction of CAT and GPx activities and GSH contents in G361 cells.

	<i>C. aromatica</i>	<i>A. galanga</i>
GPx activities	↑	↑
CAT activities	↑	-
GSH contents	↑	↑

This study aims to evaluate the roles of the plant extracts in the inhibition of cellular melanogenesis induced by UVR, although it is also crucial to carry out quantitative study of the plant extracts to ensure their quality, which is an important contribution to the development of promising herbal compounds as therapeutic agents in the future. Hence, further study is needed to conduct analytical methods e.g., HPLC or LC-MS to identify a fingerprint profile and precise possible bioactive constituents and their concentrations for quality control and potential compound synthesis. Moreover, cellular and molecular mechanisms need further elucidation by studying the signaling pathways involving in cellular antioxidant defense.

CHAPTER VII

CONCLUSION

UVA indeed induced melanogenesis in G361 cells by elevating tyrosinase activities and melanin contents. The ethanol extracts of *A. galanga* and *C. aromatica* rhizome possessing phenolic compounds and antioxidant activities yielded abilities to inhibit cellular melanogenesis caused by UVR. Both extracts could potentially provide inhibitory effects on UVA-dependent cellular melanogenesis by several mechanisms including inhibiting cell cytotoxicity and intracellular oxidative stress or ROS formation as well as improving antioxidant defense systems. *C. aromatica* extract was able to protect against UVR-induced depletion of antioxidant enzyme (both CAT and GPx) activities and GSH contents. However, *A. galanga* inhibited UVR-induced reduction of GPx activities but did not significantly prevent a decrease in CAT activities. Therefore, *A. galangal* and *C. aromatica* extracts-derived antioxidant phenolics could be further developed as effective depigmentating agents beneficial in preventing UV-induced melanogenesis.

Table 7.1 Summary table of the inhibitory effects of *A. galanga* and *C. aromatica* extracts on UVA-induced cellular melanogenesis in association with antioxidant defense system.

Assay	Effective dose ($\mu\text{g/ml}$)	
	<i>C. aromatica</i>	<i>A. galanga</i>
1. Cell viability	1.9 - 15.6	>62.5
2. Tyrosinase activities	1.9 - 62.5	3.9 - 62.5
3. Melanin contents	3.9 - 62.5	15.6 - 31.2
4. Intracellular oxidative stress	1.9 - 62.5	1.9 - 62.5
5. GSH contents	1.9 - 15.6	1.9 - 15.6
6. GPx activities	1.9 - 62.5	1.9 - 62.5
7. CAT activities	1.9 - 62.5	>62.5

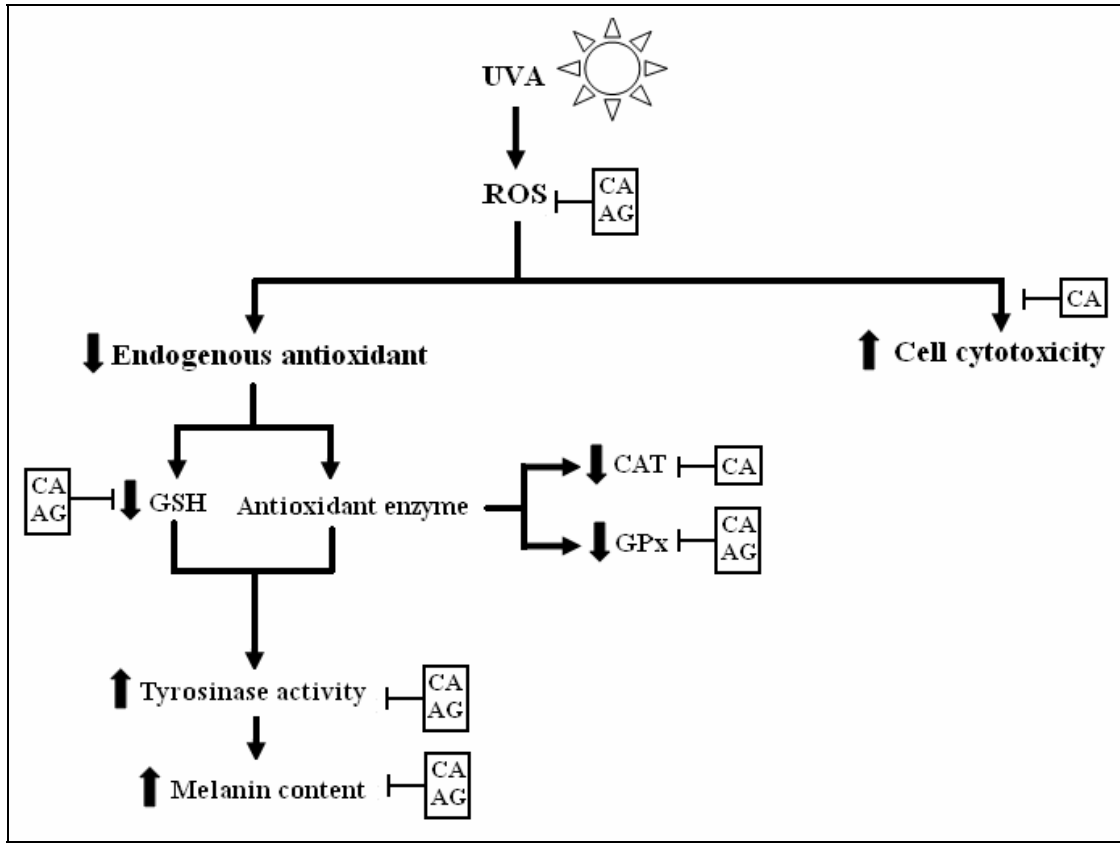


Figure 7.1 The photoprotective effect of *A. galanga* (AG) and *C. aromatica* (CA) extracts against UVA-radiation-induced the oxidative stress.

REFERENCES

1. Wassberg C. Ultraviolet Radiation and Squamous Cell Carcinoma in Human Skin. In: Department of medical Sciences, Section of Dermatology and Venereology, Faculty of medicine. Sweden: Uppsala, 2001: 53.
2. Cadet J, Sage E, Douki T. Ultraviolet radiation-mediated damage to cellular DNA. *Mutat Res* 2005; 571: 3-17.
3. Lo PK, Huang SZ, Chen HC et al. The prosurvival activity of p53 protects cells from UV-induced apoptosis by inhibiting c-Jun NH₂-terminal kinase activity and mitochondrial death signaling. *Cancer Res* 2004; 64:8736-45.
4. Kulms D, Schwarz T. Molecular mechanisms of UV-induced apoptosis. *Photodermatol Photoimmunol Photomed* 2000; 16: 195-201.
5. Ichihashi M, Ueda M, Budiyo A et al. UV-induced skin damage. *Toxicology* 2003; 189: 21-39.
6. de Gruijl FR. Ultraviolet radiation and tumor immunity. *Methods* 2002; 28: 122-9.
7. Schwarz T. Mechanism of UV-induced immunosuppression. *Keio J Med* 2005; 54(4): 165-171.
8. Mai S, Stein B, van den Berg S et al. Mechanisms of the ultraviolet light response in mammalian cells. *J Cell Sci* 1989; 94(Pt 4): 609-15.
9. Matsumura Y, Ananthaswamy NH. Short-term and long-term cellular and molecular events following UV irradiation of skin: implications for molecular medicine. *Exp Rev Mol Med* 2002, <http://www.expertreviews.org/0200532Xh.htm>
10. Hearing VJ. Biogenesis of pigment granules: a sensitive way to regulate melanocyte function. *J Dermatol Sci* 2005; 37: 3-14.
11. Sturm RA, Teasdale RD, Box NF. Human pigmentation genes: identification, structure and consequences of polymorphic variation. *Gene* 2001; 277: 49-62.

12. Rad HH, Yamashita T, Jin HY et al. Tyrosinase-related proteins suppress tyrosinase-mediated cell death of melanocytes and melanoma cells. *Exp Cell Res* 2004; 298: 317-28.
13. Sturm RA. Human pigmentation genes and their response to solar UV radiation. *Mutat Res* 1998; 422: 69-76.
14. Kang WH, Yoon KH, Lee ES et al. Melasma: histopathological characteristics in 56 Korean patients. *Br J Dermatol* 2002; 146: 228-37.
15. Victor FC, Gelber J, Rao B. Melasma: a review. *J Cutan Med Surg* 2004; 8: 97-102.
16. Balkrishnan R, McMichael AJ, Camacho FT et al. Development and validation of a health-related quality of life instrument for women with melasma. *Br J Dermatol* 2003; 149: 572-7.
17. Svobodova A, Walterova D, Vostalova J. Ultraviolet light induced alteration to the skin. *Biomed Pap Med Fac Univ Palacky Olomouc Czech Repub* 2006; 150: 25-38.
18. Kadekaro AL, Kavanagh RJ, Wakamatsu K et al. Cutaneous photobiology. The melanocyte vs. the sun: who will win the final round? *Pigment Cell Res* 2003; 16: 434-47.
19. He G, Kutala VK, Kuppusamy P et al. In vivo measurement and mapping of skin redox stress induced by ultraviolet light exposure. *Free Radic Biol Med* 2004; 36: 665-72.
20. Wondrak GT, Jacobson MK, Jacobson EL. Endogenous UVA-photosensitizers: mediators of skin photodamage and novel targets for skin photoprotection. *Photochem Photobiol Sci* 2006; 5: 215-37.
21. Valko M, Leibfritz D, Moncol J et al. Free radicals and antioxidants in normal physiological functions and human disease. *Int J Biochem Cell Biol* 2007; 39: 44-84.
22. Valko M, Rhodes CJ, Moncol J et al. Free radicals, metals and antioxidants in oxidative stress-induced cancer. *Chem Biol Interact* 2006; 160: 1-40.
23. Leccia MT, Yaar M, Allen N et al. Solar simulated irradiation modulates gene expression and activity of antioxidant enzymes in cultured human dermal fibroblasts. *Exp Dermatol* 2001; 10: 272-9.

24. Dissemond J, Schneider LA, Brenneisen P et al. Protective and determining factors for the overall lipid peroxidation in ultraviolet A1-irradiated fibroblasts: in vitro and in vivo investigations. *Br J Dermatol* 2003; 149: 341-9.
25. Hellemans L, Corstjens H, Neven A et al. Antioxidant enzyme activity in human stratum corneum shows seasonal variation with an age-dependent recovery. *J Invest Dermatol* 2003; 120: 434-9.
26. McArdle F, Rhodes LE, Parslew R et al. UVR-induced oxidative stress in human skin in vivo: effects of oral vitamin C supplementation. *Free Radic Biol Med* 2002; 33: 1355-62.
27. Cesarini JP, Michel L, Maurette JM et al. Immediate effects of UV radiation on the skin: modification by an antioxidant complex containing carotenoids. *Photodermatol Photoimmunol Photomed* 2003; 19: 182-9.
28. Shindo Y, Hashimoto T. Time course of changes in antioxidant enzymes in human skin fibroblasts after UVA irradiation. *J Dermatol Sci* 1997; 14: 225-32.
29. Ahsan H, Parveen N, Khan NU et al. Pro-oxidant, anti-oxidant and cleavage activities on DNA of curcumin and its derivatives demethoxycurcumin and bisdemethoxycurcumin. *Chem Biol Interact* 1999; 121: 161-75.
30. Gali-Muhtasib HU, Yamout SZ, Sidani MM. Plant tannins as inhibitors of hydroperoxide production and tumor promotion induced by ultraviolet B radiation in mouse skin in vivo. *Oncol Rep* 1999; 6: 847-53.
31. Saija A, Tomatino A, Lo Cascio R, Trombetta D et al. Ferulic and caffeic acids as potential protective agents against photooxidative skin damage. *J Sci Food Agric*. 1999; 79: 476-480.
32. Katiyar SK, Afaq F, Perez A et al. Green tea polyphenol (-)-epigallocatechin-3-gallate treatment of human skin inhibits ultraviolet radiation-induced oxidative stress. *Carcinogenesis* 2001; 22: 287-94.
33. Erden Inal M, Kahraman A, Koken T. Beneficial effects of quercetin on oxidative stress induced by ultraviolet A. *Clin Exp Dermatol* 2001; 26: 536-9.

34. Bonina F, Puglia C, Ventura D et al. In vitro antioxidant and in vivo photoprotective effects of a lyophilized extract of *Capparis spinosa* L buds. *J Cosmet Sci* 2002; 53: 321-35.
35. Ozkur MK, Bozkurt MS, Balabanli B et al. The effects of EGb 761 on lipid peroxide levels and superoxide dismutase activity in sunburn. *Photodermatol Photoimmunol Photomed* 2002; 18: 117-20.
36. Cesarini JP, Michel L, Maurette JM et al. Immediate effects of UV radiation on the skin: modification by an antioxidant complex containing carotenoids. *Photodermatol Photoimmunol Photomed* 2003; 19: 182-9.
37. Jeon SE, Choi-Kwon S, Park KA et al. Dietary supplementation of (+)-catechin protects against UVB-induced skin damage by modulating antioxidant enzyme activities. *Photodermatol Photoimmunol Photomed* 2003; 19: 235-41.
38. Dhanalakshmi S, Mallikarjuna GU, Singh RP et al. Dual efficacy of silibinin in protecting or enhancing ultraviolet B radiation-caused apoptosis in HaCaT human immortalized keratinocytes. *Carcinogenesis* 2004; 25: 99-106.
39. Mantena SK, Katiyar SK. Grape seed proanthocyanidins inhibit UV-radiation-induced oxidative stress and activation of MAPK and NF-kappaB signaling in human epidermal keratinocytes. *Free Radic Biol Med* 2006; 40: 1603-14.
40. Russo A, Cardile V, Lombardo L et al. Genistin inhibits UV light-induced plasmid DNA damage and cell growth in human melanoma cells. *J Nutr Biochem* 2006; 17: 103-8.
41. Psoтова J, Svobodova A, Kolarova H et al. Photoprotective properties of *Prunella vulgaris* and rosmarinic acid on human keratinocytes. *J Photochem Photobiol B* 2006; 84: 167-74.
42. Hinneburg I, Kempe S, Ruttinger HH et al. Antioxidant and photoprotective properties of an extract from buckwheat herb (*Fagopyrum esculentum* MOENCH). *Pharmazie* 2006; 61: 237-40.
43. Afaq F, Syed DN, Malik A et al. Delphinidin, an anthocyanidin in pigmented fruits and vegetables, protects human HaCaT keratinocytes and mouse skin

- against UVB-mediated oxidative stress and apoptosis. *J Invest Dermatol* 2007; 127: 222-32.
44. Lee ER, Kim JH, Kang YJ et al. The anti-apoptotic and anti-oxidant effect of eriodictyol on UV-induced apoptosis in keratinocytes. *Biol Pharm Bull* 2007; 30: 32-7.
45. Tong X, Van Dross RT, Abu-Yousif A et al. Apigenin prevents UVB-induced cyclooxygenase 2 expression: coupled mRNA stabilization and translational inhibition. *Mol Cell Biol* 2007; 27: 283-96.
46. Vankar PS, Tiwari V, Singh LW et al. Antioxidant properties of some exclusive species of zingiberaceae family of manipur. *EJEAFChe* 2006; 5(2): 1318-1322.
47. Habsah M, Amran M, Mackeen MM et al. Screening of Zingiberaceae extracts for antimicrobial and antioxidant activities. *J Ethnopharmacol* 2000; 72: 403-10.
48. Jimbow K, Minamitsuji Y. Topical therapies for melasma and disorders of hyperpigmentation. *Dermatologic Therapy* 2001; 14: 35-45.
49. Piamphongsant T. Treatment of melasma: a review with personal experience. *Int J Dermatol* 1998; 37: 897-903.
50. Haddad AL, Matos LF, Brunstein F et al. A clinical, prospective, randomized, double-blind trial comparing skin whitening complex with hydroquinone vs. placebo in the treatment of melasma. *Int J Dermatol* 2003; 42: 153-6.
51. Dell'Angelica EC. Melanosome biogenesis: shedding light on the origin of an obscure organelle. *Trends Cell Biol* 2003; 13: 503-6.
52. Chudnovsky Y, Khavari PA, Adams AE. Melanoma genetics and the development of rational therapeutics. *J Clin Invest* 2005; 115: 813-24.
53. Riley PA. Melanin. *Int J Biochem Cell Biol* 1997; 29: 1235-9.
54. Perluigi M, De Marco F, Foppoli C et al. Tyrosinase protects human melanocytes from ROS-generating compounds. *Biochemical and Biophysical Research Communications* 2003; 305: 250-256.
55. Jones K, Hughes J, Hong M et al. Modulation of melanogenesis by aloesin: a competitive inhibitor of tyrosinase. *Pigment Cell Res* 2002; 15: 335-40.

56. Sulaimon SS, Kitchell BE. The biology of melanocytes. *Vet Dermatol* 2003; 14: 57-65.
57. Kim YJ, Uyama H. Tyrosinase inhibitors from natural and synthetic sources: structure, inhibition mechanism and perspective for the future. *Cell Mol Life Sci* 2005; 62: 1707-23.
58. Slominski A, Tobin DJ, Shibahara S et al. Melanin pigmentation in mammalian skin and its hormonal regulation. *Physiol Rev* 2004; 84: 1155-228.
59. Abdel-Naser MB, Krasagakis K, Garbe C et al. Direct effects on proliferation, antigen expression and melanin synthesis of cultured normal human melanocytes in response to UVB and UVA light. *Photodermatol Photoimmunol Photomed* 2003; 19: 122-7.
60. Matsumura Y, Ananthaswamy HN. Toxic effects of ultraviolet radiation on the skin. *Toxicology and Applied Pharmacology* 2004; 195: 298-308.
61. Drobetsky EA, Turcotte Jand Chateauneuf A. A role for ultraviolet A in solar mutagenesis. *Proc Natl Acad Sci* 1995; 92: 2350-2354.
62. Ou-Yang H, Stamatias G, Kollias N. Spectral responses of melanin to ultraviolet A irradiation. *J Invest Dermatol* 2004; 122: 492-496.
63. Agar NS, Halliday GM, Barnetson RS et al. The basal layer in human squamous tumors harbors more UVA than UVB fingerprint mutations: A role for UVA in human skin carcinogenesis. *PNAS* 2004; 14: 4954-4959.
64. Emri G, Wenczl E, Erp PV et al. Low doses of UVB or UVA induce chromosomal aberrations in cultured human skin cells. *J Invest Dermatol* 2000; 115: 435-440.
65. Kvam E, Tyrrell RM. The role of melanin in the induction of oxidative DNA base damage by ultraviolet A irradiation of DNA or melanoma cells. *J Invest Dermatol* 1999; 113: 209-13.
66. Zhang H, Rosdahl I. Ultraviolet A and B differently induce intracellular protein expression in human skin melanocytes--a speculation of separate pathways in initiation of melanoma. *Carcinogenesis* 2003; 24: 1929-34.
67. Walker GJ, Hayward NK. Pathways to melanoma development: lessons from the mouse. *J Invest Dermatol* 2002; 119: 783-92.

68. Larsson P, Andersson E, Johansson U et al. Ultraviolet A and B affect human melanocytes and keratinocytes differently. A study of oxidative alterations and apoptosis. *Exp Dermatol* 2005; 14: 117-23.
69. Gasparro FP. Sunscreen, skin photobiology, and skin cancer: The need for UVA Protection and evaluation of efficacy. *Environ Health Perspect* 2000; 108(suppl 1): 71-78.
70. Haddad JJ. Redox and oxidant-mediated regulation of apoptosis signaling pathways: immuno-pharmaco-redox conception of oxidative siege versus cell death commitment. *Int Immunopharmacol* 2004; 4: 475-493.
71. Pavlovic D, Dordevic V, Kocic G. A "cross-talk" between oxidative stress and redox cell signaling. *Medicine and Biology* 2002; 9(2): 131-137.
72. Halliwell B, Whiteman M. Measuring reactive species and oxidative damage in vivo and in cell culture: how should you do it and what do the results mean? *Br J Pharmacol* 2004; 142: 231-55.
73. Scandalios JG. Oxidative stress: molecular perception and transduction of signals triggering antioxidant gene defenses. *Braz J Med Biol Res* 2005; 38(7): 995-1014.
74. Young IS, Woodside JV. Antioxidants in health and disease. *J Clin Pathol* 2001; 54: 176-186.
75. Wei YH, Lee HC. Oxidative Stress, Mitochondrial DNA Mutation, and Impairment of Antioxidant Enzymes in Aging. *Exp Biol Med* 2002; 227: 671-682.
76. Sander CS, Chang H, Salzman S et al. Photoaging is associated with protein oxidation in human skin in vivo. *J Invest Dermatol* 2002; 118: 618-25.
77. Wondrak GT, Roberts MJ, Cervantes-Laurean D et al. Proteins of the extracellular matrix are sensitizers of photo-oxidative stress in human skin cells. *J Invest Dermatol* 2003; 121: 578-86.
78. Podda M, Traber MG, Weber C et al. UV-irradiation depletes antioxidants and causes oxidative damage in a model of human skin. *Free Radic Biol Med* 1998; 24: 55-65.
79. Sakurai H, Yasui H, Yamada Y et al. Detection of reactive oxygen species in the skin of live mice and rats exposed to UVA light: a research review on

- chemiluminescence and trials for UVA protection. *Photochem Photobiol Sci* 2005; 4: 715-20.
80. He YY, Huang JL, Block ML et al. Role of phagocyte oxidase in UVA-induced oxidative stress and apoptosis in keratinocytes. *J Invest Dermatol* 2005; 125: 560-6.
81. Iwai I, Hatao M, Naganuma M et al. UVA-induced immune suppression through an oxidative pathway. *J Invest Dermatol* 1999; 112: 19-24.
82. Wondrak GT, Jacobson MK, Jacobson EL. Identification of quenchers of photoexcited States as novel agents for skin photoprotection. *J Pharmacol Exp Ther* 2005; 312: 482-91.
83. Busca R, Ballotti R. Cyclic AMP a key messenger in the regulation of skin pigmentation. *Pigment Cell Res* 2000; 13: 60-9.
84. Meewes C, Brenneisen P, Wenk J et al. Adaptive antioxidant response protects dermal fibroblasts from UVA-induced phototoxicity. *Free Radic Biol Med* 2001; 30: 238-47.
85. Maeda K, Hatao M. Involvement of photooxidation of melanogenic precursors in prolonged pigmentation induced by ultraviolet A. *J Invest Dermatol* 2004; 122: 503-9.
86. Benathan M, Alvero-Jackson H, Mooy AM, Scaletta C, Frenk E. Relationship between melanogenesis, glutathione levels and melphalan toxicity in human melanoma cells. *Melanoma Res* 1992; 2(5-6): 305-14.
87. del Marmol V, Solano F, Sels A et al. Glutathione depletion increases tyrosinase activity in human melanoma cells. *J Invest Dermatol* 1993; 101: 871-4.
88. Chakraborty AK, Ichihashi M, Mishima Y. Effect of dopa-loading on glutathione metabolising enzymes and tyrosinase in relation to 5-S-cysteinyl-dopa genesis in cultured B-16 melanoma cells. *J Dermatol Sci* 1991; 2: 329-35.
89. Inhibition of Melanogenic Activity by 4,4'-Dihydroxybiphenyl in Melanoma Cells. *Biol Pharm Bull* 2006; 29(1): 14—16.
90. Agar N, Young AR. Melanogenesis: a photoprotective response to DNA damage? *Mutat Res* 2005; 571: 121-32.

91. Gilchrest BA, Eller MS. DNA photodamage stimulates melanogenesis and other photoprotective responses. *J Invest Dermatol Symp Proc* 1999; 4: 35-40.
92. Tadokoro T, Kobayashi N, Zmudzka BZ et al. UV-induced DNA damage and melanin content in human skin differing in racial/ethnic origin. *Faseb J* 2003; 17: 1177-9.
93. Eller MS, Ostrom K, Gilchrest BA. DNA damage enhances melanogenesis. *Proc Natl Acad Sci* 1996; 93: 1087-1092.
94. Yamamura T, Onishi J, Nishiyama T. Antimelanogenic activity of hydrocoumarins in cultured normal human melanocytes by stimulating intracellular glutathione synthesis. *Arch Dermatol Res* 2002; 294: 349-54.
95. Herrling T, Fuchs J, Rehberg J et al. UV-induced free radicals in the skin detected by ESR spectroscopy and imaging using nitroxides. *Free Radic Biol Med* 2003; 35: 59-67.
96. Higuchi Y. Glutathione depletion-induced chromosomal DNA fragmentation associated with apoptosis and necrosis. *J Cell Mol Med* 2004; 8: 455-64.
97. Wu G, Fang YZ, Yang S et al. Glutathione metabolism and its implications for health. *J Nutr* 2004; 134: 489-492.
98. Benathan M, Virador V, Furumura M et al. Co-regulation of melanin precursors and tyrosinase in human pigment cells: roles of cysteine and glutathione. *Cell Mol Biol (Noisy-le-grand)* 1999; 45: 981-90.
99. Jara JR, Aroca P, Solano F et al. The role of sulfhydryl compounds in mammalian melanogenesis: the effect of cysteine and glutathione upon tyrosinase and the intermediates of the pathway. *Biochim Biophys Acta* 1988; 967: 296-303.
100. Podda M, Grundmann-Kollmann M. Low molecular weight antioxidants and their role in skin ageing. *Clin Exp Dermatol* 2001; 26: 578-82.
101. Speier C, Baker SS, Newburger PE. Relationships between in vitro selenium supply, glutathione peroxidase activity, and phagocytic function in the HL-60 human myeloid cell line. *J Biol Chem* 1985; 260: 8951-5.

102. Zubkova EV, Robaire B. Effect of glutathione depletion on antioxidant enzymes in the epididymis, seminal vesicles, and liver and on spermatozoa motility in the aging brown Norway rat. *Biol Reprod* 2004; 71: 1002-8.
103. Svobodova A, Psotova J, Walterova D. Natural phenolics in the prevention of UV-induced skin damage. A review. *Biomed Pap Med Fac Univ Palacky Olomouc Czech Repub* 2003; 147: 137-45.
104. Chirangini P, Sharma GJ, Sinha SK. Sulfur free radical reactivity with curcumin as reference for evaluating antioxidant properties of medicinal zingiberales. *J Environ Pathol Toxicol Oncol* 2004; 23: 227-36.
105. Yang X, Eilerman RG. Pungent principal of *Alpinia galangal* (L.) swartz and its applications. *J Agric Food Chem* 1999; 47: 1657-62.
106. Matsuda H, Pongpiriyadacha Y, Morikawa T et al. Gastroprotective effects of phenylpropanoids from the rhizomes of *Alpinia galanga* in rats: structural requirements and mode of action. *Eur J Pharmacol* 2003; 471: 59-67.
107. Al-Yahya MA, Rafatullah S, Mossa JS et al. Gastric antisecretory, antiulcer and cytoprotective properties of ethanolic extract of *Alpinia galanga* willd in rats. 1989
108. Kubota K, Someya Y, Yoshida R et al. Enantiomeric purity and odor characteristics of 2- and 3-acetoxy-1, 8-cineoles in the rhizomes of *Alpinia galanga* willd. *J Agric Food Chem* 1999; 47: 685-9.
109. Someya Y, Kobayashi A, Kubota K. Isolation and identification of trans-2- and trans-3-hydroxy-1,8-cineole glucosides from *Alpinia galanga*. *Biosci Biotechnol Biochem* 2001; 65: 950-3.
110. Jirovetz L, Buchbauer G, Shafi MP, Leela NK. Analysis of the essential oils of the leaves, stems, rhizomes and roots of the medicinal plant *Alpinia galanga* from southern India. *Acta Pharm* 2003; 53: 73-81.
111. Raina VK, Srivastava SK, Syamasunder KV. The essential oil of 'greater galangal' [*Alpinia galanga*(L.) Willd.] from the lower Himalayan region of India. 2001

112. Zaeoung S, Plubrukarn A, Keawpradub N. Cytotoxic and free radical scavenging activities of Zingiberaceous rhizomes. *Songklanakarin J Sci Technol* 2005; 27(4): 799-812.
113. Cheah PB, Hasim NH. Natural antioxidant extract from galangal(*Alpinia galanga*) for minced beef. *J Sci Food Agric* 2000; 80: 1565-1571.
114. Cheah PB, Gan SP. Antioxidative/Antimicrobial effects of galangal and alpha-tocopherol in minced beef. *J Food Prot* 2000; 63: 404-7.
115. Manosroi A, Manosroi J. Aromatic Volatile Oil and extracts from thai medicinal plants: Applications in pharmaceuticals and cosmetics. Faculty of pharmacy/Pharmaceutical-Cosmetic Raw Materials and Natural Products Research and Development Center, Institute for science and technology research and development Chiang Mai University, Thailand, 2005.
116. Qureshi S, Shah AH, Ageel AM. Toxicity studies on *Alpinia galanga* and *Curcuma longa*. *Planta Med* 1992; 58(2): 124-7.
117. Tohda C, Nakayama N, Hatanaka F et al. Comparison of Anti-inflammatory Activities of Six Curcuma Rhizomes: A Possible Curcuminoid-independent Pathway Mediated by *Curcuma phaeocaulis* Extract. *Evid Based Complement Alternat Med* 2006; 3: 255-60.
118. Asai A, Nakagawa K, Miyazawa T. Antioxidative effects of turmeric, rosemary and capsicum extracts on membrane phospholipid peroxidation and liver lipid metabolism in mice. *Biosci Biotechnol Biochem* 1999; 63: 2118-22.
119. Mahakunakorn P, Tohda M, Murakami Y et al. Cytoprotective and cytotoxic effects of curcumin: dual action on H₂O₂-induced oxidative cell damage in NG108-15 cells. *Biol Pharm Bull* 2003; 26: 725-8.
120. Balasubramanyam M, Koteswari AA, Kumar RS et al. Curcumin-induced inhibition of cellular reactive oxygen species generation: novel therapeutic implications. *J Biosci* 2003; 28: 715-21.
121. Kim JE, Kim AR, Chung HY et al. In vitro peroxy nitrite scavenging activity of diarylheptanoids from *Curcuma longa*. *Phytother Res* 2003; 17: 481-4.

122. Araujo MC, Antunes LM, Takahashi CS. Protective effect of thiourea, a hydroxyl-radical scavenger, on curcumin-induced chromosomal aberrations in an in vitro mammalian cell system. *Teratog Carcinog Mutagen* 2001; 21: 175-80.
123. Motterlini R, Foresti R, Bassi R, Green CJ. Curcumin, an antioxidant and anti-inflammatory agent, induces heme oxygenase-1 and protects endothelial cells against oxidative stress. *Free Radic Biol Med* 2000; 28(8): 1303-12.
124. Kim JK, Joa C, Hwangb HJ et al. Color improvement by irradiation of *Curcuma aromatica* extract for industrial application. *Radiat Phys Chem* 2006; 75: 449-452.
125. Biswas SK, McClure D, Jimenez LA et al. Curcumin induces glutathione biosynthesis and inhibits NF-kappaB activation and interleukin-8 release in alveolar epithelial cells: mechanism of free radical scavenging activity. *Antioxid Redox Signal* 2005; 7: 32-41.
126. Somparn P, Phisalaphong C, Nakornchai S et al. Comparative antioxidant activities of curcumin and its demethoxy and hydrogenated derivatives. *Biol Pharm Bull* 2007; 30: 74-8.
127. Sreejayan Rao MN. Curcuminoids as potent inhibitors of lipid peroxidation. *J Pharm Pharmacol* 1994; 46: 1013-1016.
128. Pitasawat B, Choochote W, Tuetun B et al. Repellency of aromatic turmeric *Curcuma aromatica* under laboratory and field conditions. *Journal of Vector Ecology* 2003; 12: 234-240.
129. Blume HH, Midha KK. Bio - International 92, conference on bioavailability, bioequivalence, and pharmacokinetic studies. *J Pharm Sci.* 1993; 82:1186-1189.
130. U.S. Dept of Health and Human Services FaDFCfDEaRC. Guidance for Industry: Statistical) Approaches to Establishing Bioequivalence.2001.

131. Bernerd F. Human skin reconstructed in vitro as a model to study the keratinocyte, the fibroblast and their interactions: photodamage and repair processes. *J Soc Biol* 2005; 199: 313-20.
132. Sakurai H, Yasui H, Yamada Y et al. Detection of reactive oxygen species in the skin of live mice and rats exposed to UVA light: a research review on chemiluminescence and trials for UVA protection. *Photochem Photobiol Sci* 2005; 4: 715-20.
133. Ross JA, Kasum CM. Dietary flavonoids: bioavailability, metabolic effects, and safety. *Annu Rev Nutr* 2002; 22: 19-34.
134. Kris-Etherton PM, Lefevre M et al. Bioactive compounds in nutrition and health-research methodologies for establishing biological function: The antioxidant and anti-inflammatory effects of flavonoids on atherosclerosis. *Annu Rev Nutr* 2004; 24: 511-38.
135. Rhie GE, Shin MH et al. Aging-and photoaging-dependent changes of enzymic and nonenzymic antioxidants in the epidermis and dermis of human skin in vivo. *J Invest Dermatol* 2001; 117: 1212-1217.
136. Doronicheva N, Yasui H, and Sakurai H. Chemical Structure-Dependent Differential Effects of Flavonoids on the Catalase Activity as Evaluated by a Chemiluminescent Method. *Biol Pharm Bull* 2007; 30(2): 213-217.
137. Mastore M, Kohler L and Napp AJ. Production and utilization of hydrogen peroxide associated with melanogenesis and tyrosinase-mediated oxidations of DOPA and dopamine. *FEBS Journal* 2005; 272: 2407-2415.
138. Alberto L, Sarosi G *et al.* Hydrogen peroxide increases a 55-kDa tyrosinase concomitantly with induction of p53-dependent p21 waf1 expression and a greater Bax/Bcl-2 ratio in pigmented melanoma. *Biochemical and biophysical Research Communications* 2003; 312:335-359.
139. Sander CS, Hamm F *et al.* Oxidative stress in malignant melanoma and non-melanoma skin cancer. *British Journal of Dermatology* 2003; 148: 913-922.

140. Kvam E, Dahle J. Melanin synthesis may sensitize melanocytes to oxidative DNA damage by ultraviolet A radiation and protect melanocytes from direct DNA damage by ultraviolet B radiation. *Pigment Cell Res* 2004; 17: 549-550.
141. Brian J, Liu Y, Simon JD. Aggregation of eumelanin mitigates photogeneration of reactive oxygen species. *Free Radic Biol Med* 2002; 32(8): 720-730.
142. Czarniewska E, Kasprzyk A *et al.* Effect of paraquat and metoxychlor on antioxidant enzymes in frog *Rana esculenta* L. liver. *Biol Lett* 2003; 40(2): 125-133.
143. Benathan M. Opposite regulation of tyrosinase and glutathione peroxidase by intracellular thiols in human melanoma cells. *Arch Dermatol Res* 1997; 289: 341-346.
144. Nishimura H, Yasui H, Sakurai H. Generation and distribution of reactive oxygen species in the skin of hairless mice under UVA: studies on in vivo chemiluminescent detection and tape stripping methods. *Exp Dermatol* 2006; 15: 891-899.
145. Moskaug J, Carlsen H *et al.* Polyphenol and glutathione synthesis regulation. *Am J Clin Nutr* 2005; 81(suppl): 277S-83S.

APPENDIX

I. Phosphate buffer saline (PBS)

NaCl (MW 58.44; 138 mM)	8.065 g
KCl (MW 74.55; 2.7 mM)	0.200 g
Na ₂ HPO ₄ (MW 142.0; 8 mM)	1.150 g
KH ₂ PO ₄ (MW 136.1; 1.46 mM)	0.200 g

II. Trypsin-EDTA

Trypsin 250 (Difco Laboratories)	500 mg
PBS solution	100 ml
EDTA (ethylene diamine tetra acetic acid disodium salt (C ₁₀ H ₁₄ N ₂ O ₈ Na ₂ ·2H ₂ O; MW 372.2; 5.3 mM)	197 mg

III. T-wash

ddH ₂ O	50 ml
Tris base (50mM)	302.8 mg
EDTA (10mM)	186.1 mg
Triton X-100 (1%) (v/v)	500 µl

IV. Extracted buffer

T-wash	20 ml
[Freeze] Stock PMSF (100 mg/ml in DMSO)	20 µl (100 µg/ml)
[Freeze] Stock Pepstatin A (1 mg/ml in DMSO)	20 µl (1 µg/ml)
[Freeze] Stock Leupeptin (1 mg/ml in water)	20 µl (1 µg/ml)

PUBLICATION AND PRESENTATIONS

Publications

- 2005 Jaemsak K, Tappayuthpijarn P, Wongkajornsilp A, Ninchawee C, Huabprasert S and Ketsawatsakul U. The Effects of Four Medicinal Plants on Cytotoxicity of Human Melanocyte cells *Siriraj Med J* 2005; 57: P21.
- 2005 Ketsawatsakul U, Akarasereenont P, Wongkajornsilp A, O-charoenrat P, Jaemsak K, Tappayuthpijarn P, Ninchawee C, Chotewuttakorn S, Thaworn A & Huabprasert S. The Inhibitory Effects of Thai Medicinal Plants on the Proliferation of Human Cancer cells: The Possible Role of Antioxidants. *Siriraj Med J* 2005; 57: P22.
- 2006 Jaemsak K, Tappayuthpijarn P, Wongkajornsilp A, Ninchawee C, Huabprasert S, Thaworn A, Ananta W, Akarasereenont P, Wongkajornsilp A and Ketsawatsakul U. The Phytochemical Evaluation and the Antioxidant Activity of Medicinal Plants: The Effects on Antioxidant Enzymes in Human Melanoma Cell lines *Siriraj Med J* 2006; 58: P30.
- 2006 Ketsawatsakul U, O-charoenrat P, Jaemsak K, Ninchawee C, Phonpakobsin T, Ananta W, Thaworn A & Akarasereenont P. The Anti-cancer Effects of Thai Medicinal Plants on Human Head and Neck Squamous Cell Carcinoma Cells: The Possible Roles of Antioxidant Phenolics. Proceedings the International Conference on Oral Cancer in The Asia Pacific – A Regional Update & Networking. 2006; P76.
- 2007 Jaemsak K, Thaworn A, Ananta W, Tappayuthpijarn P, Huabprasert S, Akarasereenont P, Wongkajornsilp A and Ketsawatsakul U. The effects of ultraviolet radiation on cellular antioxidants in human melanoma cells: modulation by thai medicinal plant-derived antioxidant phenolics *Siriraj Med J* 2007; 59: P32.

PUBLICATION AND PRESENTATIONS (continued)**Presentations**

- 2005 Oral presentation (1/07). The 45th Siriraj Scientific Congress, Faculty of Medicine, Siriraj Hospital, Mahidol University, Bangkok, Thailand.
- 2006 Oral presentation. (19/04)The 60th Anniversary Celebration of His Majesty's Accession to the throne Siriraj-Ramathibodi Medical Congress, Mahidol University, Bangkok, Thailand.
- 2006 Poster presentation (17-19/02). The International Conference on Oral Cancer in The Asia Pacific – A Regional Update & Networking, University of Malaya, Kuala Lumpur, Malaysia
- 2007 Oral presentation (7/03). Siriraj Medical Conference, Faculty of Medicine, Siriraj Hospital, Mahidol University, Bangkok, Thailand.

BIOGRAPHY

NAME	Miss Kannika Jaemsak
DATE OF BIRTH	August 16, 1979
PLACE OF BIRTH	Bangkok, Thailand
INSTITUTIONS ATTENDED	Silpakorn University, 1997-2001: Bachelor of Pharmacy Mahidol University, 2004-2007 Master of Science in Pharmacy (Pharmacology)
WORK EXPERIENCE	Prasart Neurological Instituted Hospital, Bangkok 2001-Present.
POSITION & OFFICE	Pharmacist Prasart Neurological Instituted Hospital, Bangkok
RESEARCH GRANT	This thesis is supported by faculty of Graduate Studies, Mahidol University, academic year 2006.